AN ABSTRACT OF THE THESIS OF

Mark Leid for the degree of Doctor of Philosophy in Pharmacy presented on 26 October 1989.

Title: Pharmacological Characterization of the Porcine Atrial A_1 Adenosine Receptor

Abstract approved: Redacted for privacy
Thomas F. Murray

Cardiac A_1 adenosine receptors mediate cardioinhibitory properties of adenosine and structural congeners. The objective of these studies was to increase our understanding of molecular processes involved in ligand interactions with receptors mediating cardioinhibitory effects of adenosine and the interactions of these receptors with guanine nucleotide binding regulatory proteins. Porcine atrial A_1 receptors receptors were characterized using both agonist (N^6-{3-[^{125}I]iodo-4-hydroxyphenylisopropyl}adenosine, [^{125}I]HPIA) and antagonist (8-cyclopentyl-1,3[^{3}H]dipropyl-xanthine, [^{3}H]DPCPX) radioligands.

[^{3}H]DPCPX was shown to be the first useful antagonist radioligand for labeling atrial A_1 adenosine receptors. The atrial adenosine receptor displayed two agonist affinity states: a guanine nucleotide-sensitive high affinity state and a guanine nucleotide-insensitive low affinity state. The former was demonstrated to be entirely the result of ternary complex formation in porcine atrial membranes (agonist-receptor-G protein).

[^{125}I]HPIA labeled a homogeneous population of membrane-bound atrial A_1 adenosine receptors which appeared to exist pre-coupled (in the absence of agonist) to a guanine nucleotide binding protein. Guanine nucleotides negatively modulated [^{125}I]HPIA binding by increasing the rate of dissociation of the agonist radioligand, providing direct evidence for ternary complex formation in porcine atrial membranes.

Solubilization of atrial adenosine receptors using a mixed detergent system (digitonin/sodium cholate) resulted in a 2.5-fold enrichment of adenosine receptor specific activity over that of porcine atrial membrane preparations. Both pharmacological specificity and receptor-G protein interactions were preserved in detergent solution. [^{125}I]HPIA interacted via a simple bimolecular reaction with solubilized atrial adenosine receptors that existed precoupled to G protein(s). Guanine nucleotide-initiated [^{125}I]-HPIA dissociation was biphasic and appeared to arise from independent, non-interconvertible populations of receptor-G protein complexes. Thus, kinetic evidence indicates that the atrial adenosine receptor is able to couple to two distinct G proteins in detergent solution.

Pharmacological Characterization of the Porcine Atrial A_1 Adenosine Receptor

by

Mark Leid

A THESIS

submitted to

Oregon State University

in partial fulfillment of
the requirements for the
degree of

Doctor of Philosophy

Completed 26 October 1989

Commencement June 1990

APPROVED:

Redacted for privacy

Associate Professor of Pharmacy in charge of major

Redacted for privacy

Dean of College of Pharmacy

Redacted for privacy

Dean of Graduate School

Date thesis is presented 26 October 1989

Typed by Mark Leid for Mark Leid

ACKNOWLEDGMENTS

I gratefully acknowledge the continuous support of my family from Little League through graduate school. In particular, the intellectual, emotional and financial support of my wife, Cassandra, over the past fifteen years is very much appreciated.

I thank the following organizations and departments for financial support during my graduate education: American Foundation for Pharmaceutical Education (predoctoral fellowship), American Heart Association (summer fellowship), Oregon State University Department of Chemistry (Tartar fellowships) and Graduate School (Bayley fellowship), Federation of American Societies for Experimental Biology (travel support) and Western Pharmacology Society (travel support).

Members of the laboratory of Professor Michael Schimerlik have made an important contribution to this work through tireless membrane preparation (Chi-Juinn Pan and Laurie Shoots) and helpful advice (Drs. Gary Peterson, Michael Tota and David Broderick). I am especially grateful to Dr. Schimerlik for his unwavering support and patience over the course of these studies. His guidance and encouragement were invaluable for completion of this work and I am honored to have had the opportunity to work with him.

I thank Drs. Paul Franklin and Joseph Siebenaller for their encouragement, insight, advice and friendship during my graduate education. The technical assistance of Janice Woelfl has been exceptionally helpful and it is with great pleasure that I acknowledge her contribution to this project.

Finally, I thank Professor Thomas F. Murray for his many years of guidance, encouragement, financial support and personal friendship. I am deeply appreciative of everything Dr. Murray has contributed to this project and my development as a scientist.

CONTRIBUTION OF CO-AUTHORS

CHAPTER II

All of the experiments discussed in this chapter were performed and analyzed by myself under the guidance of Professor Thomas Murray. Dr. Paul Franklin was consulted about some experimental details and data interpretation.

This chapter is republished with written permission of Elsevier Science Publishers and *The European Journal of Pharmacology* (Leid, M., P.H. Franklin, and T.F. Murray. Labeling of A_1 Adenosine Receptors in Porcine Atria with the Antagonist Radioligand 8-cyclopentyl-1,3[^{3}H]dipropylxanthine. *Eur. J. Pharmacol.* **147**:141-144 [1988]).

CHAPTER III

All of the experiments discussed in this chapter were performed and analyzed by myself under the guidance and in the laboratory of Professor Thomas Murray. Professor Michael Schimerlik was an invaluable source of information on all aspects of these studies but his expertise in analysis of kinetic experiments and in the synthesis of APNEA was particularly helpful. In addition, Professor Schimerlik's laboratory supplied most of the membrane preparations used in these experiments.

This chapter is republished with written permission of Williams and Wilkins Publishers, the American Society for Pharmacology and Experimental Therapeutics, and *Molecular Pharmacology* (Leid, M.,

M.I. Schimerlik, and T.F. Murray. Characterization of Agonist Radioligand Interactions with Porcine Atrial A_1 Adenosine Receptors. *Mol. Pharmacol.* 34:334-339 [1988]).

CHAPTER IV

All of the solubilizations and experiments discussed in this chapter were performed and analyzed by myself under the guidance and in the laboratory of Professor Thomas F. Murray. Professor Michael Schimerlik was an invaluable source of information on all aspects of these studies but his expertise in analysis of kinetic experiments was particularly helpful. In addition, Professor Schimerlik's laboratory supplied all of the membrane preparations used for solubilization in these experiments.

This chapter is republished with written permission of Williams and Wilkins Publishers, the American Society for Pharmacology and Experimental Therapeutics, and *Molecular Pharmacology* (Leid, M., M.I. Schimerlik, and T.F. Murray. Agonist Radioligand Interactions with the Solubilized Porcine Atrial A_1 Adenosine Receptor. *Mol. Pharmacol.* 35:450-457 [1989]).

TABLE OF CONTENTS

LIST OF FIGURES

CHAPTER III (cont'd) **PAGE**

CHAPTER IV

LIST OF TABLES

PHARMACOLOGICAL CHARACTERIZATION OF THE PORCINE ATRIAL A_1 ADENOSINE RECEPTOR

CHAPTER I

INTRODUCTION

Drury and Szent-Györgyi first described physiological properties of exogenously-administered adenosine and adenine nucleotides in 1929 (1). These pioneers studied the effects of intravenously-administered crude tissue extracts on several physiological parameters. Drury and Szent-Györgyi identified the active constituent of these extracts as adenylic acid but also noted that adenosine (prepared from hydrolysis of yeast nucleic acid) had identical physiological activity. They found that, when administered to anesthetized and atropinized animals, adenosine:

1. Produced a rapid and transient sinus bradycardia.
2. Produced a complete A-V block in guinea pigs.
3. Decreased the force with which atrial tissue contracted.
4. Reversed experimentally-induced atrial flutter and fibrillation and restored normal sinus rhythm in dogs.
5. Lowered arterial pressure (due in part to cardiac slowing and in part to a general arterial dilatation).
6. Increased perfusion of numerous tissues, most notably that of dog myocardium.

7. Decreased renal blood flow and urine production.

8. Decreased motility of the small intestine in cats.

9. Induced sedation when given to unanesthetized rabbits.

Findings 1,2 and 3 represent adenosine-induced negative chronotropy, dromotropy and inotropy, respectively, and have been experimentally and clinically confirmed repeatedly for the past sixty years. The enormity of Drury and Szent-Györgyi's work would provide the basis for a new field of biomedical research, that of purine physiology and pharmacology. As shown in Table I-1, a tremendous amount of diversity in physiological actions of adenosine is now appreciated. Analogous to many other hormone and neurotransmitter systems, much of this diversity can be explained by the existence of tissue-specific adenosine receptor subtypes (see below).

The purpose of this introductory chapter is to briefly examine the role of adenosine in myocardial function. Thus, I will consider: 1) Myocardial formation and metabolism of adenosine, 2) A general overview of receptor proteins through which the actions of adenosine are mediated, 3) The nature of the effects of adenosine on cardiovascular function with particular emphasis on the heart, and 4) Transduction mechanisms associated with cardiac adenosine receptor activation. Implicit in this thesis is that through a better understanding of the molecular nature of ligand interactions with cardiac adenosine receptors and of the latter with guanine nucleotide binding regulatory proteins, it may be possible to selectively modulate this system for therapeutic gain.

MYOCARDIAL FORMATION AND METABOLISM OF ADENOSINE. Adenosine is an ubiquitous extra- and intracellular nucleoside and, as such, is a participant in several metabolic pools (16). Three major pathways of myocardial adenosine formation have been described (17): 1) From 5′-AMP via the action of membrane-bound 5′-nucleotidase, 2) From 5′-AMP via the action of soluble 5′-nucleotidase and 3) From S-adenosylhomocysteine (SAH) via the action of S-adenosylhomocysteine hydrolase (SAH hydrolase).

Membrane-bound 5′-nucleotidase is the most important source of extracellularly-formed adenosine (18). Adenine nucleotides (ultimately AMP) which are substrates for membrane-bound 5′-nucleotidase are primarily derived from platelets, endothelial cells and/or vesicular release from nearby sympathetic terminals (18,19). Endothelial cells in heart also possess a membrane-bound 5-′nucleotidase which can contribute to myocardial adenosine formation under certain circumstances (18). However, cardiomyocytes appear the major source of adenosine formation and release in heart (18).

The dominant intracellular pathway of myocardial adenosine production is highly dependent on the metabolic state of the cell (17). Under normoxic conditions, very little intracellular adenosine is formed via the soluble 5′-nucleotidase pathway because the enzyme is strongly inhibited by normal cytoplasmic levels of ATP, ADP and creatine phosphate (17). The alternative pathway of intracellular adenosine production in heart involves SAH, a product of S-adenosyl-methionine-mediated transmethylation reactions (17, 20-22). Although

the equilibrium for SAH hydrolase lies far in the direction of SAH formation (17), significant intracellular adenosine is formed via this transmethylation pathway under normoxic conditions due to rapid product removal (see below).

During periods of hypoxia or increased workload, the cellular energy charge changes such that intracellular levels of ATP, ADP and creatine phosphate are decreased (17). The effect of this metabolic alteration is two-fold. Firstly, intracellular AMP levels rise rapidly which provides increased substrate for cytoplasmic 5'-nucleotidase. Secondly, inhibition of this enzyme by ATP, ADP and creatine phosphate is relieved. The result of these changes is that myocardial intracellular adenosine production via the soluble 5'-nucleotidase pathway increases dramatically (23-24). In contrast, flux through the transmethylation pathway is largely unaffected by the metabolic state of the myocyte (20).

The fate of intracellularly-formed adenosine is dependent on the relative activity of two enzymes (adenosine kinase and adenosine deaminase) and facilitated diffusion of the nucleoside into a extracellular compartment (18). Schrader's group has recently demonstrated that, under normoxic conditions, intracellular adenosine formed via the transmethylation pathway is rapidly shuttled back to ATP by a series phosphorylation reactions initiated by adenosine kinase (20). However, intracellular adenosine formed during hypoxia or increased workload is predominantly released into extracellular compartments (20). These homeostatic control mechanisms are likely to be very important in the modulation of myocardial responsiveness during periods of ischemia and/or catecholaminergic stimulation (25).

PURINE RECEPTORS. A major development in the field of purinoreceptor research occurred in 1970 when two groups working independently proposed the existence of cell-surface adenosine receptors based on the same observation: adenosine elevated cAMP formation in cerebral cortical slices and this effect was competitively antagonized by methylxanthines (26,27). Sir Geoffrey Burnstock later demonstrated that the effects of ATP could be separated from those of adenosine in the gastrointestinal tract and other tissues (28). This led Burnstock to suggest a classification scheme which divided purine receptors present in various tissues into P_1 and P_2 subtypes (29). P_1 receptors were those selective for adenosine and nucleoside congeners and antagonized by methylxanthines whereas P_2 receptors were selective for ATP and related nucleotides and not antagonized by methylxanthines (29). In addition, P_1 receptors (selective for adenosine) appear to require an intact ribose ring for agonist activity, whereas P_2 receptors do not (29). P_1 receptors were further subclassified when it was found that adenosine, acting through P_1 receptors, stimulated cAMP production is some tissues while inhibiting it in others (2,3,30). Thus, P_1 receptors which stimulate adenylyl cyclase activity are classified as R_a (or A_2) adenosine receptors and P_1 receptors which inhibit adenylyl cyclase activity are classified as R_i (or A_1) adenosine receptors. A_1/A_2 nomenclature is used throughout this thesis as it is now appreciated that physiological effects of adenosine are not strictly mediated through modulation of adenylyl cyclase activity (31). In addition to having opposing effects of

adenylyl cyclase activity, A_1 adenosine receptors are distinguished from A_2 receptors by the rank-order potency of agonist ligands (7). N^6-substituted agonists such as (*R*)-(phenylisopropyl)-adenosine [(*R*)-RIA], cyclopentyladenosine (CPA) and cyclohexyl-adenosine (CHA) bind with higher affinity to A_1 receptors than do non-N^6-substituted ligands such as 5′-N-(ethylcarboxamido)adenosine (NECA), 2-(phenylamino)adenosine (CV-1808) or 5′-N-(cyclopropylcarbox-amido)adenosine (CPCA,31). (*R*)-PIA is approximately 20-40-fold more potent at A_1 receptors than its less active diastereomer, (*S*)-(phenylisopropyl)adenosine [(*S*)-PIA] (31). In contrast, non-N^6-substituted analogs are more potent at A_2 receptors (31). Thus, one can summarize agonist rank-order potency at adenosine receptor subtypes as follows:

A_1 receptors: (*R*)-RIA = CPA > NECA > (*S*)-PIA >>> CV-1808.

A_2 receptors: NECA > CV-1808 > (*R*)-RIA > (*S*)-PIA > CPA.

Photoaffinity and crosslinking labeling methodology have been used to covalently incorporate agonist and antagonist radioligands into brain and adipocyte A_1 adenosine receptors (32-41). Covalent-ly labeled brain/adipocyte receptors migrate as a diffuse band on SDS-PAGE with a molecular weight of approximately 34-38 kDa. Degly-cosylation of the receptor before electrophoresis results in a reduction of the molecular weight of the labeled band to 32 kDa suggesting that the intact receptor is approximately 10% glycosylated (35,37). These molecular weight determinations have not been

corroborated by physical studies of A_1 receptors. Hydrodynamic studies performed to address physical properties of solubilized brain A_1 adenosine receptors are largely uninterpretable because the detergents used in these studies are unsuitable for such determinations (42-45). Recently, the rat brain A_1 adenosine receptor was purified to apparent homogeneity using affinity chromotography (46). The purified protein also migrated with a molecular weight of approximately 34 kDa, suggesting that this is indeed the molecular weight of the brain A_1 adenosine receptor. (46). However, in the absence of reliable hydrodynamic data, one cannot rule out the possibility of anomalous migration on SDS-PAGE or presence of a persistent artifact which may have given rise to inaccurate molecular weight estimates.

Most recently, the bovine striatal membrane A_2 adenosine receptor has been covalently radiolabeled using crosslinking methodology (47). The A_2 binding subunit migrated as a diffuse band on SDS-PAGE with an apparent molecular weight of approximately 45 kDa and the labeling displayed pharmacology appropriate for an A_2 receptor (47).

CARDIOVASCULAR EFFECTS OF ADENOSINE

VASODILATION. After the work of Drury and Szent-Györgyi (1), physiological research on adenosine and related compounds was almost non-existent until 1963 when Robert Berne noted that inosine and hypoxanthine, both of which are adenosine metabolites, were

released from ischemic myocardium (48). Berne proposed that adenosine formation served as a homeostatic control mechanism which matched local tissue flow to metabolic demand (48). The theory of Berne is now supported by a plethora of studies demonstrating that adenosine modulates blood flow in myocardial microcirculation in response to hypoxia (reviewed in 49) but may have little effect on blood flow under normoxic conditions (50,51). With the exception of kidney (52), adenosine has been demonstrated to produce vasodilation in the microcirculation of every organ or tissue in which the effects have been studied including brain (53), heart (54), smooth and skeletal muscle (53), adipose (55), gastrointestinal tract (56) and spleen (57). The rank-order potency of adenosine analogs to reduce coronary resistance (a measure of vasodilatory activity) in intact canine heart is consistent with an A_2-mediated event (58). As A_2 receptors are coupled to adenylyl cyclase in a stimulatory manner (see above), one may envision analogies between adenosine- and β_2 adrenergic receptor-induced vasodilation. However, experiments conducted with porcine carotid and canine coronary strips could not demonstrate adenosine-induced increases in cAMP formation at physiological concentrations of the nucleoside (59). Other mechanisms which have been suggested to underlie adenosine-induced vasodilation include inhibition of Ca^{++} flux, stimulation of Ca^{++} sequestration (60), attenuation of inositol phosphates accumulation (61) and A_1 receptor-mediated stimulation of particulate guanylate cyclase (62). Adenosine has been shown to indirectly produce vasodilation presynaptically (via A_1 receptor activation) by

attenuating catecholamine release from sympathetic terminals which innervate blood vessels (63).

NEGATIVE CHRONOTOPY. Negative chronotropic properties of adenosine were originally described by Drury and Szent-Györgyi (1). Adenosine depresses SA node activity and causes a "pacemaker shift." The first cells to activate during normal atrial impulse generation are the primary pacemaker cells of the SA nodal region (31). Under adenosinergic modulation, the site of impulse generation shifts toward the subsidiary pacemaker cells of the crista terminalis region (31). In addition, West and Belardinelli have shown that, at high concentrations, adenosine can cause complete SA exit block in rabbits (64). Considered together, the above findings indicate that pacemaker cells in the SA nodal region are exquisitely sensitive to the effects of adenosine. Although adenosine has potent effects on the action potentials of atrial and SA nodal cells, it does not affect impulse propagation in atrial tissue (31). Other pacemaker cells exhibiting sensitivity to the modulatory effects of adenosine have been described in the His bundle region and Purkinje fibers (see below) (31,65). The rank-order potency of adenosine analogs to produce atrial and/or ventricular negative chronotropy in both *in-vitro* and *in- situ* preparations is consistent with an A_1 receptor-mediated event (66-68).

NEGATIVE DROMOTROPY. Drury and Szent-Györgyi were also the first to demonstrate negative dromotropic properties of adenosine (1). Adenosine appears to directly affect function of the AV node (69). Belardinelli's group has shown that adenosine prolongs A $\rightarrow$ H

(*A*tria → Bundle of *H*is), but not H → V (Bundle of *H*is → *V*entricle), conduction time (70). The nature of adenosine-induced negative dromotropy has recently been more precisely defined as a direct depressant effect on AV nodal cell excitability: depression of amplitude, duration and rate of rise of AV nodal cell action potentials (71). Based on agonist rank-order potency profiles, an A_1 adenosine receptor mediates the negative dromotropic effect of the nucleoside (71). The pronounced sensitivity of conduction fibers to inhibition by adenosine may be explained, in part, by the finding that these cells possess a high density of A_1 adenosine receptors relative to cardiac myocytes (72).

The relative sensitivities of SA nodal, AV nodal, Hisian bundle or Purkinje fiber cells to the depressant effects of adenosine appears to be species-specific (1). The primary effect of adenosine on guinea pig heart is AV block, whereas sinus block is the predominant action in cat, dog and rabbit heart (1).

NEGATIVE INOTROPY. Adenosine produces a negative inotropic effect via A_1 receptor activation in both atrial and ventricular tissue (68,73-76). However, the response observed in the former is qualitatively distinct from that of the latter (31). In atria, adenosine reduces contractility directly and attenuates catecholaminergic-stimulated increases in contractility and adenylyl cyclase activity (77-79). Modulation of myocardial responsiveness to catecholaminergic stimulation has been referred to as the "anti-adrenergic" property of adenosine (31). In contrast, adenosine

does not directly reduce ventricular contractility, but does reverse that stimulated by catecholamines as well as attenuating catecholaminergic-stimulated adenylyl cyclase activity (80,81).

TRANSDUCTION MECHANISMS OF THE CARDIAC ADENOSINE RECEPTOR

Figure I-1 is a schematic diagram of transduction systems known to be associated with activation of cardiac adenosine receptors. Experimental evidence which forms the basis of this model is briefly summarized below.

ACTIVATION OF POTASSIUM CONDUCTANCE. Adenosine, acting through A_1 receptors, activates $^{42}K^+$ efflux in guinea pig atrial trabeculae (82) and $^{86}Rb^+$ efflux in whole guinea pig atria (H. Tawfik-Schlieper, personal communication). Adenosine has also been shown to activate a K^+ conductance in cardiac membrane patches analogous to that activated by muscarinic acetylcholine receptors in that the effect is GTP-dependent and exhibits pertussis toxin sensitivity and the channel shows inward rectification (83,84). Moreover, the effects of acetylcholine and adenosine on K^+ conductance are not additive (84). Both muscarinic acetylcholine and A_1 adenosine receptors couple to this type of K^+ channel via an interaction with a guanine nucleotide binding regulatory protein, presumedly, G_i (83,84). It has been suggested that A_1 adenosine receptor activation of this inward-rectifying, which results in cardiac myocyte hyperpolarization, is the molecular basis of

adenosine-induced negative chronotropy in atria (31,84). Although it is generally believed that similar mechanisms (activation of an inward-rectifying K^+ channel) are responsible for the effect of adenosine on AV nodal function (31), this has yet to be directly demonstrated.

INHIBITION OF ADENYLYL CYCLASE ACTIVITY. As discussed above and throughout this thesis, the adenosine receptor present in myocardium is of the A_1 subtype. A_1 adenosine receptors are coupled in an inhibitory manner to adenylyl cyclase in other tissues such as brain (reviewed in 7) and adipocytes (2). Overwhelming evidence indicates that adenosine directly inhibits adenylyl cyclase activity in atria (85-89, Leid et al., unpublished observations). However, adenosine-mediated inhibition of adenylyl cyclase in ventricular preparations is apparent only after prior stimulation of the enzyme by catecholamines or forskolin (80,81). As the latter observation closely parallels negative inotropic effects of adenosine in ventricular tissue, it appears that adenosine receptor-mediated inhibition of catecholamine-stimulated adenylyl cyclase activity may represent the molecular basis of the so-called antiadrenergic effect of adenosine (31). Isenberg and Belardinelli have shown that adenosine attenuates β adrenergic receptor-stimulated, but not basal, Ca^{++} influx in isolated ventricular myocytes (90). Therefore, it is likely that the negative inotropic properties of adenosine in ventricle are related to A_1 receptor-mediated inhibition of catecholamine-induced increases in cAMP formation, cAMP-dependent protein kinase activation, Ca^{++} channel

phosphorylation and Ca^{++} influx (31). However, a more direct effect of adenosine on Ca^{++} channel function, such as a G protein-dependent but adenylyl cyclase-independent pathway, cannot be excluded at the present time.

INHIBITION OF INOSITOL PHOSPHATES (IPx) FORMATION. Activation of A_1 adenosine receptors on rat pituitary GH_3 cells attenuates TRH-stimulated accumulation of inositol phosphates (91). This effect has also been demonstrated in rat cerebral cortical slices in which IP accumulation was stimulated by histamine (92,93). We have observed a similar effect in chick heart: adenosine analogs inhibited carbachol-stimulated IP accumulation in primary cultures of chick embryonic myocytes (Leid et al., unpublished data). The mechanism(s) responsible for this effect is (are) unknown but two candidate transduction pathways are: 1) A_1 adenosine receptor activation may lead to generation of excess G protein $\beta\gamma$ subunits which then bind to and inhibit activated G protein α subunits responsible for receptor-stimulated phospholipase C activity and IPx formation. Alternatively or additionally, 2) A_1 adenosine receptor activation may produce activated G protein α subunits which directly inhibit the catalytic activity of phospholipase C.

OBJECTIVES

The intent of these studies was to increase our understanding of molecular processes involved in ligand interactions with receptors mediating cardioinhibitory actions of adenosine and the interactions of these receptors with guanine nucleotide binding regulatory proteins.

Chapter II describes experiments in which an A_1-selective antagonist radioligand, [^{3}H]DPCPX, was used to label membrane-bound porcine atrial adenosine receptors. Salient features of this work are: 1) [^{3}H]DPCPX was shown to be the first useful antagonist radioligand for labeling cardiac adenosine receptors: [^{3}H]DPCPX bound to a homogeneous population of cardiac adenosine receptors with high affinity and a pharmacological profile consistent with that of an A_1 adenosine receptor, 2) The mechanism of [^{3}H]DPCPX binding to the membrane-bound receptor was consistent with that of a simple bimolecular interaction, 3) Agonist titration of [^{3}H]DPCPX binding in the absence of guanine nucleotide allowed quantification of two agonist affinity states of the cardiac adenosine receptor, and 4) Agonist titration of [^{3}H]DPCPX binding in the presence of guanine nucleotide suggested that the high agonist affinity state of the receptor was entirely due to formation of a ternary complex in porcine atrial membranes (agonist-receptor-G protein).

Chapter III describes studies done using an agonist radioligand, [^{125}I]HPIA, to label membrane-bound porcine atrial adenosine receptors. Noteworthy results of these experiments are: 1) [^{125}I]-

HPIA labeled a homogenous population of A_1 adenosine receptors which appeared to exist pre-coupled (in the absence of agonist) to a guanine nucleotide binding protein, 2) The association of [^{125}I]-HPIA with the membrane-bound cardiac adenosine receptor was via a simple bimolecular interaction, and 3) Guanine nucleotides negatively modulated [^{125}I]HPIA binding by increasing the rate of dissociation of the agonist radioligand. The latter finding provided direct evidence for the ternary complex formation in porcine atrial membranes.

Chapter IV details detergent solubilization of the porcine atrial adenosine receptor and characterization of agonist ([^{125}I]HPIA) radioligand interactions with this solubilized receptor. The most significant observations of this chapter are: 1) Solubilization of cardiac adenosine receptors using a mixed detergent system (digitonin/sodium cholate) resulted in a 2.5-fold enrichment of adenosine receptor specific activity over that of porcine atrial membrane preparations and a tremendously enhanced signal to noise ratio of [^{125}I]HPIA binding, 2) Both pharmacological specificity and receptor-G protein interactions were preserved in detergent solution, 3) [^{125}I]HPIA interacted via a simple bimolecular reaction with solubilized atrial adenosine receptors that existed precoupled to G protein(s), and 4) Guanine nucleotide-initiated [^{125}I]HPIA dissociation was biphasic and appeared to arise from independent, non-interconvertible populations of receptor-G protein complexes. Thus, kinetic evidence indicates that the atrial adenosine receptor is able to couple to two distinct G proteins in detergent solution.

FIGURE I-1

Schematic diagram of transduction mechanisms known to be associated with adenosine receptor activation. A_1 and A_2 represent currently defined adenosine receptor subtypes. G_i and G_s are guanine nucleotide binding regulatory proteins which couple receptors to adenylyl cyclase (C) in an inhibitory and stimulatory manner, respectively. G_x represents a guanine nucleotide binding regulatory protein of unknown identity which couples A_1 adenosine receptors to phospholipase C in an inhibitory manner. DAG and IP_3 represent diacylglycerol and inositol trisphosphate, respectively. P is a purine binding site intimately associated with adenylyl cyclase which mediates the inhibitory effects of intracellular purines on the activity of the enzyme. The physiological significance of the P site is unknown (7).

Adenosine Receptor Transduction and Effector Systems

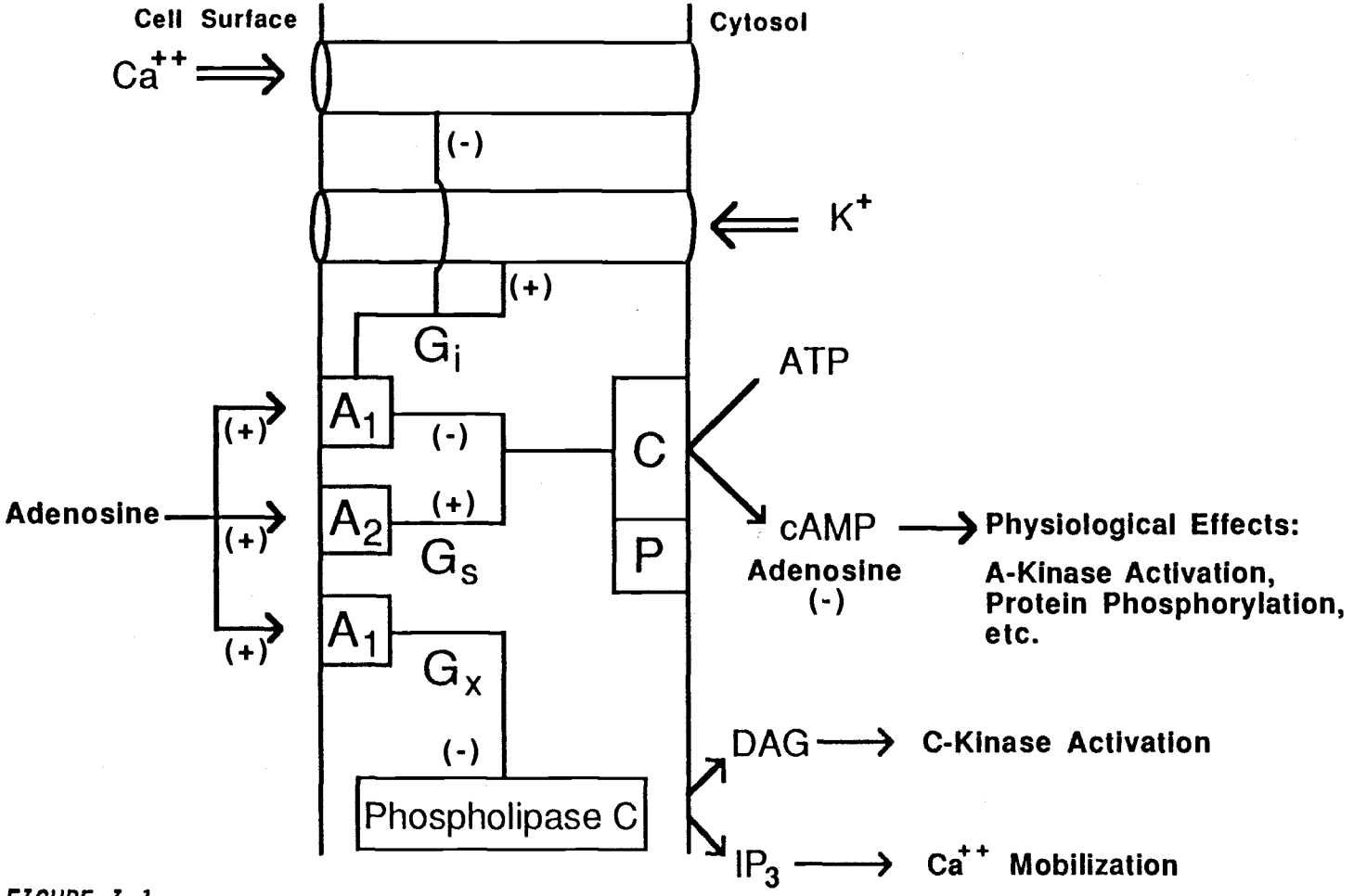

FIGURE I-1

TABLE I-1 Adenosine receptor distribution and physiological effects of the nucleoside. References given generally represent the original observation.

TISSUE/CELL	RESPONSE	REFERENCE
Adipocyte	Inhibition of lipolysis	2
Adrenals	Stimulation of steroidogenesis	3
Brain	Sedation	4
	Inhibition of transmitter release	5
	Anticonvulsant	6
Heart	Negative chronotropy	1
	Negative dromotropy	1
	Negative inotropy	1
Liver	Stimulation of gluconeogenesis	7
Lymphocytes	Inhibition of function	8
Mast cells	Enhancement of mediator release	9
Pancreas	Potentiation of glucagon release	10
Platelets	Inhibition of aggregation	11
Smooth muscle	Relaxation (except tracheal)	12 (13)
Striated muscle	Relaxation (centrally-mediated)	14
Testis	Unknown	15

CHAPTER II

Labeling of A_1 Adenosine Receptors in Porcine Atria with the Antagonist Radioligand 8-cyclopentyl-1,3[^{3}H]dipropylxanthine

ABSTRACT

The antagonist radioligand, 8-cyclopentyl-1,3-[^{3}H]dipropyl-xanthine ([^{3}H]DPCPX), has been used to label adenosine receptors in porcine atrial membranes. [^{3}H]DPCPX bound saturably, reversibly and with high affinity to an apparently homogenous population of receptors with a B_{max} of 32 ± 1 fmol/mg of protein and a K_D of (3.9 ± 0.5) x 10^{-10} *M*. A kinetically-derived dissociation constant (9.3 x 10^{-10} *M*) was in reasonable agreement with that parameter obtained from experiments conducted at equilibrium, assuming a simple bimolecular binding mechanism. Prototypic adenosine receptor agonists and antagonists inhibited [^{3}H]DPCPX binding in a manner consistent with the labeling of an A_1 adenosine receptor. Agonist, but not antagonist, titration curves yielded indirect Hill slopes significantly less than unity which were best described by a two-site model composed of high and low affinity states. However, in the presence of GTP (100 μM), these titration curves were monophasic and of low agonist affinity indicating that the high affinity component of agonist titration curves results from formation of a ternary complex consisting of agonist, adenosine receptor and G protein. [^{3}H]DPCPX appears to be the first useful antagonist radioligand for characterization of cardiac adenosine receptors.

ABBREVIATIONS

B_{max}, maximum binding capacity; 2-CADO, 2-chloroadenosine; CPA, N^6-cyclopentyladenosine; CV-1808, 2-phenylaminoadenosine; [^{3}H]DPCPX, 8-cyclopentyl-1,3[^{3}H]dipropylxanthine; K_D, equilibrium dissociation constant; k_{+1}, association rate constant; k_{-1}, dissociation rate constant; NECA, 5′-(N-ethylcarboxamido)-adenosine; *(R)*-PIA, N^6-(R-phenylisopropyl)adenosine; *(S)*-PIA, N^6-(S-phenylisopropyl)adenosine; τ and τ^{-1}, relaxation time and reciprocal relaxation time, respectively.

INTRODUCTION

Negative chronotropic properties of adenosine were initially described by Drury and Szent-Györgyi (1). Others have confirmed this finding and, in addition, adenosine has been shown to have negative inotropic and dromotropic properties in isolated atrial, ventricular or whole mammalian heart preparations (74,94). Cardioinhibitory responses of adenosine are believed to be mediated via an interaction with receptors of the A_1 subtype (95). Adenosine recognition sites in myocardial membrane preparations have been radiolabeled using high specific activity (^{125}I) agonist probes (94-96). Recently, intense interest has focused on development of highly selective A_1 receptor antagonists (94,97). Reports of A_1 adenosine receptor selectivity, relatively high specific activity (95-120 Ci/mmol) and antagonist properties contribute to make [^{3}H]DPCPX a potentially useful ligand for the characterization of cardiac adenosine receptors. The results of the present studies indicate that [^{3}H]DPCPX labels adenosine receptors in porcine atrial membranes with high affinity and a pharmacological profile consistent with that of an A_1 adenosine receptor. Kinetic experiments suggest that the interaction of [^{3}H]DPCPX with membrane-bound cardiac adenosine receptors is adequately described by a simple bimolecular binding mechanism. In addition, results of titration experiments have allowed the first quantification of multiple agonist affinity states of a cardiac adenosine receptor.

MATERIALS AND METHODS

[^{3}H]DPCPX (95 Ci/mmol) was purchased from Amersham (Chicago, IL). *(R)*- and *(S)*-PIA, NECA and adenosine deaminase were obtained from Boehringer-Mannheim (Mannheim, West Germany). Unlabeled DPCPX, CPA and CV-1808 were obtained from Research Biochemicals (Wayland, MA). GTP, theophylline, caffeine and CADO were from Sigma Chemical Company (St. Louis, MO) and CHA was obtained from Calbiochem (La Jolla, CA). Particularly insoluble adenosine analogs were initially dissolved in 100% DMSO and diluted to yield a final DMSO concentration of 0.5%. Therefore, all tubes in each experiment contained 0.5% DMSO.

MEMBRANE PREPARATION AND BINDING ASSAY. Porcine atrial membrane preparations were generously provided by Professor Michael I. Schimerlik of the Department of Biochemistry and Biophysics at Oregon State University. Membranes were prepared as previously described (98) yielding a P_3 fraction which was then incubated with adenosine deaminase (5 units/ml) for 30 minutes at 22°C and used directly in binding assays. Binding reactions were carried out at 18°C in volume of 250 μL which contained 25 m*M* imidazole buffer (pH 7.4) and 5 m*M* $MgCl_2$. Reactions were terminated by rapid filtration over Whatman GF/C filters using a Brandel Cell Harvester (Model M-24R, Brandel Instruments, Gaithersburg, MD). Filter strips were presoaked in 0.5% polyethyleneimine (Sigma) to reduce non-specific binding. Filter disks were allowed to elute overnight in 9ml Biocount Scintillation cocktail (Research Products

International Corp., Mount Prospect, IL) and then counted using a Beckman LS6800 scintillation counter at an efficiency of approximately 50%.

ANALYSIS OF BINDING DATA. Saturation data were analyzed by use of an iterative curve fitting routine, Lundon I Saturation Analysis Software (Lundon Software, Cleveland, OH). FITFUN on the PROPHET II system was used to analyze [^{3}H]DPCPX association rate experiments, fitting data to a monoexponential equation:

$$B = B_0(1 - e^{-t/\tau}) \qquad \text{(Eq. II-1)}$$

Where B_0 and B are the amount of [^{3}H]DPCPX bound at equilibrium and time t, respectively, and τ is the relaxation time for the single kinetic phase. Similarly, [^{3}H]DPCPX dissociation experiments were analyzed by fitting to a monophasic decay equation:

$$B = B_0 e^{-t/\tau} \qquad \text{(Eq. II-2)}$$

Competition experiments were analyzed using the iterative public procedure NEWFITSITES2 on the PROPHET system assuming a one-site model:

$$B = \frac{B_T}{1 + ([L]/IC_{50})^n} \qquad \text{(Eq. II-3)}$$

where B is the amount of [^{3}H]DPCPX bound, B_T is the total number of binding sites labeled by the [^{3}H]DPCPX in the absence of competing drug, IC_{50} is the concentration of competing ligand that inhibits 50% of [^{3}H]DPCPX specific binding, L is the concentration of competing ligand and *n* is the Hill coefficient. Agonist titration curves were also analyzed according to a two-site model:

$$B = \frac{B_1}{1 + ([L]/IC_{50(1)})} + \frac{B_2}{1 + ([L]/IC_{50(2)})} \qquad \text{(Eq. II-4)}$$

where B is the total amount of [^{3}H]DPCPX bound, B_1 and B_2 the amplitudes of each affinity state labeled by the [^{3}H]DPCPX, L is the concentration of competing ligand and $IC_{50(1)}$ and $IC_{50(2)}$ are the concentrations of competing ligand that inhibit 50% of the [^{3}H]DPCPX binding to each receptor state, respectively. Since this analysis assumes that the interaction of competitors with each receptor state obeys mass action principles, the Hill coefficients are assumed to be one.

The F value for comparing the two models was calculated from an analysis of residuals according to the equation:

$$F = \frac{(SS_1 - SS_2)/(df_1 - df_2)}{(SS_2/df_2)} \qquad \text{(Eq. II-5)}$$

where SS_1 and SS_2 are the residual sums of squares with corresponding degrees of freedom df_1 and df_2 associated with the simpler and more complex models, respectively.

The apparent K_D values for competitors were calculated from IC_{50} values using the method of Cheng and Prusoff (99):

$$K_D = \frac{IC_{50}}{1 + \frac{[D^*]}{K_{D*}}} \qquad \text{(Eq. II-6)}$$

where K_D is the equilibrium dissociation constant for the competitor (which is analogous to the K_I) and D^* and K_{D*} are the concentration and equilibrium dissociation constant of [^{3}H]DPCPX, respectively.

PROTEIN DETERMINATIONS. Aliquots of membrane suspension were dissolved in 0.5N NaOH and protein concentration determined by the method of Lowry et al. (100) using crystalline bovine serum albumin (Sigma) was used as the standard.

RESULTS

SATURATION ANALYSIS. [^{3}H]DPCPX bound saturably, reversibly and with high affinity to an apparently homogenous receptor population with a B_{max} of 32 ± 1 fmol/mg of protein and a K_D of (3.9 ± 0.4) x 10^{-10} *M* (Fig. II-1A). Transformation of saturation data generated a monophasic Scatchard-Rosenthal plot with nearly identical parameter estimates (Fig. II-1B) and a Hill plot with a slope of 1.03 ± 0.08 (data not shown). Specific binding of [^{3}H]DPCPX was approximately 80% of total binding at a ligand concentration equal to its K_D.

KINETIC ANALYSIS. To address the mechanism of [^{3}H]DPCPX binding to the membrane-bound porcine atrial membrane adenosine receptor, association rate experiments were conducted under pseudo-first order conditions at several radioligand concentrations (Fig. II-2A). Values of the reciprocal relaxation time (τ^{-1}) were obtained at each concentration of [^{3}H]DPCPX by fitting data to equation II-1. Values of τ^{-1} were then replotted vs. [^{3}H]DPCPX concentration (Fig. II-3) and the resultant plot analyzed by fitting with a weighted linear regression procedure which yielded a slope and y-intercept of (4.1 ± 0.7) x 10^7 M^{-1} min^{-1} and (3.8 ± 2.6) x 10^{-2} min^{-1}, respectively. Data points were weighted by the reciprocal of the standard error of τ^{-1} estimates to minimize the contribution of points with relatively large error to the fitting procedure (such as those estimates made at high [^{3}H]DPCPX concentrations). The slope and y-intercept

represent k_{+1} and k_{-1}, respectively, and can be used to calculate a kinetically-derived equilibrium dissociation constant of 9.3 x 10^{-10} *M*, assuming a simple bimolecular binding mechanism. This value is in reasonable agreement with that parameter obtained from equilibrium experiments (see above).

The value of k_{-1} was directly determined by addition of theophylline (final concentration of 1 m*M*) to an equilibrated mixture of [^{3}H]DPCPX and porcine atrial membranes (Fig. II-2B). These data were fitted using equation II-2 to determine k_{-1}. The experimentally-determined value for k_{-1} was (4.6 ± 0.2) x 10^{-2} min^{-1}, which was very similar to the value of this parameter obtained by extrapolation of the τ^{-1} vs. [[^{3}H]DPCPX] replot (see above).

TITRATION EXPERIMENTS. Several adenosine receptor ligands inhibited the specific binding of [^{3}H]DPCPX (Fig. II-4, Table II-1). Agonist rank order potency was (*R*)-PIA = CPA > CHA > (*S*)-PIA > NECA > CADO >> CV-1808. (*R*)-PIA was 18-fold more potent than its less active diastereomer, (*S*)-PIA. CV-1808, an A_2-selective ligand, was approximately 3-4 orders of magnitude less potent than other A_1-active ligands. Considered together, these findings are consistent with the labeling of an A_1 adenosine receptor in porcine atrial membranes. Indirect Hill slopes for agonist competition curves were consistently less than unity (Table II-1). These complex titration curves could be resolved into two phases using an iterative curve-fitting routine (Equation 2.4) and were found to correspond to high and low agonist affinity states.

Two-site modeling consistently provided a significant improvement in fit compared to that obtained from the one-site model (Table II-1). To test the hypothesis that the high affinity component of agonist titration curves arose from ternary complex formation and, thus, exhibited guanine nucleotide-sensitivity, CPA titration of [^{3}H]DPCPX was performed in the presence and absence of GTP (Fig. II-5, Table II-2). As above, CPA titration curves done in the absence of GTP were shallow and easily resolved into two phases. However, in the presence of GTP, CPA titration curves were monophasic (n_H = 0.90 ± 0.05) and of low agonist affinity. In the presence of GTP, the apparent K_D for CPA was very similar to the low affinity phase obtained by two-site modeling in the absence of GTP (13.8 ± 1.0 and 10 ± 3 n*M*, respectively). Therefore, biphasic agonist titration of [^{3}H]DPCPX binding appears to be the result of ternary complex formation in porcine atrial membranes.

Prototypic adenosine receptor antagonists also inhibited [^{3}H]DPCPX binding (Fig. II-6, Table II-1). Most notably, the potency with which unlabeled DPCPX displaced [^{3}H]DPCPX is consonant with saturation-derived affinity (0.5 and 0.4 n*M*, respectively). Indirect Hill slopes for all antagonist titration curves did not significantly differ from unity. Collectively, these findings provide further evidence that [^{3}H]DPCPX labels an adenosine receptor of the A_1 subtype in porcine atrial membranes preparations.

DISCUSSION

The number of recognition sites labeled by [^{3}H]DPCPX in myocardial membranes is virtually identical to that labeled by the iodinated adenosine receptor agonist [^{125}I]hyrodxyphenylisopropyl-adenosine (95,96). Likewise, the affinity with which [^{3}H]DPCPX labels these sites is very similar to that reported for rat brain A_1 adenosine receptors (97) and for DPCPX-mediated antagonism of *(R)*-PIA-induced inhibition of adenylate cyclase in adipocytes (101). Three additional findings are highly suggestive that the adenosine receptor of porcine atrial membranes labeled by [^{3}H]DPCPX is of the A_1 subtype: 1) The rank-order potency of adenosine agonists to inhibit the [^{3}H]DPCPX binding is consistent with that expected of an interaction at an A_1 receptor (102), 2) An A_2-selective ligand, CV-1808, is approximately 3-4 orders of magnitude less potent as an inhibitor of [^{3}H]DPCPX binding than other A_1-active ligands, and 3) CPA, *(R)*-PIA and CADO have been shown to dose- and GTP-dependently inhibit basal and forskolin-stimulated adenylate cyclase activity in this preparation (96). The latter finding provides functional evidence for the existence of A_1 adenosine receptors in porcine atrial membranes.

A_1 adenosine receptors have been shown to exist in two affinity states for agonists (103). Correspondingly, each agonist titration curve was significantly better described by a two- rather than a one-site model (Table II-1). However, agonist titration curves done in the presence of a guanine nucleotide were adequately described by

one-site modeling and no improvement in fit could be obtained by more complex fitting procedures. This finding is consistent with formation of a ternary complex in porcine atrial membranes which possesses high affinity for adenosine receptor agonists (104). Guanine nucleotides presumedly destabilize the complex resulting in component dissociation and an uncoupled receptor which has lower affinity for agonists (104). Accordingly, CPA titration curves done in the presence of GTP were monophasic and of low agonist affinity. In contrast, antagonists (such as [^{3}H]DPCPX) apparently do not differentiate between coupled and uncoupled receptors (104). This hypothesis is supported by monophasic [^{3}H]DPCPX saturation (Fig. II-2) and unlabeled antagonist titration experiments (Fig. II-6, Table II-1). The cardiac A_1 adenosine receptor appears to be similar to that of brain and adipocyte membranes in exhibiting two agonist affinity states, one of which is characterized as having high, guanine nucleotide-sensitive affinity for agonists.

Linear dependence of τ^{-1} on [^{3}H]DPCPX concentration suggests that this antagonist radioligand interacts with the porcine atrial A_1 adenosine receptor via a simple bimolecular binding mechanism of the type:

$$[^3\text{H}]\text{DPCPX} + R \underset{k_{-1}}{\overset{k_{+1}}{\rightleftharpoons}} [^3\text{H}]\text{DPCPX-R} \qquad \text{(Eq. II-7)}$$

which is described by the pseudo-first order rate equation:

$$\tau^{-1} = k_{+1}([^3\text{H}]\text{DPCPX}) + k_{-1} \qquad \text{(Eq. II-8)}$$

Such a hypothesis is further supported by: 1) Consistency between kinetically- and equilibrium-derived [^{3}H]DPCPX dissociation constants, and 2) An experimentally-determined k_{-1} (Fig. II-2B) which closely agreed with that obtained by extrapolation of the pseudo-first order plot (Fig. II-3). Thus, under these experimental conditions and over this range of radioligand concentration, the interaction of [^{3}H]DPCPX with membrane-bound porcine atrial A_1 adenosine receptors is adequately described by a simple bimolecular binding mechanism.

In summary, [^{3}H]DPCPX is the first useful antagonist radioligand for the characterization of cardiac adenosine receptors. The percentage of [^{3}H]DPCPX binding which is specific (80% at a concentration equal to its K_D) is far better than other radioligands commonly used in this tissue. The kinetics of [^{3}H]DPCPX association and dissociation appear to be relatively straightforward and easily quantified. Titration of [^{3}H]DPCPX by agonists has allowed the first demonstration and quantification of high and low agonist affinity states of a cardiac adenosine receptor. High affinity, selectivity, antagonist properties and a favorable signal to noise ratio of [^{3}H]DPCPX binding render this radioligand useful for further characterization of the cardiac adenosine receptor.

FIGURE II-1

A, [^{3}H]DPCPX saturation isotherm in a porcine atrial membrane preparation. Non-specific binding (not shown) was defined as that occurring in the presence of 100μM CADO and was approximately 80% of total binding at a ligand concentration equal to the K_D of [^{3}H]DPCPX. The curve shown is based on fitted parameter estimates obtained by non-linear regression analysis: B_{max} = 32 ± 1 fmol/mg protein, K_D = (4.0 ± 0.5) x 10^{-10} *M*.
B, Scatchard replot of saturation isotherm. The theoretical line drawn is based on parameter estimates obtained from linear regression analysis: B_{max} = 33 fmol/mg protein, K_D = 4.5 x 10^{-10} *M*.
Shown is an representative experiment done in duplicate.

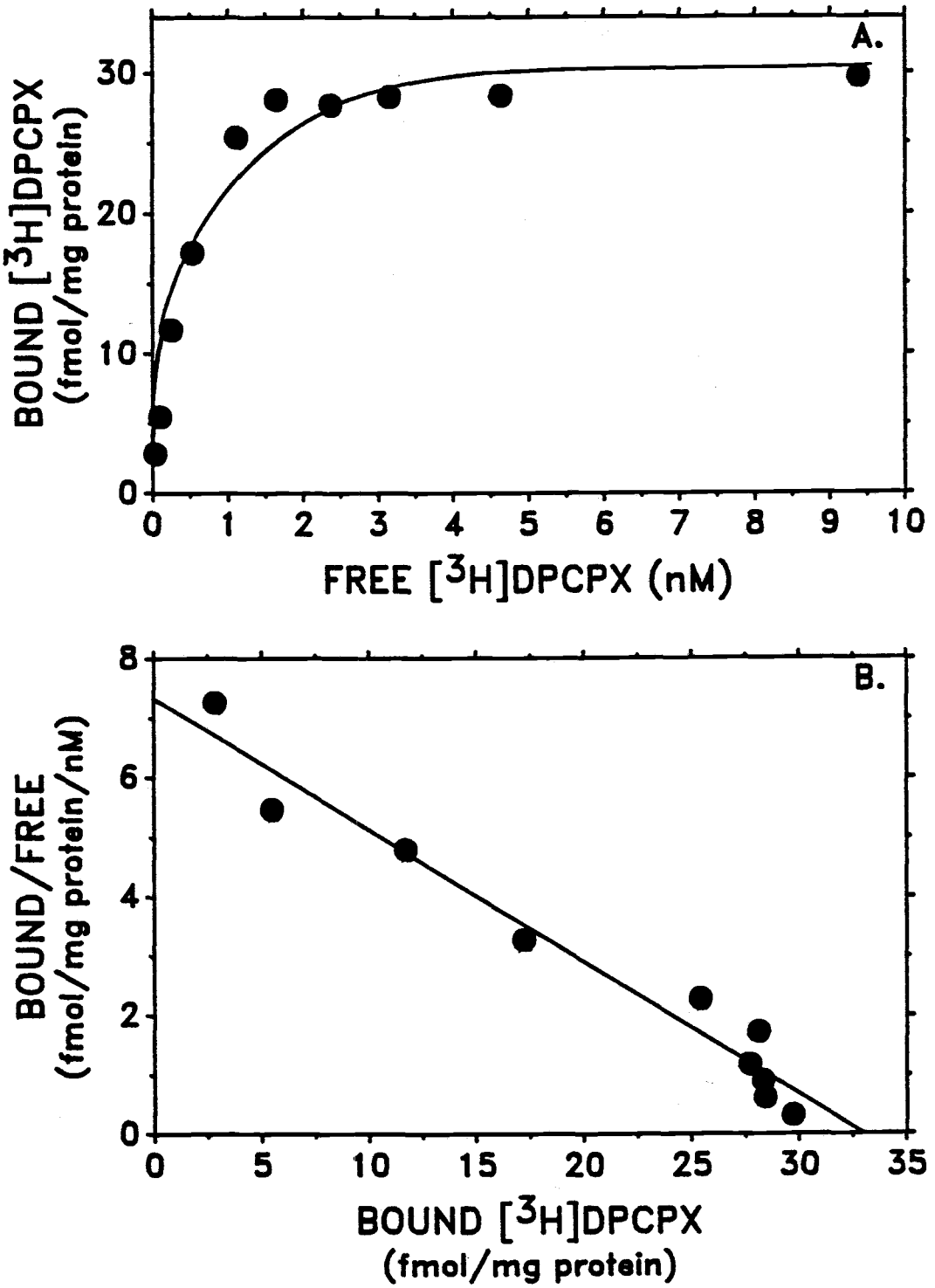
A.
BOUND [3H]DPCPX
(fmol/mg protein)
0
10
20
30
0 1 2 3 4 5 6 7 8 9 10
FREE [3H]DPCPX (nM)
B.
BOUND/FREE
(fmol/mg protein/nM)
0
2
4
6
8
0 5 10 15 20 25 30 35
BOUND [3H]DPCPX
(fmol/mg protein)

FIGURE II-1

FIGURE II-2

A, [^{3}H]DPCPX association experiment in a porcine atrial membrane preparation. [^{3}H]DPCPX and receptor concentrations were 2.1 n*M* and 50 p*M*, respectively, and the experiment was carried out at 22°C. The line drawn is based on parameter estimates obtained by fitting data with equation II-1 (τ^{-1} = [2.1 ± 0.1] x 10^{-1} min^{-1}). *B*, [^{3}H]DPCPX dissociation experiment in a porcine atrial membrane preparation. Theophylline (final concentration = 1 m*M*) was added to the above membrane preparation at t = 60 minutes and 250 μL samples were filtered at the times indicated. The line shown is based on parameter estimates obtained by fitting data with equation II-2 (k_{-1} = [4.6 ± 0.2] x 10^{-2} min^{-1}).

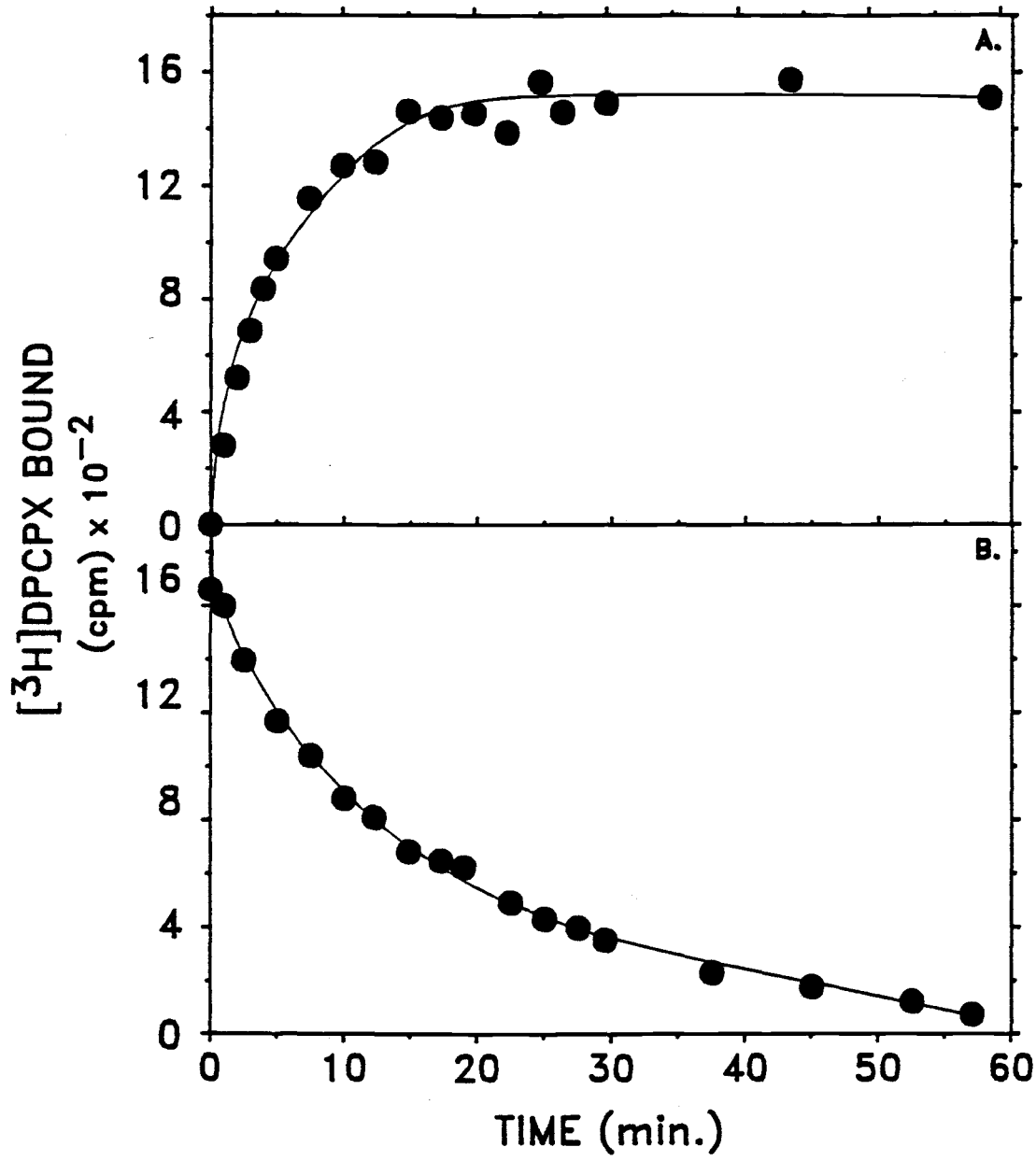
A.
B.
16
12
8
4
0
16
12
8
4
0
0
10
20
30
40
50
60
TIME (min.)
[3H]DPCPX BOUND
(cpm) x 10-2

FIGURE II-2

FIGURE II-3

Reciprocal relaxation time (τ^{-1}) as a function of [^{3}H]DPCPX concentration in porcine atrial membrane preparations. Association rate experiments were performed at several radioligand concentrations and τ^{-1} determined as described in the legend of Fig. II-2. The fit shown was determined by a weighted linear regression procedure which yielded a slope and intercept of (4.1 ± 0.7) x 10^7 M^{-1} min^{-1} and (3.8 ± 2.6) x 10^{-2} min^{-1}, respectively. These parameters correspond to k_{+1} and k_{-1}, respectively, and can be used to calculate a kinetically-derived K_D of 9.3 x 10^{-10} M. Data points were weighted by the reciprocal of the standard error of τ^{-1} estimates to minimize the contribution of points with relatively large error (such as those made at high [^{3}H]DPCPX concentrations) to the fitting procedure.

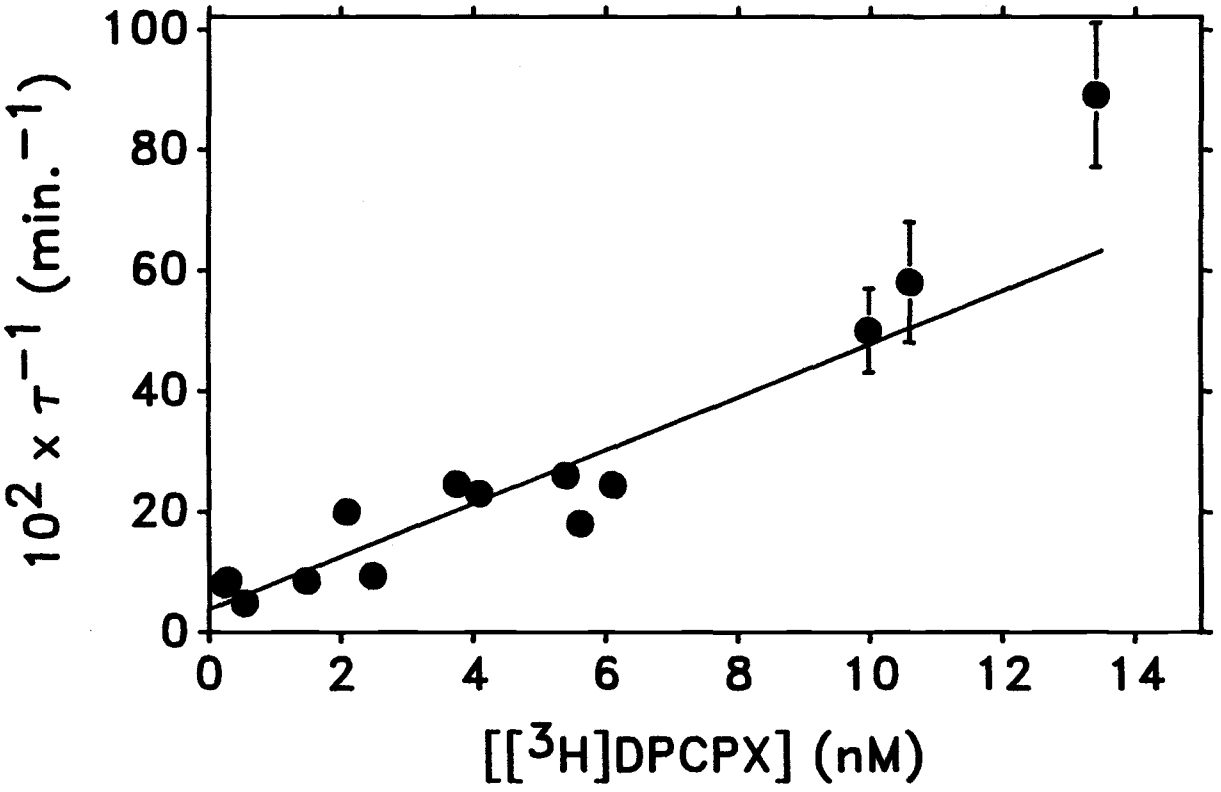

FIGURE II-3

FIGURE II-4

Agonist titration of [^{3}H]DPCPX binding in a porcine atrial membrane preparation. [^{3}H]DPCPX and receptor concentration were 2.8 n*M* and 50 p*M*, respectively. Curves drawn are based on theoretical one-site parameter estimates given in table II-1.

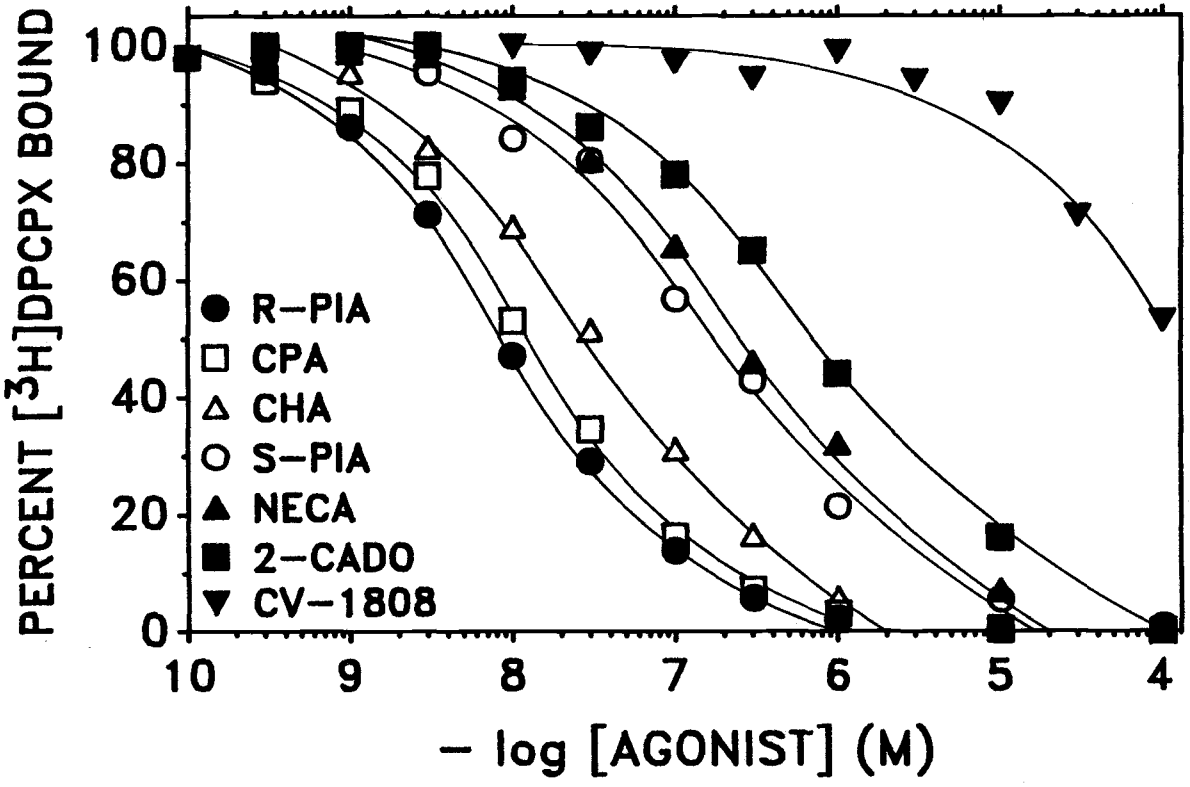
PERCENT [3H]DPCPX BOUND
100
80
60
40
20
0
10
9
8
7
6
5
4
– log [AGONIST] (M)
R–PIA
CPA
CHA
S–PIA
NECA
2–CADO
CV–1808

FIGURE II-4

FIGURE II-5

CPA titration of porcine atrial membrane [^{3}H]DPCPX binding in the presence (●) and absence (o) of 100 μM GTP. Experimental conditions are given in the legend of Fig. II-4. Curves drawn are based on theoretical parameter estimates given in Table II-2.

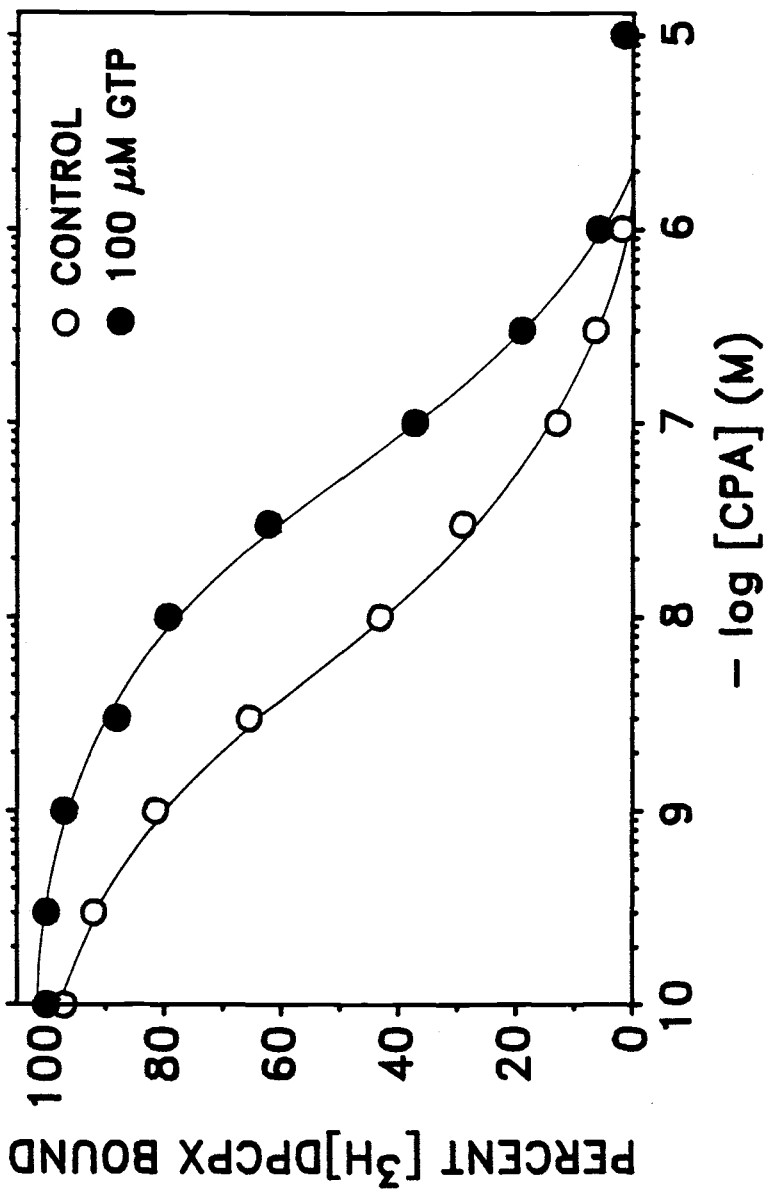
PERCENT [3H]DPCPX BOUND
100
80
60
40
20
0
10
9
8
7
6
5
− log [CPA] (M)
○ CONTROL
● 100 μM GTP

FIGURE II-5

FIGURE II-6

Antagonist titration of [^{3}H]DPCPX binding in a porcine atrial membrane preparation. Experimental conditions and the basis for theoretical curves shown are given in the legend of Fig. II-4. *Theo. = Theophylline.*

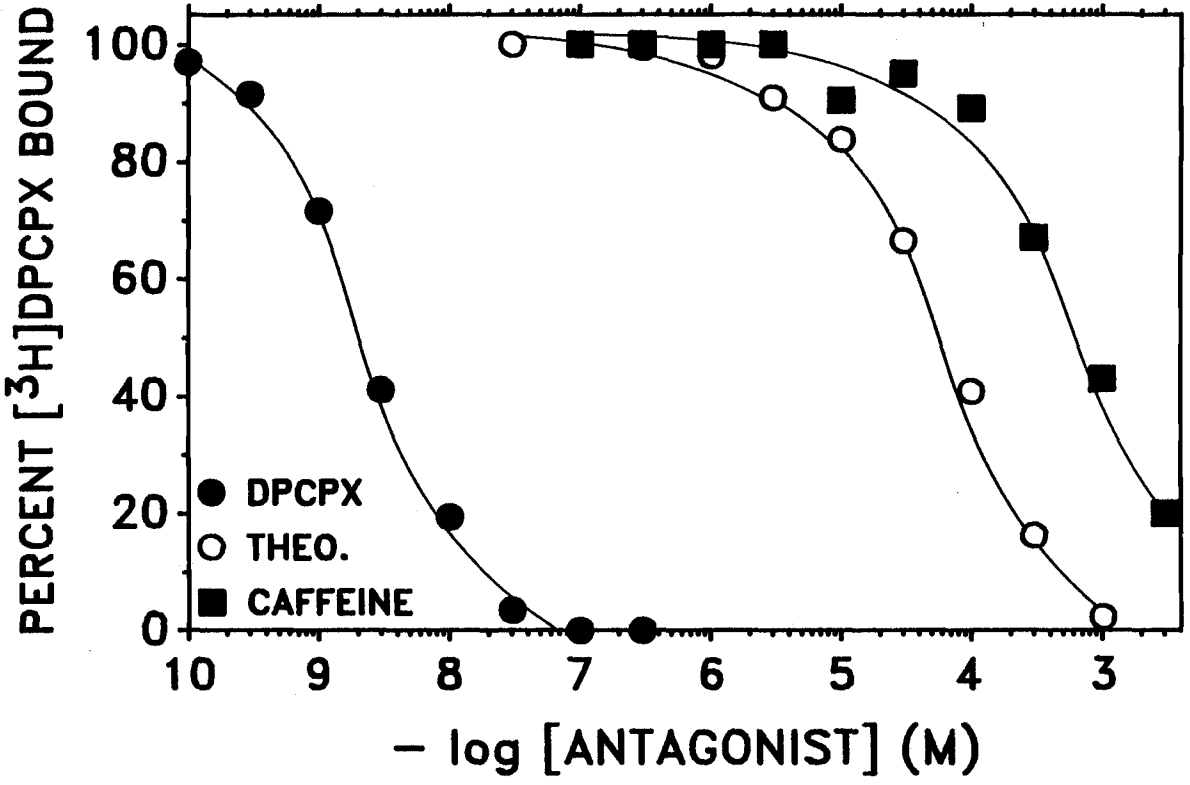
PERCENT [3H]DPCPX BOUND
100
80
60
40
20
0
DPCPX
THEO.
CAFFEINE
10
9
8
7
6
5
4
3
– log [ANTAGONIST] (M)

FIGURE II-6

TABLE II-1

Potency of adenosine analogs to inhibit specific binding of [^{3}H]DPCPX in porcine atrial membrane preparations. Experimental conditions were as described in the legend of Fig. II-4. Parameter estimates were determined by fitting data with Equations II-3, 4 and 5. F values for improvement in fit were calculated using Equation II-6. P values represent significance in the improvement of fit when comparing two- to one-site models.

TABLE II-1

COMPOUND	ONE-SITE		TWO-SITES					
			SITE 1		SITE 2			
	K_I (n*M*)	n_H	%	K_I (n*M*)	%	K_I (n*M*)	F	P
AGONISTS								
(*R*)-PIA	2.1 ± 0.1	0.79 ± 0.02	70 ± 4	1.0 ± 0.1	30 ± 4	12 ± 2	205	0.0001
(*S*)-PIA	38 ± 4	0.71 ± 0.04	38 ± 15	5.6 ± 4.2	62 ± 15	113 ± 50	12	0.008
CPA	2.9 ± 0.3	0.81 ± 0.04	69 ± 20	1.4 ± 0.6	31 ± 21	15 ± 13	8	0.02
CHA	7.5 ± 1.2	0.80 ± 0.05	46 ± 8	1.5 ± 0.6	54 ± 9	25 ± 6	49	0.0005
NECA	62 ± 8	0.71 ± 0.04	58 ± 5	15 ± 3	42 ± 5	428 ± 117	91	0.0001
CADO	167 ± 37	0.71 ± 0.06	40 ± 11	19 ± 12	60 ± 12	634 ± 306	11	0.01
CV-1808	> 10,000	---	---	---	---	---	--	---
ANTAGONISTS								
Theophylline	14,100 ± 1580	1.09 ± 0.08	---	---	---	---	--	---
Caffeine	160,000 ± 16100	0.92 ± 0.08	---	---	---	---	--	---
DPCPX	0.52 ± 0.24	1.16 ± 0.34	---	---	---	---	--	---

TABLE II-2. CPA titration of porcine atrial membrane [^{3}H]DPCPX binding in the presence and absence of 100 μM GTP. Experimental conditions are as described in the legend of Fig. II-4. Parameter estimates, F and P values were calculated as described in the legend of Table II-1.

COMPOUND	ONE-SITE		TWO-SITES					
			SITE 1		SITE 2			
	K_I (nM)	n_H	%	K_I (nM)	%	K_I (nM)	F	P
CPA (-) GTP	1.6 ± 0.2	0.72 ± 0.03	61 ± 6	0.5 ± 0.1	39 ± 7	10 ± 3	75	0.0001
CPA (+) GTP	13.8 ± 1.0	0.90 ± 0.05	---	---	---	---	--	NS

ACKNOWLEDGEMENTS

The authors thank Dr. Michael Schimerlik and co-workers for providing membrane preparations. M.L. is a Fellow of the American Foundation for Pharmaceutical Education. This work was supported by a grant from the Oregon Affiliate of the American Heart Association to T.F.M.

CHAPTER III

Characterization of Agonist Radioligand Interactions with Porcine Atrial A_1 Adenosine Receptors

ABSTRACT

The agonist radioligand (-)-N^6-[^{125}I]-p-hydroxyphenylisopropyladenosine ([^{125}I]HPIA) was used to characterize adenosine recognition sites in porcine atrial membranes. [^{125}I]HPIA showed saturable binding to an apparently homogenous population of sites with a maximum binding capacity of 35 ± 3 fmol/mg protein and a equilibrium dissociation constant of 2.5 ± 0.4 n*M*. Kinetic experiments were performed to address the molecular mechanism of [^{125}I]HPIA binding in porcine atrial membranes. [^{125}I]HPIA apparently interacts with the cardiac adenosine receptor in a simple bimolecular reaction. A kinetically-derived [^{125}I]HPIA dissociation constant (2.4 n*M*) was in good agreement with that parameter measured at equilibrium. Guanine nucleotides negatively modulated [^{125}I]HPIA binding by increasing its rate of dissociation. This finding is consonant with the formation of a ternary complex in porcine atrial membranes consisting of ligand, receptor and guanine nucleotide binding protein. Prototypic adenosine receptor agonists and antagonists inhibited specific binding in a manner consistent with the labeling of an A_1 adenosine receptor. The results of these experiments suggest that the adenosine receptor present in porcine atrial membranes as labeled by [^{125}I]HPIA is of the A_1 subtype.

ABBREVIATIONS

APNEA, N^6-2-(4-aminophenyl)ethyladenosine; B_{max}, maximum binding capacity; 2-CADO, 2-chloroadenosine; CPA, N^6-cyclopentyladenosine; CHA, N^6-cyclohexyladenosine; CV-1808, 2-phenylaminoadenosine; DMSO, dimethylsulfoxide; DPCPX, 8-cyclopentyl-1,3-dipropylxanthine; [^{3}H]DPCPX, 8-cyclopentyl-1,3[^{3}H]dipropylxanthine; DPX, 1,3-diethyl-8-phenylxanthine; Gpp(NH)p, Guanyl-5′-yl-imidodiphosphate; GTPγS, Guanosine-5′-(3-O-thio)-triphosphate; HPIA, N^6-(hydroxyphenylisopropyl)adenosine; [^{125}I]HPIA, N^6-3([^{125}I]-Iodo-4-hydroxyphenylisopropyl)adenosine; IBMX, 3-isobutyl-1-methylxanthine; K_D, equilibrium dissociation constant; K_I, inhibition constant; k_{+1}, association rate constant; k_{-1}, dissociation rate constant; NECA, 5′-N-(ethylcarboxamido)adenosine; PACPX, 1,3-dipropyl-8-(2-amino-4-chlorophenyl)xanthine; PMSF, phenylmethanesulfonyl fluoride; *(R)*-PIA, N^6-(R-phenylisopropyl)adenosine; *(S)*-PIA, N^6-(S-phenylisopropyl)adenosine; pSPT, 8-(p-sulfophenyl)theophylline; τ and τ^{-1}, relaxation time and reciprocal relaxation time, respectively.

INTRODUCTION

Adenosine has been identified as a putative neurotransmitter or neuromodulator in the central nervous system as well as a physiological regulator in several peripheral cell types (105,106). Effects of adenosine on the myocardium are uniformly inhibitory in nature (107). Negative chronotropy was among the first physiological effects ascribed to the endogenous nucleoside nearly six decades ago (1). Adenosine and its analogs also exert negative inotropic and dromotropic effects on isolated atrial, ventricular or whole mammalian heart preparations (66,68,74,94,108). Consonant with its modulatory role in other tissues (105,106), adenosine attenuates myocardial responsiveness to catecholaminergic stimulation (81,109). This may serve as an important regulatory mechanism as catecholaminergic stimulation has been shown to rapidly increase adenosine release from the myocardium (81). Physiological effects of adenosine on the isolated myocardium are competitively antagonized by xanthine derivatives, indicative of a receptor-mediated event (66,94,110).

Cardioinhibitory effects of adenosine are believed to be mediated via an interaction with adenosine receptors of the A_1 subtype (3). Three general lines of evidence support this hypothesis: 1) Agonist rank order potencies in *in-vitro* physiological studies are consistent with an A_1-mediated event (66,68,74). 2) Adenosine recognition sites in myocardial membranes have been directly radiolabeled using agonist probes [^{125}I]HPIA (95) and [^{125}I]aminobenzyladenosine (111) and an A_1-selective antagonist

probe [^{3}H]DPCPX (112,113). The rank order potency profile of agonists inhibiting specific binding of these radioligands is consistent with that of an A_1 adenosine receptor. 3) Activation of adenosine receptors on dispersed rat cardiac myocytes (85,87) or in guinea pig myocardial membranes (88) inhibits catecholamine-stimulated and basal adenylyl cyclase activity, respectively. This finding is consistent with the presumed A_1 nature of the cardiac adenosine receptor (106). Adenosine also activates a potassium conductance in cardiac membrane patches which is analogous to that activated by acetylcholine in that it shows inward rectification and pertussis toxin sensitivity (83,84). Both adenosine and acetylcholine receptors couple to this type of K^+ channel via an interaction with a guanine nucleotide binding protein, presumedly G_i (83,84). Activation of this K^+ channel may represent the molecular basis of adenosine-induced negative chronotropy (84). Adenosine also attenuates catecholaminergic-stimulated calcium conductance in bovine ventricular myocytes voltage-clamped in the whole cell configuration (90). Whether this is related to adenosine-mediated inhibition of adenylyl cyclase activity or coupling of cardiac adenosine receptors to calcium channels is unknown.

The objective of the present study was threefold: 1) To determine if porcine atria represent an acceptable model for the characterization of cardiac adenosine receptors in terms of density and pharmacological specificity, 2) To directly address the kinetic mechanism of binding of an adenosine receptor agonist radioligand

and, 3) To assess the influence of guanine nucleotides on agonist equilibrium binding and dissociation kinetics. The results of our pharmacological characterization suggest that the porcine atrial adenosine receptor labeled by [^{125}I]HPIA is of the A_1 subtype. The kinetics of [^{125}I]HPIA binding were consistent with those expected for a simple bimolecular reaction. The homogenous population of cardiac adenosine receptors labeled by [^{125}I]HPIA presumably represents binding to the high affinity form of the receptor as [^{125}I]HPIA binding is sensitive to negative modulation by guanine nucleotides. Thus, the porcine atria may represent a suitable model for further characterization of cardiac adenosine receptors.

MATERIALS AND METHODS

[^{125}I]HPIA (1800-2200 Ci/mmol) was purchased from Amersham (Chicago, IL). (*R*)- and (*S*)-PIA, NECA, HPIA, GTPγS, Gpp(NH)p, GDP, GMP, PMSF and adenosine deaminase were from Boehringer Mannheim (Mannheim, West Germany). CPA, CV-1808, DPCPX, PACPX, and pSPT were obtained from Research Biochemicals, Inc. (Wayland, MA). CHA, IBMX and DPX were from Calbiochem (La Jolla, CA). 2-CADO, theophylline, caffeine and GTP were obtained from Sigma Chemical Company (St. Louis, MO). Ultrapure DMSO was obtained from Pierce Chemical Company (Rockford, IL). APNEA was synthesized by the method of Stiles et al. (32).

MEMBRANE PREPARATION AND EXPERIMENTAL PROTOCOL. Membranes used in all binding assays were prepared as previously described (98). Immediately prior to binding assays, this P3 fraction was resuspended at a protein concentration of 1-2 mg/mL and incubated with 5 units/mL adenosine deaminase for 30 minutes at 22°C. Adenosine deaminase-treated homogenates were used directly in binding assays.

All binding experiments were carried out at 37°C in a final volume of 0.25 mL containing 25 m*M* imidazole (pH 7.4), 5 m*M* $MgCl_2$ and 0.3-0.5 mg membrane protein. Non-specific binding was defined as that occurring in the presence of 100 μ*M* (*R*)-PIA, 100 μ*M* 2-CADO or 1 m*M* theophylline (which gave identical values). Concentrated stock solutions of insoluble adenosine receptor agonists and antagonists were prepared in 100%

ultrapure DMSO which were diluted such that the final concentration of DMSO in binding assays was 0.5%. Therefore, all binding experiments (except those with guanine nucleotides) were carried out in 0.5% DMSO. Equilibrium binding experiments were carried out for 90-120 minutes and terminated by rapid filtration over GF/C filters using a Brandel Cell Harvester (M-24R, Gaithersburg, MD). GF/C filters were presoaked in 0.5% polyethyleneimine to reduce non-specific binding. Kinetic experiments were carried out for varying time intervals and terminated similarly. Additional saturation isotherms were carried out using the dilution method of Green (114). Filter-trapped radioactivity was quantified by use of a Beckman 4000 gamma counter at a counting efficiency of 75%. Protein concentration determined by the method of Lowry et al. (100).

DATA ANALYSIS. Saturation data were analyzed using Lundon I Saturation Analysis Software (Lundon Software, Cleveland, OH). Agonist, antagonist and guanine nucleotide titration experiments were also analyzed using an iterative curve-fitting procedure (EBDA (Elsevier-Biosoft, Cambridge, UK) assuming a one-site model:

$$B = \frac{B_T}{1 + ([L]/IC_{50})^n} \qquad \text{(Eq. III-1)}$$

where B is the amount of [^{3}H]DPCPX bound, B_T is the total number of binding sites labeled by the [^{3}H]DPCPX in the absence of competing drug, IC_{50} is the concentration of competing ligand that inhibits 50% of [^{3}H]DPCPX specific binding, L is the concentration of competing ligand and n is the Hill coefficient. The apparent

K_D values for competitors were calculated from IC_{50} values using the method of Cheng and Prusoff (99).

Association rate experiments were analyzed by linear transformation of binding data to a natural logarithm plot:

$$\ln ([B_{eq} - B_t]/[B_{eq}]) = -t/\tau \qquad \text{(Eq. III-2)}$$

where B_{eq} and B_t are the amounts of [^{125}I]HPIA specifically bound at equilibrium and time t, respectively. Fitting kinetic data to this equation generates a plot with a slope corresponding to $(-)\tau^{-1}$, the reciprocal relaxation time.

[^{125}I]HPIA dissociation experiments were analyzed by fitting data to mono-:

$$B = B_0 e^{-t/\tau} \qquad \text{(Eq. III-3)}$$

or biexponential:

$$B = B_1 e^{-t/\tau_1} + B_2 e^{-t/\tau_2} \qquad \text{(Eq. III-3)}$$

decay equations using an iterative curve fitting routine (KINETIC, ELSEVIER-BIOSOFT). For the monoexponential equation, B_0 and B are the amounts of [^{125}I]HPIA bound at equilibrium and time t, respectively, and τ is the relaxation time for the single kinetic phase. Similarly, for the biexponential equation, B is the amount of [^{125}I]HPIA bound at time t, and $B_{1,2}$ and $\tau_{1,2}$ are the amplitude and relaxation time for each kinetic phase, respectively.

RESULTS

SATURATION ANALYSIS. [^{125}I]HPIA bound saturably, reversibly and with high affinity to an apparently homogenous population of recognition sites with a B_{max} of 35 ± 3.0 fmol/mg protein and a K_D of 2.5 ± 0.4 n*M* (Fig. III-1A). Parameter estimates for a two-site model could not be obtained for these data using an iterative curve fitting routine (Lundon I). A Scatchard-Rosenthal replot of saturation data was monophasic in the concentration range of [^{125}I]HPIA employed (Fig. III-1B inset). It was not possible to exceed the maximal concentration shown (approximately 4 n*M*) due to high levels of non-specific binding with attendant unfavorable signal to noise ratios. At a ligand concentration equal to its K_D approximately 35% of total [^{125}I]HPIA binding was specific. A Hill plot of saturation data yielded a slope of 1.0 ± 0.1 and an apparent K_D of 2.5 ± 0.6 n*M* (data not shown). At the concentrations of radioligand used, this binding presumably represents the labeling of the high affinity state of the porcine atrial adenosine receptor. Additional saturation experiments were performed using the dilution method of Green (114) to achieve greater fractional occupancy of adenosine receptors in equilibrium binding experiments. The binding of a fixed concentration of [^{125}I]HPIA (0.2 n*M*) was determined in the presence of 0.2 to 20 n*M* unlabeled HPIA in these experiments. Under these conditions, HPIA labeled a single population of recognition sites with a B_{max} of 49.1 ± 2.2 fmol/mg protein and a

K_D of 7.4 ± 0.8 n*M* (Fig. III-2A). A Scatchard-Rosenthal replot of these data was monophasic over this expanded concentration range (Fig. III-2B inset). A Hill plot of these data yielded a slope of 1.09 ± 0.07 and an apparent K_D of 7.7 ± 0.4 n*M* (data not shown). Moreover, parameter estimates for a two-site model could not be obtained from these data using an iterative curve-fitting procedure (Lundon I). Therefore, a one-site model adequately described [^{125}I]HPIA equilibrium binding isotherms in all saturation experiments.

KINETIC EXPERIMENTS. Kinetic experiments were undertaken to address the mechanism of [^{125}I]HPIA binding in porcine atrial membranes. In order to maintain pseudo-first order reaction conditions, ligand concentrations employed were always five-fold greater than that of receptor (approximately 50 p*M*). Values of τ^{-1} was determined at several ligand concentrations (Fig. III-3A) and plotted versus [^{125}I]HPIA concentration (Fig. III-3B). The latter plot was linear (R^2 = 0.99) with a slope of (1.9 ± 0.1) x 10^7 M^{-1} min^{-1} and a y-intercept of (4.5 ± 0.2) x 10^{-2} min^{-1}. These parameters represent k_{+1} and k_{-1}, respectively. Dividing k_{-1} by k_{+1} yields a kinetically-derived K_D of 2.4 n*M* which is in excellent agreement with that parameter determined in equilibrium binding experiments (2.5 ± 0.4 n*M*, above and Fig. III-1). The dependence of τ^{-1} on [^{125}I]HPIA concentrations greater than 4 n*M* could not be determined due to diminished signal to noise ratios.

GUANINE NUCLEOTIDE EXPERIMENTS. To determine the effects of guanine nucleotides on [^{125}I]HPIA dissociation kinetics, dissociation of [^{125}I]HPIA was initiated by addition of 2-CADO (100 μM), GTP (300 μM) or the combination of 2-CADO and GTP to an equilibrated incubate (Fig. III-4). [^{125}I]HPIA dissociation induced by 2-CADO was described by a monoexponential yielding a k_{-1} of (1.6 ± 0.2) x 10^{-2} min^{-1}. However, biphasic dissociation kinetics were observed when dissociation was initiated by simultaneous addition of 2-CADO and GTP. Initially, a rapid dissociation occurred in which approximately 66 ± 9% of specifically bound [^{125}I]HPIA dissociated yielding a k_{-1R} of 1.2 ± 0.1 min^{-1}. This burst phase was followed by a slower dissociation (k_{-1S} = [1.5 ± 0.2] x 10^{-2} min^{-1}) which was estimated to account for the remaining 34 ± 2% [^{125}I]HPIA specifically bound. The mean value for k_{-1S} is nearly identical to the off-rate determined by addition of 2-CADO in the absence of GTP. Finally, dissociation initiated by addition of 300 μM GTP alone occurs very rapidly (k_{-1} = 1.3 ± 0.13 min^{-1}) and is essentially complete within one minute. Approximately 53 ± 6% of specifically bound [^{125}I]HPIA was sensitive to dissociation induced by GTP alone. Both the rate and extent of [^{125}I]HPIA dissociation initiated by GTP were very similar to that observed in the rapid phase of dissociation induced by the combination of 2-CADO and GTP. These kinetic data are consistent with the formation of a ternary complex in porcine atrial membranes consisting of ligand, receptor and guanine nucleotide binding protein which possesses high affinity for

agonists. GTP presumedly causes a dissociation of this complex resulting in loss of high affinity agonist binding sites (104). The affinity of the guanine nucleotide binding protein-uncoupled receptor for [^{125}I]HPIA would appear to be sufficiently low such that this interaction could not be measured by the methodology employed (rapid filtration).

To further characterize guanine nucleotide modulation of [^{125}I]HPIA binding in porcine atrial membranes, titration experiments for several guanine nucleotides were performed. Guanine nucleotides negatively modulated specific binding of [^{125}I]HPIA in porcine atrial membranes with the following rank order potency: Gpp(NH)p > GTPγS > GDP = GTP >> 5′-GMP (Fig. III-5). 5′-GMP was essentially ineffective as a negative modulator of [^{125}I]HPIA binding in concentrations up to 3 m*M*. With the exception of GTPγS, maximal inhibition of [^{125}I]HPIA binding by guanine nucleotides was approximately 75%. GTPγS, however, inhibited 100% of [^{125}I]HPIA specific binding. These data provide further evidence for the formation of a ternary complex in porcine atrial membranes which is sensitive to negative modulation by guanine nucleotides.

AGONIST AND ANTAGONIST TITRATION EXPERIMENTS. In order to address the pharmacological specificity of the porcine atrial adenosine receptor, the rank order potency profile for a series of adenosine receptor ligands as inhibitors of [^{125}I]HPIA binding was determined (Fig. III-6A and B, Table III-1). CPA and (*R*)-PIA were the most potent inhibitors of [^{125}I]HPIA binding in porcine

atrial membranes. *(R)*-PIA was 22-fold more potent than its diastereomer *(S)*-PIA. CV-1808, an adenosine A_2 receptor-selective ligand, was approximately three orders of magnitude less potent than A_1-active ligands. Overall adenosine receptor agonist rank order potency was as follows: CPA $\geq$ *(R)*-PIA > HPIA $\geq$ CHA > APNEA > NECA $\geq$ *(S)*-PIA > 2-CADO >> CV-1808. This agonist rank order potency profile is consistent with the labeling of an A_1 adenosine receptor in porcine atrial membranes. With the exception of HPIA and CV-1808, indirect Hill slopes for agonist competition curves did not differ significantly from unity.

Prototypic adenosine receptor antagonists inhibited the binding of [^{125}I]HPIA in porcine atrial membranes (Fig. III-7, Table III-1). DPCPX and PACPX, adenosine A_1-selective ligands, were the most potent antagonist inhibitors of [^{125}I]HPIA specific binding. DPCPX was approximately 10-fold more potent as an inhibitor of [^{125}I]HPIA specific binding than PACPX. Overall rank order potency of antagonists inhibiting the binding of [^{125}I]HPIA in porcine atrial membranes was as follows: DPCPX > PACPX > IBMX > DPX > pSPT > Theophylline > Caffeine. Indirect Hill slopes for DPCPX and IBMX were unexpectedly but reproducibly less than unity. The reasons for this observation are unclear. Interestingly, these compounds represent two of the most lipophilic adenosine receptor ligands used in these experiments.

DISCUSSION

The number of porcine atrial membrane recognition sites labeled by [^{125}I]HPIA is very similar to that previously reported for the adenosine receptor antagonist [^{3}H]DPCPX (35 ± 3 and 32 ± 1 fmol/mg protein, respectively) (113). At the concentrations of radioligand employed in the present study, [^{125}I]HPIA labeled only the high affinity state of the adenosine receptors. Thus, the labeling of equivalent numbers of recognition sites in porcine atrial membranes by [^{125}I]HPIA and [^{3}H]DPCPX suggests that the inclusion of 5 m*M* $MgCl_2$ in the incubate and carrying the reaction out at 37°C resulted in a quantitative conversion of adenosine receptors from a low to a high affinity state. This was also demonstrated using a dilution procedure for equilibrium saturation experiments. Employing concentrations of HPIA up to 20 n*M*, we were unable to detect a second, presumably lower affinity recognition site. Thus, under these incubation conditions, [^{125}I]HPIA apparently labels the high affinity recognition state of the porcine atrial adenosine receptor.

The relationship between τ^{-1} and [^{125}I]HPIA concentration has not previously been evaluated. The demonstration of a linear dependence of τ^{-1} on [^{125}I]HPIA concentration suggests a simple bimolecular association reaction. From these data it may be inferred that under the assay conditions employed the porcine atrial A_1 adenosine receptor population exists precoupled with a G protein. However, the possibility of a ligand-induced isomerization

of the porcine atrial adenosine receptor cannot be completely excluded at the present time. Such a phenomenon would yield values of τ^{-1} which were hyperbolically dependent on [^{125}I]HPIA concentration (115-118). In the present study, concentrations of [^{125}I]HPIA employed in association experiments may have generated τ^{-1} values which merely represented the initial linear phase of a rectangular hyperbola. To more rigorously characterize such a possibility would require use of [^{125}I]HPIA concentrations considerably higher than those employed. Unfortunately, use of [^{125}I]HPIA concentrations greater than 4.0 n*M* severely compromises the signal to noise ratio and therefore were not feasible. Nonetheless, excellent agreement exists between saturation- and kinetically-derived affinities assuming a simple bimolecular reaction.

Guanine nucleotides negatively modulated the specific binding of [^{125}I]HPIA in porcine atrial membranes in both kinetic and equilibrium experiments (Figs. III-4 and 5). This is consistent with guanine nucleotides and adenosine receptor agonists participating in negative heterotropic binding interactions (104). Simultaneous addition of GTP and 2-CADO to agonist-occupied receptors resulted in a very rapid dissociation of [^{125}I]HPIA followed by a slow terminal dissociation with a rate constant nearly identical to that measured when dissociation was initiated by addition of 2-CADO alone. Dissociation initiated by addition of GTP (300 μM) was characterized by a similar burst phase but lacked a terminal (slow) dissociation phase. Approximately 53% of specifically bound

[^{125}I]HPIA rapidly dissociated upon addition of this concentration of GTP. This finding was not unexpected as the concentration of GTP used in these experiments approximated its IC_{50} as a negative modulator of [^{125}I]HPIA binding in equilibrium experiments.

In studies carried out at equilibrium, Gpp(NH)p and GTPγS were observed to be the most potent negative modulators of [^{125}I]HPIA binding in porcine atrial membranes (Fig. III-5). GTP and GDP were essentially equipotent and 5′-GMP was devoid of efficacy as a modulator of [^{125}I]HPIA binding. The finding that GTP and GDP were equipotent may be related to the GTPase activity of porcine atrial membranes. These experiments were carried out at 37°C in 5 m*M* $MgCl_2$ with a high protein concentration (300-500 μg protein/assay tube) and without a GTP regenerating system. These incubation conditions may contribute to low negative modulatory potencies which were observed for hydrolyzable guanine nucleotides. With the exception of GTPγS, maximal inhibition of [^{125}I]HPIA binding was approximately 75-80%. The remaining 20-25% of [^{125}I]HPIA bound is insensitive to negative modulation by guanine nucleotides. The reasons for this insensitivity are not known but may involve diffusional barriers within the membrane creating a subpopulation of high affinity agonist recognition sites which are inaccessible to guanine nucleotides. The finding that GTPγS inhibits 100% of [^{125}I]HPIA binding was unique and possibly related to differing partitioning properties for this non-hydrolyzable ligand.

Adenosine agonists inhibited the specific binding of [^{125}I]HPIA in a manner consistent with the labeling of an A_1 adenosine receptor (Fig. III-6A and B, Table III-1 [102,119]). This hypothesis is supported by the rank order potency of adenosine analogs as inhibitors of [^{125}I]HPIA binding ((*R*)-PIA > NECA ≥ (*S*)-PIA), the finding that CV-1808 (an A_2-selective ligand) is approximately three orders of magnitude less potent than other A_1-active ligands and the potency of A_1-selective antagonists as inhibitors of the specific binding of [^{125}I]HPIA (see below). The cardiac adenosine receptor derived from porcine atria appears to be similar to that of bovine ventricular origin in that the potency of N^6-substituted agonists is enhanced over that of non-N^6-substituted agonists (NECA and (*S*)-PIA are essentially equipotent) (112).

Adenosine receptor antagonists were also useful in the classification of the porcine atrial membrane adenosine receptor. DPCPX and PACPX were the most potent inhibitors of [^{125}I]HPIA binding (DPCPX was approximately 10-fold more potent than PACPX). However, a discrepancy exists between the apparent K_D of DPCPX as an inhibitor of [^{125}I]HPIA binding and either its K_D from [^{3}H]DPCPX saturation experiments or its K_I as an inhibitor of [^{3}H]DPCPX binding in the same tissue (2.4 ± 0.2 vs. 0.4 ± 0.05 or 0.5 ± 0.2 n*M*) (113). This inconsistency is most likely due to incubation conditions of the competition experiments (5 m*M* $MgCl_2$). Yeung and coworkers observed decreased potency (2-10 fold) of IBMX as an inhibitor of [^{3}H](*R*)-PIA binding in cholate-

solubilized rat brain membranes when competition experiments were carried out in the presence of $MgCl_2$ (45). $MgCl_2$ (3 m*M*) increased the amount of [^{3}H]*R*-PIA bound and the affinity of adenosine receptors for this agonist (45). Mg^{++} apparently promotes and/or stabilizes the formation of the ternary complex (104). Therefore, in the presence of 5 m*M* $MgCl_2$, the potency of antagonists as inhibitors of [^{125}I]HPIA binding may be reduced over that observed in its absence.

In summary, radioligand binding experiments suggest that the adenosine receptor present in porcine atrial membranes is of the A_1 subtype. [^{125}I]HPIA appears to label a single population of high affinity recognition sites. The mechanism of [^{125}I]HPIA binding to porcine atrial membrane adenosine receptors is apparently a simple bimolecular reaction. Cardiac adenosine receptors are similar to other rhodopsin-like hormone and neurotransmitter receptors in that agonist binding is subject to negative heterotropic regulation by guanine nucleotides. Thus, porcine atria appear to represent an acceptable model for further characterization of cardiac adenosine receptors.

FIGURE III-1

A, [^{125}I]HPIA saturation isotherm in porcine atrial membranes. Non-specific binding was defined as that occurring in the presence of 100 μM (*R*)-PIA. The fit shown was obtained using Lundon I Saturation Analysis software which yielded a B_{max} of 35 ± 3 fmol/mg protein and a K_D of 2.5 ± 0.4 n*M*. *B*, Scatchard-Rosenthal replot of saturation data. This fit was determined as above generating identical binding parameters. Shown is a representative experiment, done in duplicate and replicated once. At a ligand concentration equal to its K_D, approximately 35% of total [^{125}I]HPIA binding was specific.

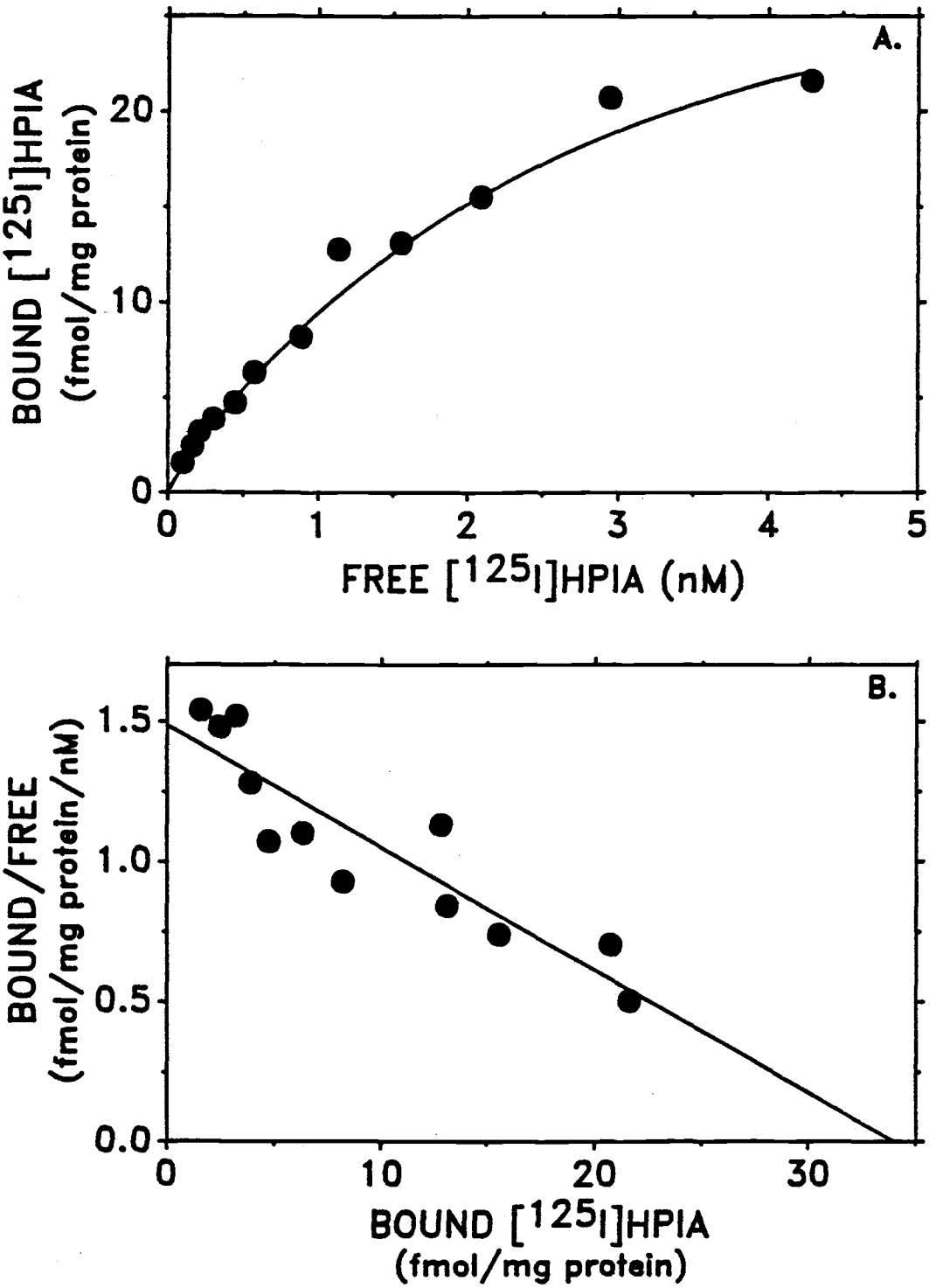
A.
BOUND [125I]HPIA
(fmol/mg protein)
0
10
20
0
1
2
3
4
5
FREE [125I]HPIA (nM)
B.
BOUND/FREE
(fmol/mg protein/nM)
0.0
0.5
1.0
1.5
0
10
20
30
BOUND [125I]HPIA
(fmol/mg protein)

FIGURE III-1

FIGURE III-2

A, HPIA saturation isotherm in porcine atrial membranes. The concentration of [^{125}I]HPIA was fixed at 0.2 n*M* and varying concentrations of unlabeled HPIA added (0.2-20 n*M*). The fit shown was obtained using Lundon I Saturation Analysis software which generated a B_{max} of 49.1 ± 2.2 fmol/mg protein and a K_D of 7.4 ± 0.8 n*M*. *B*, Scatchard-Rosenthal replot of saturation data. This fit was determined as above generating similar parameter estimates. Shown are the pooled results of three individual experiments each employing different membrane preparations.

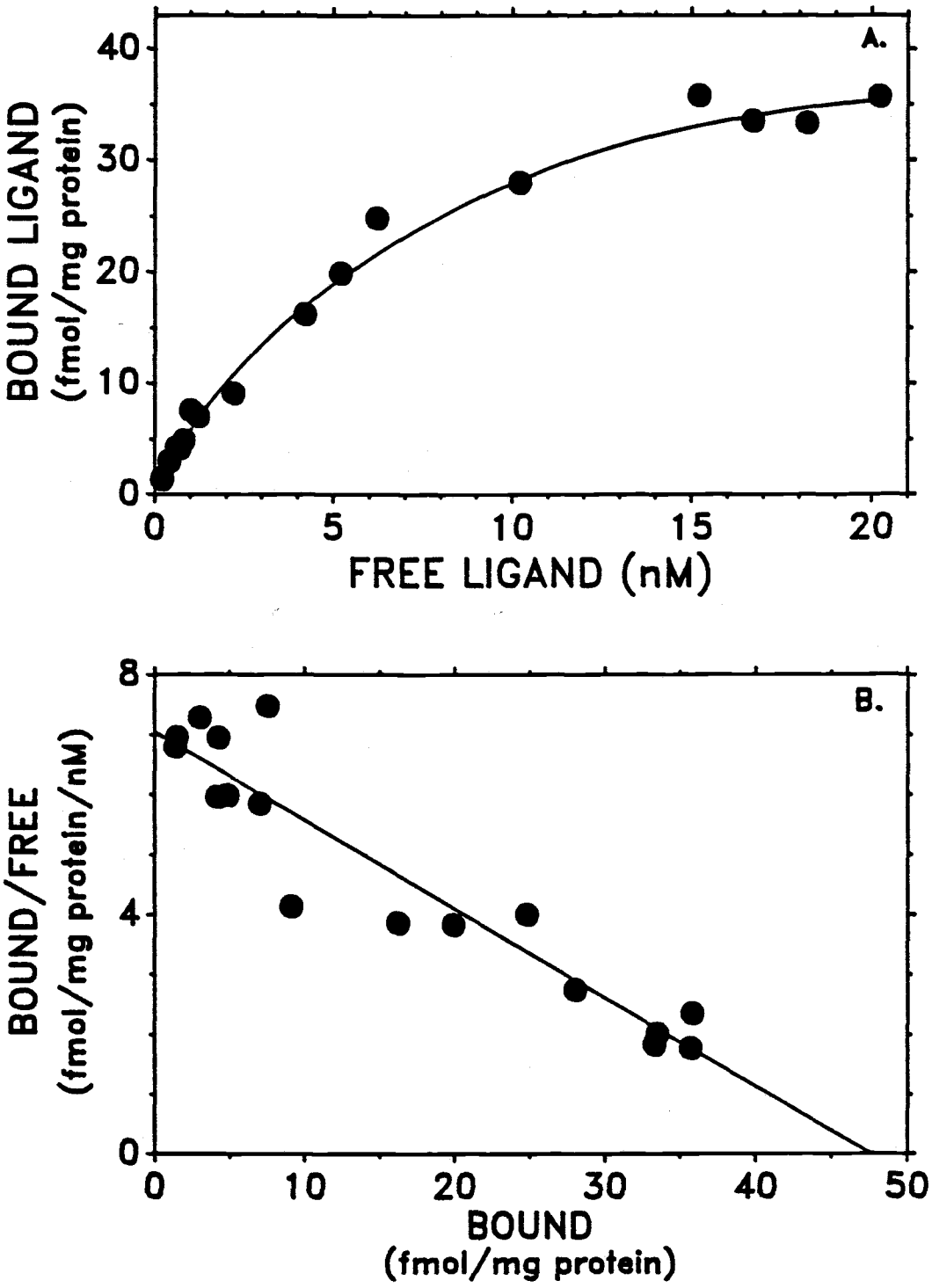
A.
BOUND LIGAND
(fmol/mg protein)
40
30
20
10
0
0
5
10
15
20
FREE LIGAND (nM)
B.
BOUND/FREE
(fmol/mg protein/nM)
8
4
0
0
10
20
30
40
50
BOUND
(fmol/mg protein)

FIGURE III-2

FIGURE III-3

A, [^{125}I]HPIA association experiments in porcine atrial membranes. Experiments were carried out with a receptor concentration of 50 p*M* and indicated ligand concentrations. Binding data were linearly transformed to a ln (% receptors open) vs. time plot. Lines drawn represent best fits as determined by linear regression. Slopes of these lines correspond to $(-)\tau^{-1}$ for that concentration of [^{125}I]HPIA. This yielded the following values for τ^{-1}: 0.253 n*M*, (4.5 ± 0.2) x 10^{-2} min^{-1}; 0.469 n*M*, (5.4 ± 0.4) x 10^{-2} min^{-1}; 0.742 n*M*, (6.1 ± 0.2) x 10^{-2} min^{-1}; 1.15 n*M*, (6.8 ± 0.3) x 10^{-2} min^{-1}; 1.61 n*M*, (7.6 ± 0.3) x 10^{-2} min^{-1}; 3.305 n*M*, (10.5 ± 0.5) x 10^{-2} min^{-1}. Experiments were conducted on the same day using the same membrane preparation. These findings were replicated twice under similar conditions. *B*, τ^{-1} as function of [^{125}I]HPIA concentration in porcine atrial membranes. The line drawn represents the best fit as determined by linear regression (R^2 = 0.99). The slope ([1.9 ± 0.2] x 10^7 M^{-1} min^{-1}) and y-intercept ([4.5 ± 0.1] x 10^{-2} min^{-1}) of this plot represent k_{+1} and k_{-1}, respectively.

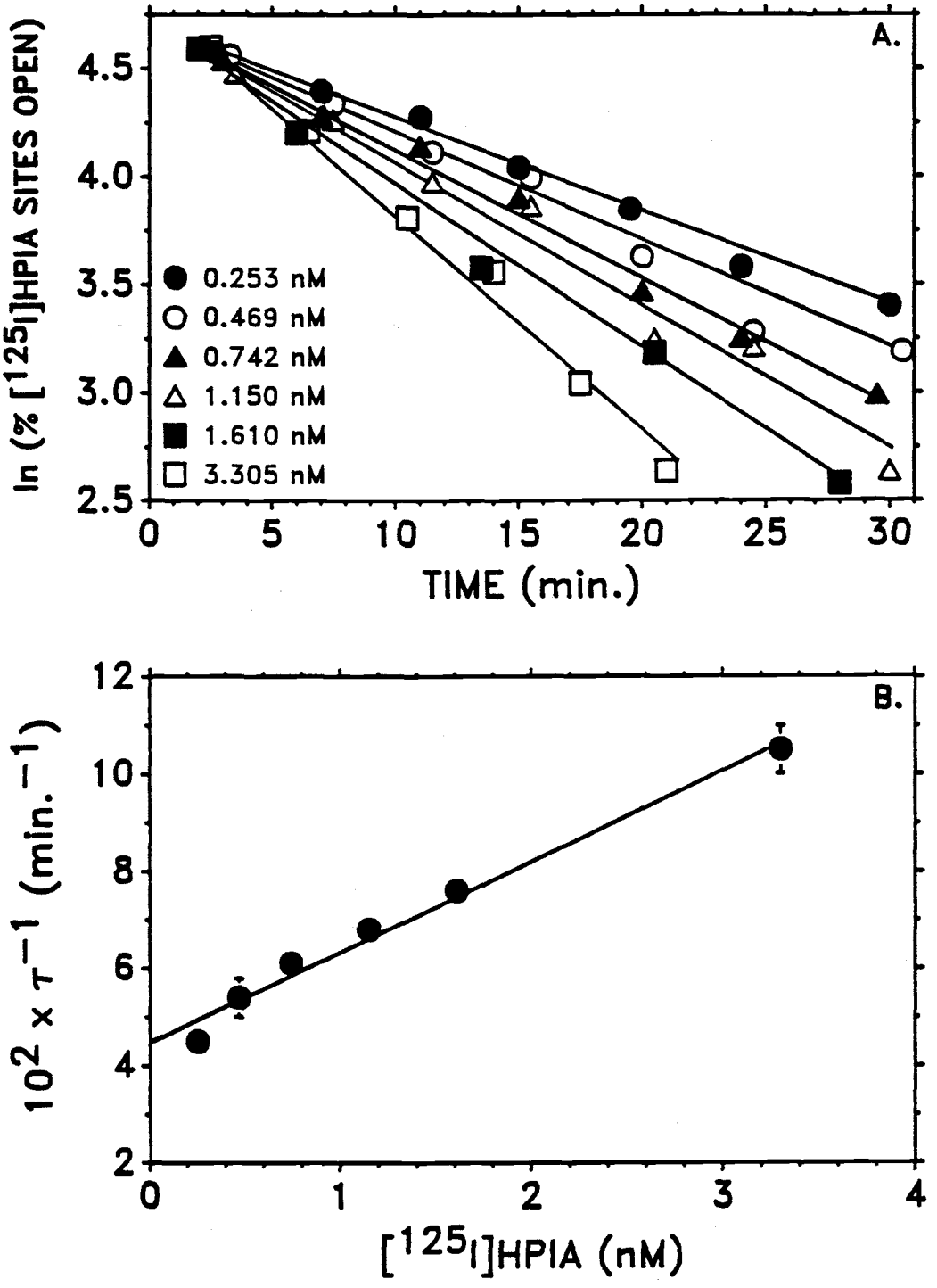
A.
ln (% [125I]HPIA SITES OPEN)
4.5
4.0
3.5
3.0
2.5
0
5
10
15
20
25
30
TIME (min.)
0.253 nM
0.469 nM
0.742 nM
1.150 nM
1.610 nM
3.305 nM
B.
10^2 x τ^-1 (min.^-1)
12
10
8
6
4
2
0
1
2
3
4
[125I]HPIA (nM)

FIGURE III-3

FIGURE III-4

Dissociation of specifically bound [^{125}I]HPIA from porcine atrial membranes. 0.25-0.5 n*M* [^{125}I]HPIA was allowed to equilibrate with porcine atrial membranes (receptor concentration = 50 p*M*) for 60 minutes, at which time dissociation was initiated as indicated. The values of k_{-1} were determined to be (1.6 ± 0.2) x 10^{-2} min^{-1} and 1.3 ± 0.13 min^{-1} for 2-CADO and GTP alone, respectively. For the combination of 2-CADO and GTP: 66 ± 9% [^{125}I]HPIA dissociated with a k_{-1} of 1.2 ± 0.1 min^{-1} and 34 ± 2% dissociated with a k_{-1} of (1.5 ± 0.2) x 10^{-2} min^{-1}. Parameters given were obtained by fitting data with equations III-2 and 3 using the least squares curve fitting routine KINETIC (Elsevier-Biosoft). Shown is a representative experiment which was replicated twice.

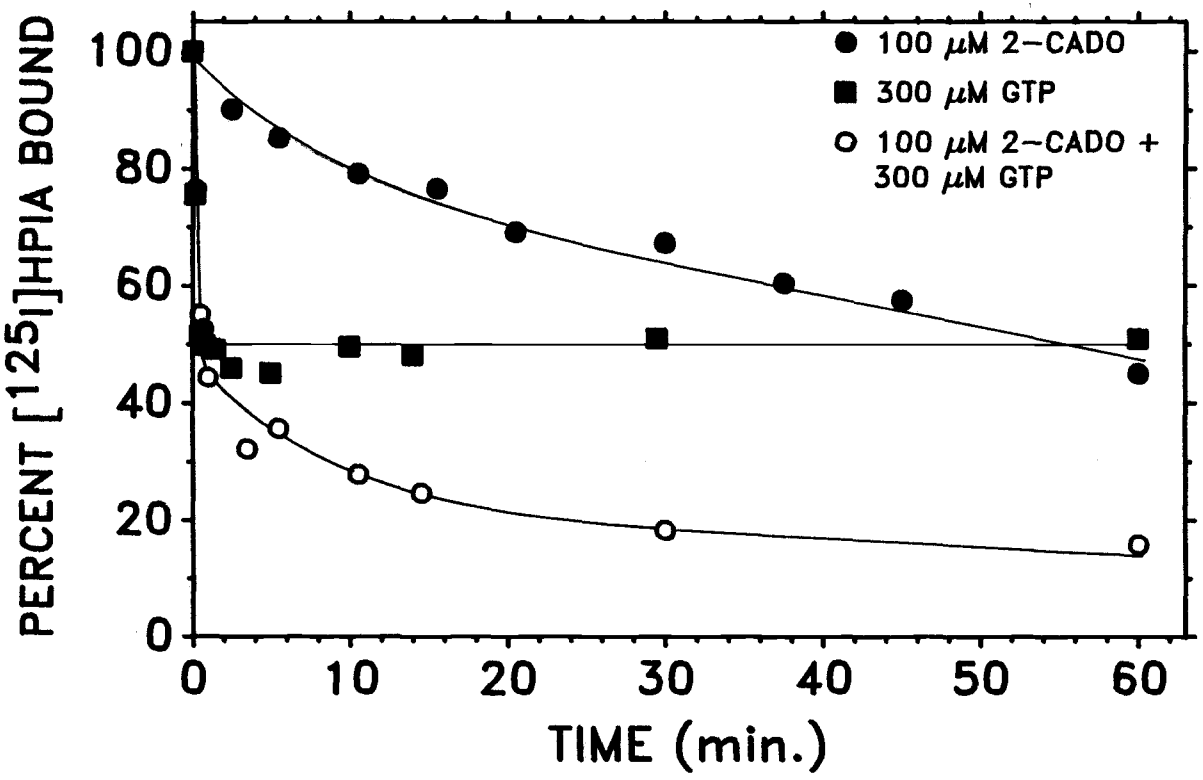
PERCENT [125I]HPIA BOUND
100
80
60
40
20
0
0
10
20
30
40
50
60
TIME (min.)
100 μM 2-CADO
300 μM GTP
100 μM 2-CADO +
300 μM GTP

FIGURE III-4

FIGURE III-5

Guanine nucleotides inhibiting the specific binding of [^{125}I]HPIA in porcine atrial membranes. Receptor and [^{125}I]HPIA concentration were approximately 40 and 500 p*M*, respectively. Shown is a representative experiment which was replicated 2-4 times. Titration curves drawn represent best fits as determined by fitting data with equation III-2 using an iterative curve fitting procedure (EBDA). This gave the following parameter estimates (IC_{50} [μM] ± S.E.): Gpp(NH)p, 2.5 ± 0.6; GTPγS, 19.4 ± 3.0; GDP, 231 ± 102; GTP, 376 ± 112; 5′-GMP > 3000.

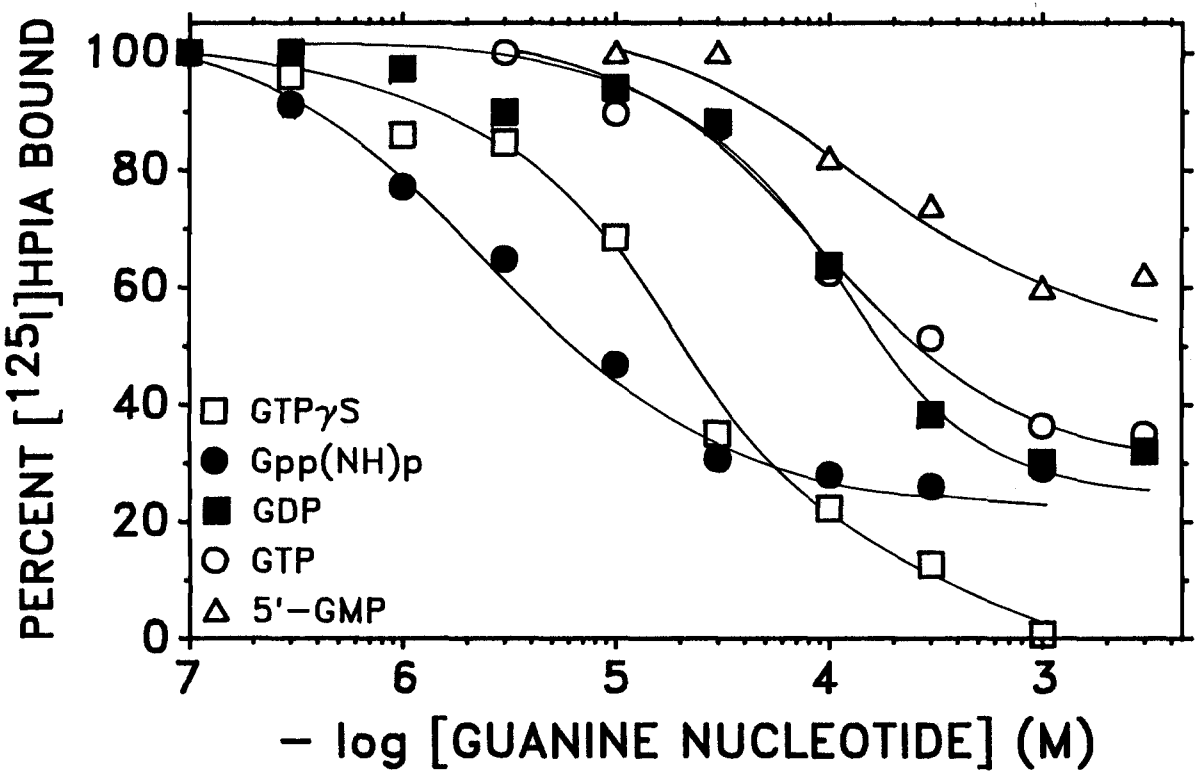
PERCENT [125I]HPIA BOUND
100
80
60
40
20
0
7
6
5
4
3
– log [GUANINE NUCLEOTIDE] (M)
GTPγS
Gpp(NH)p
GDP
GTP
5'–GMP

FIGURE III-5

FIGURE III-6

A, N^6 adenosine receptor agonists inhibiting specific binding of [^{125}I]HPIA in porcine atrial membranes. *B*, Non-N^6-substituted adenosine receptor agonists inhibiting the specific binding of [^{125}I]HPIA in porcine atrial membranes. Experimental conditions and curve fitting for *A* and *B* are as described in the legend of Fig. III-5. Shown are representative experiments which were replicated 3-6 times.

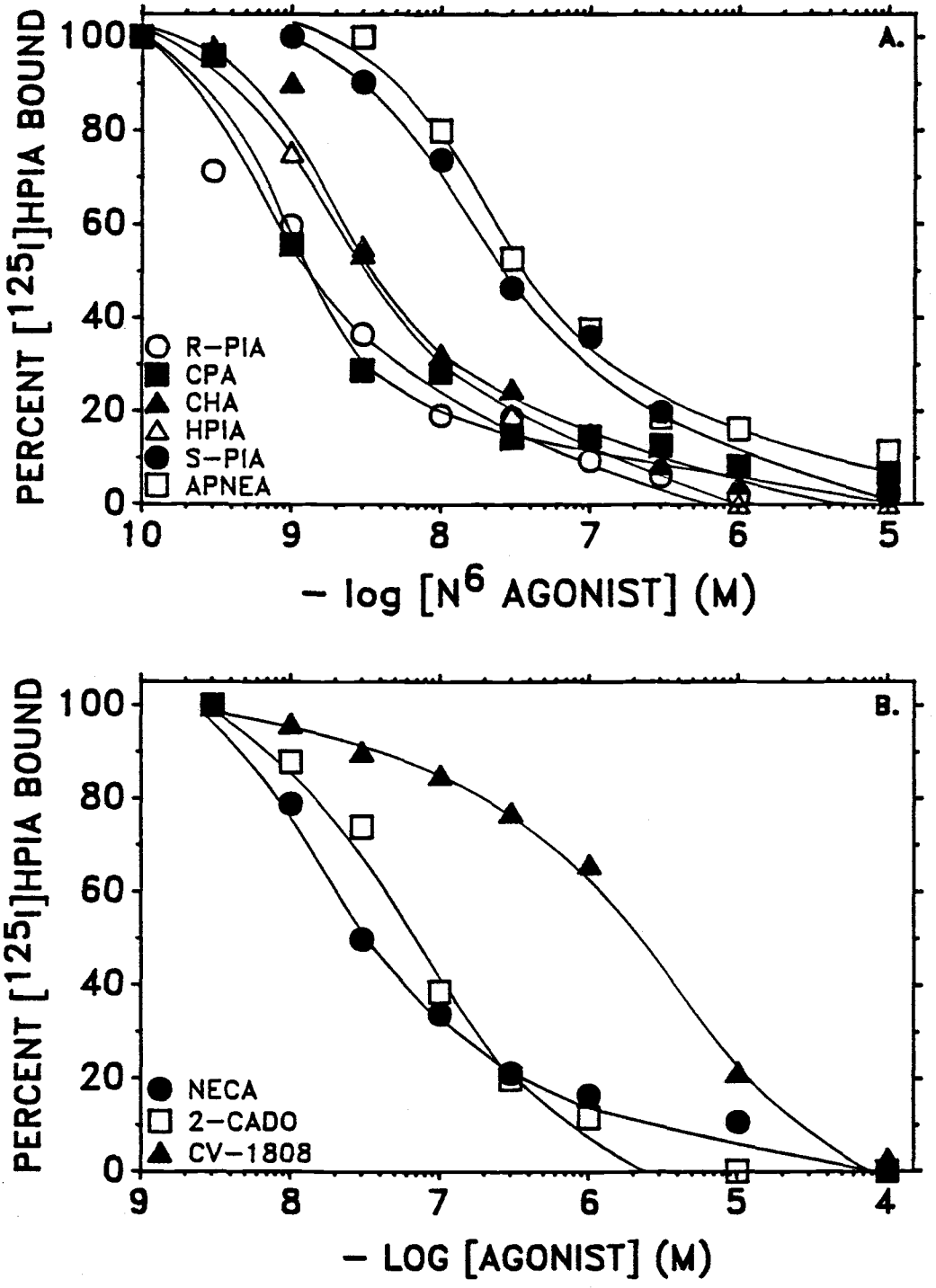
A.
PERCENT [125I]HPIA BOUND
100
80
60
40
20
0
R-PIA
CPA
CHA
HPIA
S-PIA
APNEA
10
9
8
7
6
5
– log [N6 AGONIST] (M)
B.
PERCENT [125I]HPIA BOUND
100
80
60
40
20
0
NECA
2-CADO
CV-1808
9
8
7
6
5
4
– LOG [AGONIST] (M)

FIGURE III-6

FIGURE III-7

Adenosine receptor antagonists inhibiting the specific binding of [^{125}I]HPIA in porcine atrial membranes. Experimental conditions and curve fitting are as described in the legend of Fig. III-5. Shown is a representative experiment which was replicated 1-3 times.

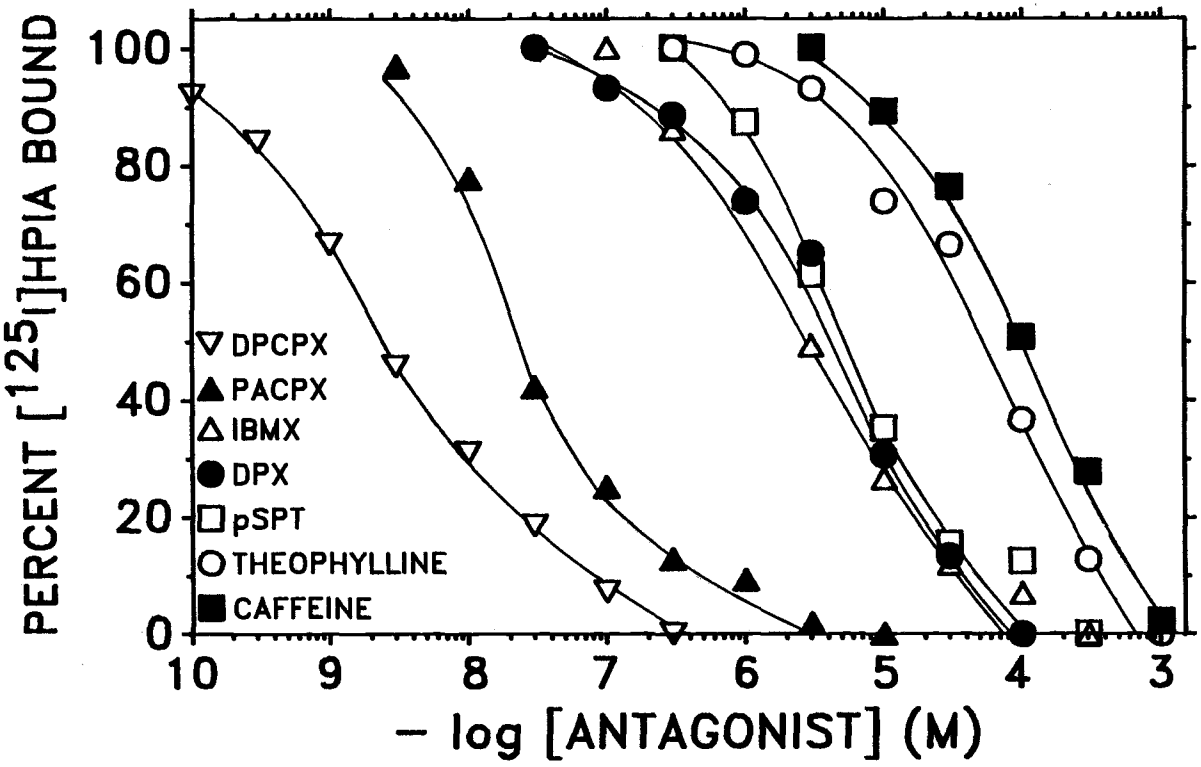
PERCENT [125I]HPIA BOUND
100
80
60
40
20
0
10
9
8
7
6
5
4
3
− log [ANTAGONIST] (M)
DPCPX
PACPX
IBMX
DPX
pSPT
THEOPHYLLINE
CAFFEINE

FIGURE III-7

TABLE III-1

Adenosine receptor agonists and antagonists inhibiting the specific binding of [^{125}I]HPIA in porcine atrial membranes. Experimental conditions and curve fitting are as described in the legend of Fig. III-5. Parameter estimates as described and represent the mean of 3-6 experiments (agonists) or 2-3 experiments (antagonists).

TABLE III-1

COMPOUND	K_I(n*M*) ± S.E.M.	SLOPE FACTOR ± S.E.M.
	AGONISTS	
CPA	1.04 ± 0.14	0.94 ± 0.30
(*R*)-PIA	1.38 ± 0.60	0.82 ± 0.17
HPIA	2.95 ± 0.40	0.78 ± 0.06
CHA	3.61 ± 0.60	0.83 ± 0.16
APNEA	25.4 ± 0.1	1.04 ± 0.23
NECA	27.1 ± 12.5	0.83 ± 0.14
(*S*)-PIA	30.0 ± 12.4	0.83 ± 0.14
2-CADO	64.5 ± 12.2	0.86 ± 0.16
CV-1808	2310 ± 355	0.74 ± 0.06
	ANTAGONISTS	
DPCPX	2.4 ± 0.2	0.70 ± 0.04
PACPX	22.0 ± 4.1	0.98 ± 0.14
IBMX	2770 ± 343	0.82 ± 0.08
DPX	4096 ± 593	1.00 ± 0.11
pSPT	4479 ± 586	0.99 ± 0.11
THEOPHYLLINE	45,888 ± 7295	1.02 ± 0.13
CAFFEINE	90,130 ± 25,283	1.15 ± 0.30

ACKNOWLEDGMENTS

The authors gratefully acknowledge skillful membrane preparation done by C.J. Pan and Laurie Shoots and the helpful advice of Drs. Paul H. Franklin, Gary L. Peterson and Michael R. Tota.

CHAPTER IV

Agonist Radioligand Interactions with the Solubilized Porcine Atrial A_1 Adenosine Receptor

ABSTRACT

Porcine atrial adenosine receptors have been solubilized using a detergent system consisting of digitonin and sodium cholate and characterized with the agonist radioligand N^6-([^{125}I]hydroxyphenylisopropyl)adenosine ([^{125}I]HPIA). [^{125}I]HPIA labeled an apparently homogeneous population of solubilized recognition sites with a B_{max} of 88 ± 4 fmol/mg of protein and a K_D of 1.4 ± 0.1 n*M*. Solubilization resulted in a 2.5-fold enrichment of adenosine receptor specific activity and an enhanced signal to noise ratio over that observed for porcine atrial membrane preparations. Solubilized cardiac adenosine receptors were relatively stable and exhibited many of the properties of membrane-bound receptors. The rank order potency of adenosine receptor agonists inhibiting the binding of [^{125}I]HPIA was consistent with the labeling of a solubilized A_1 adenosine receptor. Association rate experiments suggested that the interaction of [^{125}I]HPIA with solubilized cardiac adenosine receptors was consistent with that of a simple bimolecular reaction. The dissociation constant calculated from kinetic data (0.73 n*M*) was in good agreement with that determined by equilibrium binding measurements (1.4 n*M*). The interaction of cardiac A_1 adenosine receptors and guanine nucleotide binding protein(s) was retained in this detergent system. Addition of GTPγS to an equilibrated mixture of solubilized cardiac adenosine receptors and [^{125}I]HPIA resulted in a rapid and complete dissociation of [^{125}I]HPIA. This dissociation was resolved into

two kinetic phases which appear to arise from two populations of independent, non-interconvertible receptor-G protein complexes which display differing sensitivities to guanine nucleotides. The A_1 adenosine receptor-G protein complex solubilized in digitonin/cholate appears to provide an excellent system by which agonist radioligand-receptor-G protein interactions can be further studied.

ABBREVIATIONS

B_{max}, maximum binding capacity; 2-CADO, 2-chloroadenosine; CPA, N^6-cyclopentyladenosine; CHAPS, 3[(3-cholamidopropyl)dimethyl-ammonio]-1-]propanesulfonate; CV-1808, 2-phenylaminoadenosine; DTT, dithiothreitol; Gpp(NH)p, guanine-5′-yl-imidodiphosphate; GTPγS, guanosine-5′-(3-O-thio)-triphosphate; [^{125}I]HPIA, N^6-3([^{125}I]-Iodo-4-hydroxyphenylisopropyl)adenosine; K_D, equilibrium dissociation constant; k_{+1}, association rate constant; k_{-1}, dissociation rate constant; Na_2EDTA, disodium ethylenediamine tetraacetic acid; NECA, 5′-(N-ethylcarboxamido)adenosine; PMSF, phenylmethylsulfonyl fluoride; *(R)*-PIA, N^6-(R-phenyliso-propyl)adenosine; *(S)*-PIA, N^6-(S-phenylisopropyl)adenosine; τ and τ^{-1}, relaxation time and reciprocal relaxation time, respectively.

INTRODUCTION

A_1 adenosine receptors in myocardial membranes mediate cardioinhibitory effects of adenosine and its structural congeners (66,68,71,94,108). Transduction mechanisms associated with cardiac adenosine receptor activation include activation of an inward-rectifying potassium channel (84) and inhibition of adenylyl cyclase activity (85-89). The former seems likely to represent the molecular mechanism of adenosine receptor-mediated negative chronotropy (84). Inhibition of adenylyl cyclase activity is not temporally correlated with negative chronotropy in the developing atria of the embryonic chick (89) but may be involved in adenosine receptor-mediated negative inotropy or catecholamine antagonism inasmuch as adenosine attenuates catecholaminergic-stimulated positive inotropy (81) and calcium influx (90).

Molecular properties of membrane-bound rat (86,111), bovine (95,112), chick (120) and porcine (113,121) cardiac adenosine receptors have been characterized. Solubilization of brain, but not cardiac, A_1 adenosine receptors has previously been reported (42,43,45,122,123). Solubilized bovine (122) and rat (42,45,123) brain adenosine receptors display high affinity agonist binding which is sensitive to negative modulation by guanine nucleotides indicating that receptor-G protein interactions are preserved in detergent extracts of brain membranes. Guanine nucleotide-sensitive agonist binding to detergent-solubilized receptors has also been reported for the muscarinic receptor of rat myocardium (124) and rat striatal D-1

dopamine receptors (125). These findings are in contrast to results obtained for detergent-solubilized porcine atrial muscarinic receptors (126), or a variety of catecholaminergic receptors (127-129) which do not display guanine nucleotide-sensitive high affinity agonist binding. Thus, brain A_1 adenosine receptors and rat cardiac muscarinic and striatal D-1 dopamine receptors apparently exist tightly coupled to guanine nucleotide binding protein(s).

Results of the present studies suggest that molecular properties of porcine atrial adenosine receptors are not grossly altered in digitonin/cholate. Adenosine receptor-G protein interactions are also well preserved in this detergent system. Thus, the solubilized cardiac A_1 adenosine receptor provides a potential model for the study of receptor-G protein interactions in detergent solution.

MATERIALS AND METHODS

Digitonin and sodium cholate were obtained from Sigma (St. Louis, MO). [^{125}I]HPIA (1930 Ci/mmol) and all other compounds were purchased from sources previously described (121).

MEMBRANE PREPARATION AND RECEPTOR SOLUBILIZATION. Porcine atrial membranes were prepared and solubilized as previously described for the atrial muscarinic receptor (98) with minor modifications. Briefly, digitonin and sodium cholate were added to a porcine atrial membrane P3 preparation to give a final concentration of 0.4% w/v digitonin, 0.08% w/v sodium cholate and 4.95 mg of protein/mL. This mixture was then centrifuged at 100,000 x *g* for 1 hour at 4°C in a Beckman L8-55M Ultracentrifuge. The supernatant (E1) was discarded and the pellet resuspended to give a protein concentration of 10 mg/mL, assuming a 30% protein loss during the first extraction. Digitonin and sodium cholate were added to this membrane suspension to give a final concentration of 0.8% w/v digitonin, 0.16% w/v sodium cholate and 8 mg of protein/mL. After a 10 min. incubation at 22°C, the membrane-detergent mixture was then diluted 2-fold and centrifuged as above. The supernatant from this second extraction contained solubilized cardiac A_1 adenosine receptors in approximately 50% yield (in [^{125}I]HPIA sites) and was used for all experiments described here. Prior to the second solubilization step, membranes were incubated with 5 m*M* $MgCl_2$ and 1 m*M* DTT on ice for 30 min. Preincubation with Mg^{++} and DTT improved both the yield and stability of the solubilized cardiac

A_1 adenosine receptor. Protease inhibitors present during all solubilization procedures were PMSF (0.1 m*M*), Na_2EDTA (1 m*M*), egg white tryspin inhibitor (100 μg/mL), leupeptin (0.7 μg/mL) and bacitracin (0.01% w/v). Solubilized receptor preparations were used immediately or stored on ice. Storage on ice for up to 7 days did not adversely affect receptor specific activity. Immediately before radioligand binding studies, solubilized receptor preparations (~ 1 mg of protein/mL) were warmed to 22°C and incubated with 5 units/mL of adenosine deaminase for 30 minutes. Adenosine deaminase-treated extracts were then used directly in radioligand binding experiments (the concentration of adenosine deaminase was approximately 4 units/mL in assay tubes).

RADIOLIGAND BINDING EXPERIMENTS. All equilibrium radioligand binding experiments were carried out for 120 minutes at 37°C in a volume of 95 μl containing 20 m*M* imidazole (pH 7.4), 4 m*M* $MgCl_2$, 0.3% w/v digitonin, 0.06% sodium cholate, and 30-70 μg protein. Non-specific binding was defined as that occurring in the presence of 100 μM 2-CADO, 3 m*M* theophylline or 1 m*M* GTP (which gave identical values) and amounted to approximately 10% of total [^{125}I]HPIA binding at a concentration equal to its K_D. Bound [^{125}I]HPIA was separated from free radioligand by rapid filtration (Brandel Cell Harvester M-24R, Brandel Scientific, Gaithersburg, MD) over Schleicher and Schuell #32 glass-fiber filters which had been presoaked in 0.5% w/v polyethyleneimine, similar to the method described by Bruns (130). Kinetic experiments were carried out under identical conditions for varying time intervals and

were terminated by rapid filtration. Radioactivity on the filters was quantified by use of a Beckman 4000 γ-counter at a counting efficiency of 75%. Protein concentration was determined by the method of Lowry et al. (100).

DATA ANALYSIS. Results of saturation and competition experiments were analyzed by use of Lundon I Saturation Analysis Software (Lundon Software, Cleveland, OH) and EBDA (Elsevier-Biosoft, Cambridge, UK), respectively. [^{125}I]HPIA association experiments were analyzed by linear transformation of binding data to a natural logarithm plot:

$$\ln ([B_0 - B_t]/[B_0]) = (-)t/\tau \qquad \text{(Eq. IV-1)}$$

where B_0 and B_t are the amounts of [^{125}I]HPIA specifically bound at equilibrium and time t, respectively, and τ is the relaxation time for the single kinetic phase. Fitting kinetic data to this equation generates a plot with a slope corresponding to $(-)\tau^{-1}$. Values of τ^{-1} were plotted vs. [^{125}I]HPIA concentration and fitted with the pseudo-first order rate equation for a simple bimolecular association reaction:

$$\tau^{-1} = k_{+1}[[^{125}\text{I}]\text{HPIA}] + k_{-1} \qquad \text{(Eq. IV-2)}$$

where k_{+1} and k_{-1} are the association and dissociation rate constants for [^{125}I]HPIA binding, respectively. [^{125}I]HPIA dissociation experiments were analyzed by fitting data to monophasic

or biphasic decay equations:

$$B_t = B_0 e^{-t/\tau} \qquad \text{(Eq. IV-3A)}$$

$$B = B_1 e^{-t/\tau_1} + B_2 e^{-t/\tau_2} \qquad \text{(Eq. IV-3B)}$$

The values of $\tau_{1,2}$ are the relaxation times and $B_{1,2}$ the amplitudes of each kinetic phase. Reciprocal relaxation times for fast and slow phases of GTPγS-initiated [^{125}I]HPIA dissociation were plotted vs. GTPγS concentration (Fig. IV-6B and C, respectively). Values of τ_1^{-1} and τ_2^{-1} appeared to increase in a hyperbolic manner as GTPγS concentration increased. Therefore, these data were analyzed according to equation IV-4 using an iterative curve-fitting routine:

$$\tau^{-1} = \frac{k_{-1}[GTP\gamma S]}{K_D + [GTP\gamma S]} \qquad \text{(Eq. IV-4)}$$

where τ^{-1}, k_{-1} and K_D represent the reciprocal relaxation time, the rate constant for [^{125}I]HPIA dissociation and the dissociation constant for GTPγS in each kinetic phase, respectively.

RESULTS

SATURATION ANALYSIS. [^{125}I]HPIA showed saturable binding to a homogeneous population of high affinity solubilized cardiac recognition sites with a B_{max} of 88 ± 4 fmol/mg of protein and a K_D of 1.4 ± 0.1 n*M* (Fig. IV-1A). A B_{max} of 88 fmol/mg of protein represents a 2.5-fold enrichment over that previously reported for the membrane-bound adenosine receptor of porcine atria (113,121). In addition, solubilization in this mixed detergent system resulted in a greatly enhanced signal to noise ratio inasmuch as 90% of total [^{125}I]HPIA binding was specific at a concentration equal to its K_D. In contrast, the corresponding percentage of [^{125}I]HPIA specific binding in porcine atrial membranes preparations is approximately 35% (121).

Saturation binding data were linearly transformed and fitted by least squares regression analysis to generate a Scatchard-Rosenthal plot (Fig. IV-1B). This plot was monophasic over a 100-fold range of [^{125}I]HPIA concentration, yielding a B_{max} of 91 ± 3 fmol/mg of protein and a K_D of 1.5 ± 0.2 n*M*.

ASSOCIATION AND DISSOCIATION KINETICS. Kinetic experiments were undertaken to determine the mechanism by which [^{125}I]HPIA binds to solubilized cardiac A_1 adenosine receptors. Under pseudo-first order reaction conditions, [^{125}I]HPIA association experiments were performed over a broad range of radioligand concentration. Values for τ^{-1} were obtained at each concentration of radioligand by fitting association data to

equation IV-1 (Fig. IV-2A) and then plotted versus [^{125}I]HPIA concentration (Fig. IV-2B). The latter plot was fitted with equation IV-2 giving a k_{+1} equal to (3.36 ± 0.10) x 10^7 M^{-1} min^{-1} and a value of k_{-1} equal to (2.45 ± 0.40) x 10^{-2} min^{-1}. The linear dependence of τ^{-1} on ligand concentration suggests that [^{125}I]HPIA interacts with the solubilized cardiac A_1 adenosine receptor in simple bimolecular reaction under the reaction conditions employed (4 m*M* Mg^{++} and 37°C). Values of k_{-1} and k_{+1} can be used to calculate an equilibrium dissociation constant of 0.73 n*M*, assuming a simple bimolecular binding mechanism. This value is in reasonable agreement with the dissociation constant obtained from equilibrium binding experiments (see above and Fig. IV-1). The value of k_{-1} was independently determined by addition of 2-CADO (final concentration of 100 μM in a volume which represented 2% of incubate volume) to an equilibrated mixture of [^{125}I]HPIA and solubilized porcine atrial adenosine receptors (Fig. IV-3). Dissociation of [^{125}I]HPIA initiated by 2-CADO was monophasic with a k_{-1} of (1.6 ± 0.1) x 10^{-2} min^{-1} or a half-time for dissociation of approximately 43 minutes, in good agreement with the value determined from the analysis of association kinetics (Fig. IV-2B). All of the present kinetic data agree with those observed for [^{125}I]HPIA binding to the membrane-bound adenosine receptor of porcine atria (121) which were also consistent with a simple bimolecular binding mechanism.

GUANINE NUCLEOTIDE TITRATION EXPERIMENTS. As a means of investigating guanine nucleotide modulation of [^{125}I]HPIA binding

to solubilized cardiac A_1 adenosine receptors, titration experiments for a series of guanine nucleotides were performed (Fig. IV-4). The purpose of these experiments was to determine if the binding of this agonist radioligand demonstrates sensitivity to guanine nucleotides as had been reported for solubilized brain adenosine receptors and was suggested by the high affinity nature of [^{125}I]HPIA binding (see above). The rank order potency for guanine nucleotides negatively modulating specific binding of [^{125}I]HPIA was as follows: GTPγS > Gpp(NH)p > GTP > GDP. 5′-GMP, in concentrations up to 1 m*M*, was ineffective as a negative modulator of [^{125}I]HPIA binding (data not shown). All active guanine nucleotides inhibited 100% of [^{125}I]HPIA binding to solubilized cardiac A_1 adenosine receptors. This finding is in contrast to experiments using the membrane-bound adenosine receptor of porcine atria in which all guanine nucleotides (except GTPγS) maximally inhibited 70-80% of [^{125}I]HPIA binding (121). These titration experiments provide evidence that [^{125}I]HPIA, solubilized cardiac A_1 adenosine receptors and guanine nucleotide binding protein(s) interact to form a ternary complex which possesses high affinity for adenosine receptor agonists. The sensitivity of high affinity agonist binding to negative modulation by guanine nucleotides is consistent with a negative heterotropic binding interaction (104).

KINETICS OF GUANINE NUCLEOTIDE-INDUCED [^{125}I]HPIA DISSOCIATION. The kinetic nature of guanine nucleotide destabilization of high affinity agonist binding was studied by following the binding of [^{125}I]HPIA after addition of saturating concentrations of guanine nucleotides to an equilibrated mixture of solubilized receptors and radioligand. The purpose of these experiments was to determine the kinetic characteristics of [^{125}I]HPIA dissociation from the guanine nucleotide-sensitive binding component. In contrast to monophasic kinetics observed when dissociation was initiated by 2-CADO (Fig. IV-3), [^{125}I]HPIA dissociation induced by guanine nucleotides appeared biphasic (Fig. IV-5). The magnitude of dissociation rate constants (0.1 - 0.2 min^{-1}) and amplitude (50 - 60% in the fast phase, 40 - 50% in the slow phase) of each kinetic phase was relatively constant for all guanine nucleotides tested. As a means of addressing molecular mechanisms involved in the generation of biphasic [^{125}I]HPIA dissociation kinetics, dissociation rate experiments were conducted over a large range of GTPγS concentration (Fig. IV-6A). Biphasic dissociation kinetics were observed over the entire range of GTPγS concentrations tested (10 n*M* - 30 μ*M*). These data were fitted with equation IV-3B) to determine the values of the reciprocal relaxation times (τ_1^{-1}, τ_2^{-1}) and amplitudes (B_1, B_2) of each kinetic phase as a function of GTPγS concentration. A plot of the reciprocal relaxation times for fast and slow kinetic phases vs. GTPγS concentration appeared hyperbolic (Figs. IV-6B and C, respectively). Fitting these data

with equation IV-4 generated the following parameter estimates: fast phase, k_{-1} = (1.3 ± 0.1) x 10^{-1} min^{-1}, K_D for GTPγS = 86 ± 20 n*M*; slow phase, k_{-1} = (7.6 ± 0.3) x 10^{-2} min^{-1}, K_D for GTPγS = 481 ± 76 n*M*.

PHARMACOLOGICAL SPECIFICITY OF SOLUBILIZED CARDIAC ADENOSINE RECEPTORS. To address pharmacological specificity of solubilized cardiac adenosine receptors the rank order potency of several adenosine receptor agonists and antagonists as inhibitors of [^{125}I]HPIA binding was determined. The adenosine A_1 receptor-selective agonists, CPA and (*R*)-PIA were the most potent inhibitors of [^{125}I]HPIA binding whereas an A_2-selective ligand, CV-1808, was approximately 3 orders of magnitude less potent than these A_1-active ligands (Fig. IV-7 and table IV-1). (*R*)-PIA was approximately 42-fold more potent as an inhibitor of [^{125}I]HPIA binding than its less active diastereomer, (*S*)-PIA. Indirect Hill slopes for all agonist and antagonist inhibitors of [^{125}I]HPIA binding did not differ from unity, providing evidence that this concentration of [^{125}I]HPIA (~ 750 p*M*) labels a homogeneous receptor population. With the exception of (*S*)-PIA, absolute potencies of all inhibitors of [^{125}I]HPIA binding are reasonably similar for studies employing either solubilized or membrane-bound porcine atrial adenosine receptors (121). These titration experiments suggest that the A_1 receptor-subtype selectivity of the cardiac adenosine receptor is well maintained in this detergent system.

DISCUSSION

The mixed detergent system employed in these studies effectively solubilized porcine atrial adenosine receptors in good yield and provided sufficient stability to allow biochemical characterization. Solubilization of brain A_1 adenosine receptors has previously been reported to result in a either a marginal (42,123) or a negative enrichment of adenosine receptor specific activity (43,45,122). Such findings suggest that these solubilization protocols were not optimized for selective solubilization of adenosine receptors and/or solubilized brain adenosine receptors were unstable in the detergents employed. It is, therefore, noteworthy that this double-extraction procedure employing a mixed detergent system solubilized cardiac adenosine receptors in good yield, resulted in an enrichment of adenosine receptor specific activity and provided stability adequate for biochemical characterization. The solubilization protocol used here was originally optimized for selective solubilization of porcine atrial muscarinic receptors (98) and modified only slightly for the present studies (Mg^{++} and DTT preincubation). In addition to the enrichment of adenosine receptor specific activity, a dramatic increase in the [^{125}I]HPIA binding signal to noise ratio was observed upon solubilization. [^{125}I]HPIA, a marginally useful radioligand for the characterization of membrane-bound cardiac adenosine receptors (35% specific binding at K_D), appears to be an excellent agonist radioligand for the characterization of solubilized cardiac A_1 adenosine receptors (90% specific binding at K_D).

Saturation data were clearly monophasic over the 100-fold range of [^{125}I]HPIA concentration used. These data would appear to suggest that cardiac adenosine receptors, solubilized in this detergent system and assayed in the presence of high Mg^{++} and at 37°C, exist as a homogeneous population displaying high affinity for agonists.

Kinetic experiments were performed to address the mechanism of [^{125}I]HPIA binding to solubilized cardiac A_1 adenosine receptors. Data from association experiments are consistent with [^{125}I]HPIA binding to the solubilized cardiac A_1 adenosine receptor in a simple bimolecular reaction of the type:

$$L + R \underset{k_{-1}}{\overset{k_{+1}}{\rightleftharpoons}} LR \qquad \text{(Eq. IV-5)}$$

which is described by the pseudo-first order rate equation presented above (equation IV-2). This mechanism of binding is consistent with that observed for [^{125}I]HPIA interacting with membrane-bound cardiac adenosine receptors (121). Under these experimental conditions, we found no evidence for a ligand-dependent conformational change in receptor which would create a high affinity complex, such as [LR] interacting with a G protein(s). Rather, as postulated for its interaction with membrane-bound cardiac adenosine receptors, [^{125}I]HPIA appears to interact via a simple bimolecular reaction with solubilized cardiac A_1 adenosine receptors which exist precoupled to a G protein(s), i.e.,

$$L + RG \underset{k_{-1}}{\overset{k_{+1}}{\rightleftharpoons}} LRG \qquad \text{(Eq. IV-6)}$$

Brain adenosine receptors solubilized in sodium cholate (45,122), digitonin (42) or CHAPS (123) maintain the ability to interact with G proteins as evidenced by negative modulation of agonist binding by guanine nucleotides. Guanine nucleotides were two orders of magnitude more potent modulators of [^{125}I]HPIA binding to solubilized- than membrane-bound porcine atrial adenosine receptors and all active guanine nucleotides inhibited 100% of [^{125}I]HPIA binding. In contrast, guanine nucleotides inhibited only 75-80% of [^{125}I]HPIA binding to membrane-bound porcine atrial adenosine receptors (121). The inability of guanine nucleotides to inhibit 100% of [^{125}I]HPIA binding to membrane-bound porcine atrial adenosine receptors is likely to be the result of diffusional barriers in the membrane creating a subpopulation of high affinity agonist binding sites which are inaccessible and thus, insensitive to negative modulation by polar guanine nucleotides. Solubilization of porcine atrial membranes with digitonin/cholate would appear to remove these diffusional barriers.

At saturating concentrations, all guanine nucleotides initiate a maximal rate of [^{125}I]HPIA dissociation of 0.1 - 0.2 min^{-1}. This value is reasonably close to the rate constant for GDP dissociation from G_i in a reconstituted system (131). However, GDP release is unlikely to be the rate-limiting step in guanine nucleotide-induced [^{125}I]HPIA dissociation in the present studies. The system has

been primed by a preincubation with [^{125}I]HPIA which should decrease the affinity of G_i for GDP and thus allow for rapid binding of other guanine nucleotides. Indeed, the finding that GDP potently and rapidly modulated [^{125}I]HPIA binding provided direct evidence that preincubation with agonist resulted in dissociation of native GDP from the ternary complex.

Biphasic dissociation kinetics were observed for guanine nucleotide-initiated [^{125}I]HPIA dissociation. The magnitude of the reciprocal relaxation times for both fast and slow kinetic phases was hyperbolically dependent on GTPγS concentration. The simplest mechanism to explain this is the occurrence of two parallel reactions:

$$LRG_1 + N \underset{}{\overset{K_1}{\rightleftharpoons}} LRG_1N \xrightarrow{k_{-1}} L + R + G_1N \quad \text{(Eq. IV-7A)}$$

$$LRG_2 + N \underset{}{\overset{K_2}{\rightleftharpoons}} LRG_2N \xrightarrow{k_{-2}} L + R + G_2N \quad \text{(Eq. IV-7B)}$$

where L, R, G and N represent [^{125}I]HPIA, solubilized cardiac adenosine receptor, G protein(s) and GTPγS, respectively, and LRG_1 and LRG_2 are independent, non-interconvertible populations of receptor-G protein complexes. $K_{1,2}$ and $k_{-1,-2}$ represent the dissociation constant for GTPγS and the rate constant for GTPγS-initiated [^{125}I]HPIA dissociation for each parallel reaction, respectively. This model implies that biphasic [^{125}I]HPIA dissociation involves the interaction of guanine nucleotides with a heterologous population of LRG complexes differing

in G rather than R. The basis for this hypothesis is that [^{125}I]HPIA apparently labels a homogenous population of solubilized receptors as evidenced by monophasic Scatchard-Rosenthal, Hill (data not shown), association rate and 2-CADO-induced dissociation rate plots. Therefore, biphasic guanine nucleotide-induced [^{125}I]HPIA dissociation appears to arise from G protein, rather than receptor, heterogeneity. Heart contains considerable amounts of both G_i and G_o (132-137). Nathanson and coworkers, using quantitative immunoblotting, have reported that the level of $G_{o\alpha}$ in adult rat atria is approximately 60% that of $G_{i\alpha}$ (138). One potential explanation for the appearance of two independent, non-interconvertible populations of receptor-G protein complexes is interaction of cardiac adenosine receptors with both of these G proteins. Other G protein-coupled receptors, such as cloned M2 muscarinic receptors, have been shown to interact with two distinct G proteins related to inositol phosphate metabolism and inhibition of adenylyl cyclase activity (139). Functional consequences of adenosine receptor activation in heart which are known to be mediated via an interaction with G proteins include the activation of an inward-rectifying K^+ channel (84) and inhibition of adenylyl cyclase activity (85-89), both of which could be explained by the coupling of cardiac adenosine receptors to G_i. Brown and coworkers have reported the existence of G_o-modulated K^+ channels in brain (140), however, the functional significance of G_o in heart and the possibility of adenosine receptor-G_o coupling remain unknown.

One must also consider the possibility that artifacts of detergent solubilization may have given rise to the appearance of two populations of receptor-G protein complexes. Detergent solubilization most certainly alters the microenvironment in which the cardiac adenosine receptor exists. Effectors, with which the receptor is not associated in the membrane (potentially G_o), will gain access to the receptor provided these effectors and the receptor cosolubilize. Alternatively, the presence of detergent may have altered guanine nucleotide-initiated [^{125}I]HPIA dissociation kinetics. This hypothesis is supported by the finding that GTP-initiated [^{125}I]HPIA dissociation from membrane-bound porcine atrial adenosine receptors is monophasic and occurs with a rate constant of approximately 1.3 min^{-1} (121), one order of magnitude greater than was observed in detergent solution. However, the present results are in accordance with the demonstration that guanine nucleotide-induced dissociation of the agonist radioligand [^{3}H]oxotremorine-M was slower in solubilized- than membrane-bound cardiac muscarinic receptor preparations (129). Questions involving the validity of the present kinetic measurements may be addressed in the absence of detergent by using purified components of the ternary complex in a reconstituted system.

Several potential reaction mechanisms are inconsistent with the kinetic behavior of GTPγS-initiated [^{125}I]HPIA dissociation. A bifurcated reaction scheme such as:

$$\begin{array}{ccccccccc} LRG & + & N & \rightleftharpoons & LRGN & \longrightarrow & L & + & R & + & GN \\ & & & & \downarrow\uparrow & & & & & & \\ & & & & L & + & RGN & & & & \end{array} \qquad \text{(Eq. IV-7)}$$

would not explain the observed biphasic GTPγS-initiated [^{125}I]HPIA dissociation kinetics. Such a reaction mechanism would predict that, at increasing concentrations of N, the fast phase of [^{125}I]HPIA dissociation would dominate the observed kinetics. However, consistent with the hypothesis of two parallel dissociation reactions described above, the amplitude of the slow phase increased with increasing nucleotide concentration. Rebinding of agonist is also unlikely to account for biphasic guanine nucleotide-initiated [^{125}I]HPIA dissociation kinetics. The results of [^{125}I]HPIA dissociation experiments in which 100 *μM* 2-CADO was added simultaneously with guanine nucleotide (GDP) were not qualitatively or quantitatively different from dissociation experiments done in the absence of 2-CADO (data not shown). This finding suggests that, at least in the instance of GDP-initiated [^{125}I]HPIA dissociation, rebinding of agonist does not contribute to the observed biphasic dissociation kinetics.

Adenosine receptor agonists inhibited [^{125}I]HPIA binding in a manner consistent with an interaction at A_1 adenosine receptors (102). Relative and absolute potencies of adenosine receptor agonists inhibiting [^{125}I]HPIA binding to solubilized cardiac adenosine receptors were nearly identical to experiments employing membrane-bound receptors (121). This finding indicates that the

pharmacological specificity of solubilized cardiac A_1 adenosine receptors is preserved in this detergent system. Interestingly, both the relative and absolute potency of (*S*)-PIA in the present experiments were decreased when compared to studies employing membrane-bound receptors (121). NECA and (*S*)-PIA were essentially equipotent inhibitors of [^{125}I]HPIA binding to membrane-bound porcine atrial adenosine receptors, whereas a 2-fold difference in apparent K_D values exists in solubilized receptor experiments. Moreover, the potency ratio for the diastereomers of PIA in the present experiments is 2-fold greater than that observed in experiments conducted with the membrane-bound receptors. These findings suggest that the enhanced potency of (*S*)-PIA in higher mammalian tissues (112,113,121) may not be a function of differences in receptor proteins *per se*, but rather due to other membrane-related factors such as differing lipid composition.

In summary, a detergent system consisting of digitonin and sodium cholate effectively solubilized cardiac A_1 adenosine receptors in good yield, afforded reasonable stability and preserved receptor-G protein interactions as well as pharmacological specificity. This solubilization procedure appears to be useful for biochemical characterization of cardiac adenosine receptors and the interaction of agonist radioligands with receptor-G protein complexes in detergent solution. Further studies are required to delineate to molecular events involved in the generation of two independent, non-interconvertible populations of cardiac adenosine receptor-G protein complexes.

FIGURE IV-1

A, [^{125}I]HPIA saturation isotherm in digitonin/cholate extracts of porcine atrial membranes. Specific binding (o) was defined as total binding (not shown) minus that occurring in the presence of 100 μM 2-CADO (o). Incubation conditions are described in *Methods*. The theoretical fit shown was obtained using Lundon I Saturation Analysis Software and is based on a B_{max} of 88 ± 4 fmol/mg protein and a K_D of 1.4 ± 0.1 nM. At a ligand concentration equal to its K_D, approximately 90% of total [^{125}I]HPIA binding was specific. *B*, Transformation of saturation binding data shown in *A* to a Scatchard-Rosenthal replot. The line drawn represents a best fit as determined by linear regression (R = 0.98) and gives a B_{max} of 91 ± 3 fmol/mg of protein and a K_D of 1.5 ± 0.2 nM. All points in Fig. IV-1 represent the mean ± S.E.M. of three independent experiments done in duplicate.

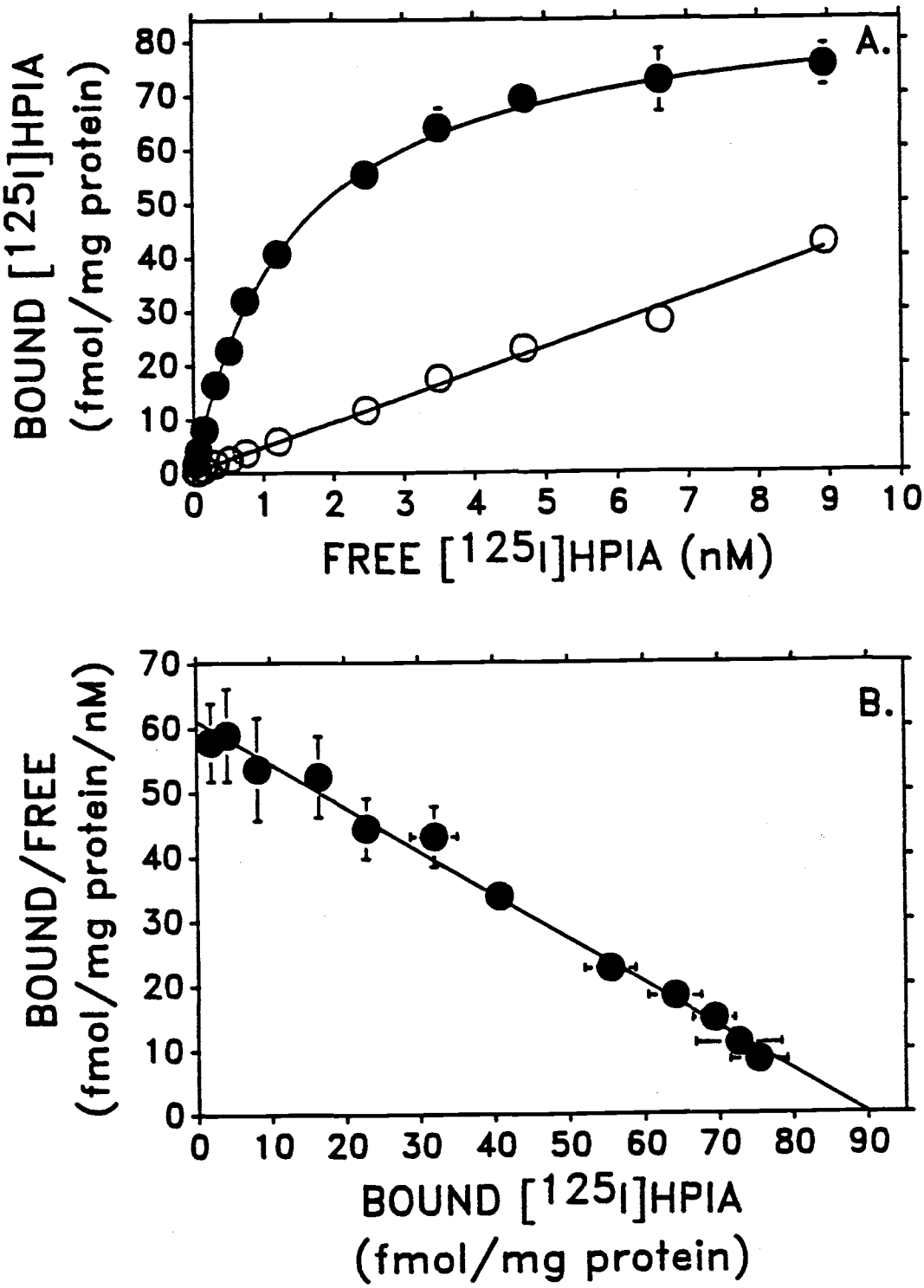
A.
BOUND [125I]HPIA
(fmol/mg protein)
FREE [125I]HPIA (nM)
B.
BOUND/FREE
(fmol/mg protein/nM)
BOUND [125I]HPIA
(fmol/mg protein)

FIGURE IV-1

FIGURE IV-2

A, [^{125}I]HPIA association experiments with the solubilized porcine atrial adenosine receptor. Experiments were carried out with a receptor concentration of 15-40 p*M* and indicated [^{125}I]HPIA concentrations (see below). Binding data were linearly transformed to a ln (percent [^{125}I]HPIA sites open) vs. time plot and fitted to equation IV-1 (lines drawn are based on these theoretical fits). Slopes of these lines correspond to $(-)\tau^{-1}$ for that concentration of [^{125}I]HPIA. This analysis yielded the following values for τ^{-1} (min^{-1}): 0.077 n*M* (●), (2.4 ± 0.1) x 10^{-2}; 0.44 n*M* (o), (3.6 ± 0.1) x 10^{-2}; 0.955 n*M* (x), (5.9 ± 0.3) x 10^{-2}; 1.86 n*M* (□), (9.6 ± 0.4) x 10^{-2}; 2.05 n*M* (▲), (1.0 ± 0.1) x 10^{-1}; 3.65 n*M* (△), (1.4 ± 0.1) x 10^{-1}; 4.51 n*M* (■), (1.66 ± 0.06) x 10^{-1}; 7.94 n*M* (◍), (3.0 ± 0.5) x 10^{-1}. All experiments were conducted over the course of 36 hours in the same solubilized receptor preparation. *B*, τ^{-1} as a function of [^{125}I]HPIA concentration in the solubilized receptor preparation. The line drawn represents that obtained by fitting data to equation IV-2 which yields a k_{+1} of (3.4 ± 0.1) x 10^7 M^{-1} min^{-1} and a k_{-1} of (2.45 ± 0.40) x 10^{-2} min^{-1}, giving a kinetically-derived K_D of 0.73 n*M*.

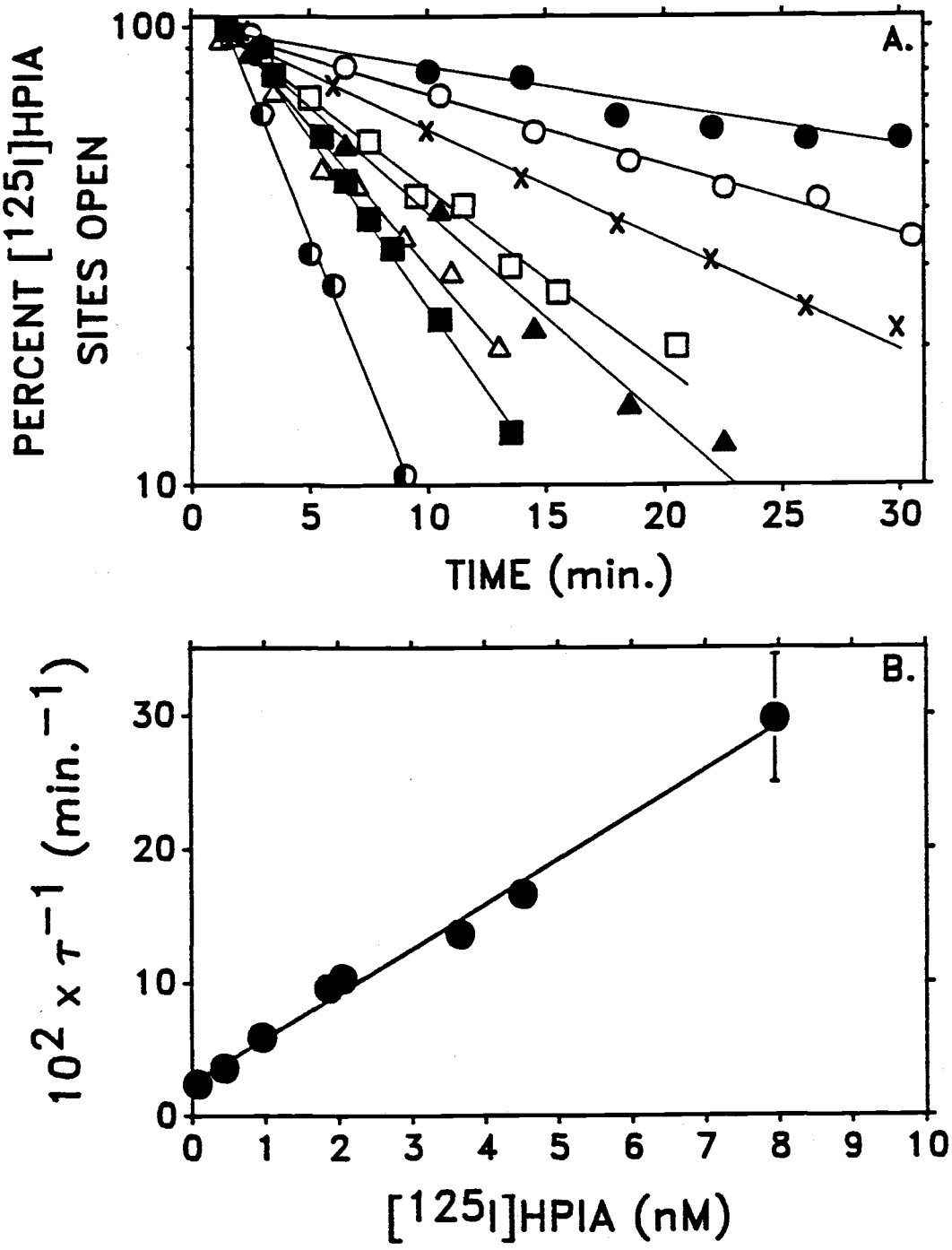
A.
PERCENT [125I]HPIA SITES OPEN
100
10
0
5
10
15
20
25
30
TIME (min.)
B.
$10^2 \times \tau^{-1}$ (min.$^{-1}$)
30
20
10
0
0
1
2
3
4
5
6
7
8
9
10
[125I]HPIA (nM)

FIGURE IV-2

FIGURE IV-3

[^{125}I]HPIA dissociation initiated by addition of 100 μM 2-CADO to an equilibrated mixture of [^{125}I]HPIA and solubilized cardiac A_1 adenosine receptors. Receptor and [^{125}I]HPIA concentration were approximately 50 and 750 pM, respectively. Data were fitted to equation IV-3A (line drawn is based on that fit) which gave a dissociation rate constant of (1.6 ± 0.1) x 10^{-2} min^{-1}. *Inset*, Semi-logarithmic transformation of dissociation data which was fitted by linear regression and generated an identical estimate for k_{-1}. This figure depicts an experiment representative of 3 such experiments.

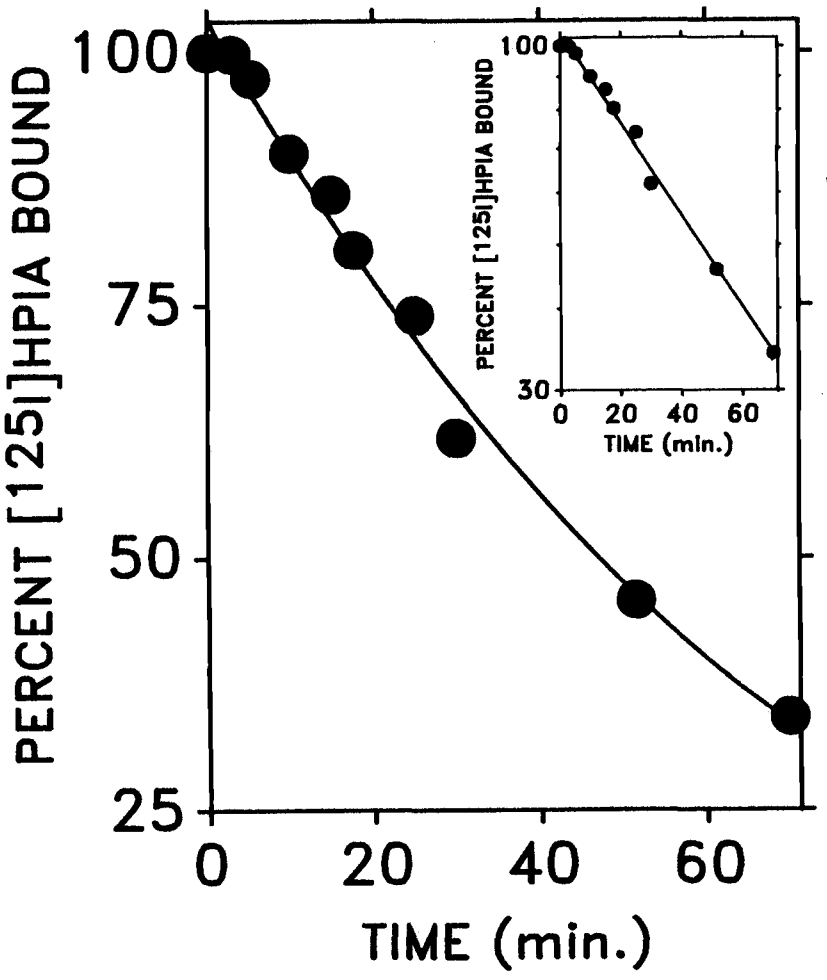
PERCENT [125I]HPIA BOUND
100
75
50
25
0
20
40
60
TIME (min.)
PERCENT [125I]HPIA BOUND
100
30
0
20
40
60
TIME (min.)

FIGURE IV-3

FIGURE IV-4

Guanine nucleotide modulation of [^{125}I]HPIA binding in solubilized porcine atrial adenosine receptor preparations. Receptor and [^{125}I]HPIA concentrations were approximately 40 and 750 p*M*, respectively. Each point represents the mean ± S.E.M. of 3-7 individual experiments. Titration curves drawn represent best fits as determined by EBDA software and give the following parameter estimates (IC_{50} ± S.E.M, n*M*): GTPγS, 64.1 ± 12; Gpp(NH)p, 138 ± 13; GTP, 2600 ± 700; GDP, 8000 ± 6500.

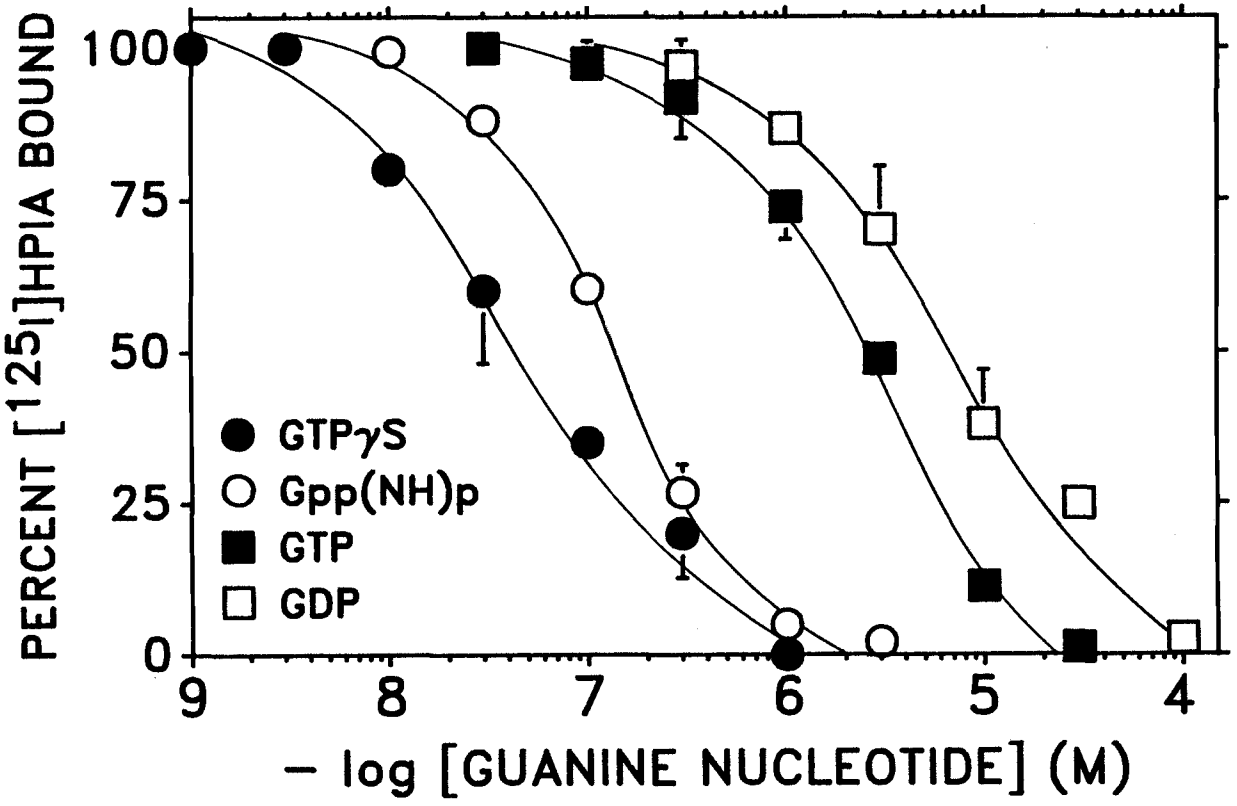
PERCENT [125I]HPIA BOUND
100
75
50
25
0
9
8
7
6
5
4
GTPγS
Gpp(NH)p
GTP
GDP
– log [GUANINE NUCLEOTIDE] (M)

FIGURE IV-4

FIGURE IV-5

Semi-logarithmic plot of percent [^{125}I]HPIA bound vs. time after addition of a saturating concentration of guanine nucleotide. Experimental conditions are as described in the legend of Fig. IV-4. Data were fitted to equation IV-3B (lines drawn are the results of those fits) which yielded the following parameter estimates (units of τ^{-1} are min^{-1}): GTPγS: 67% fast, $(\tau_1)^{-1}$ = (15.0 ± 0.3) x 10^{-2}, 33% slow, $(\tau_2)^{-1}$ = (7.6 ± 1.0) x 10^{-2}; Gpp(NH)p: 37% fast, $(\tau_1)^{-1}$ = (11.7 ± 0.7) x 10^{-2}, 63% slow, $(\tau_2)^{-1}$ = (3.7 ± 0.2) x 10^{-2}; GTP: 53% fast, $(\tau_1)^{-1}$ = (19.5 ± 2.1) x 10^{-2}, 47% slow, $(\tau_2)^{-1}$ = (5.9 ± 0.4) x 10^{-2}; GDP: 54% fast, $(\tau_1)^{-1}$ = (9.0 ± 0.5) x 10^{-2}, 46% slow, $(\tau_2)^{-1}$ = (3.2 ± 0.4) x 10^{-2}.

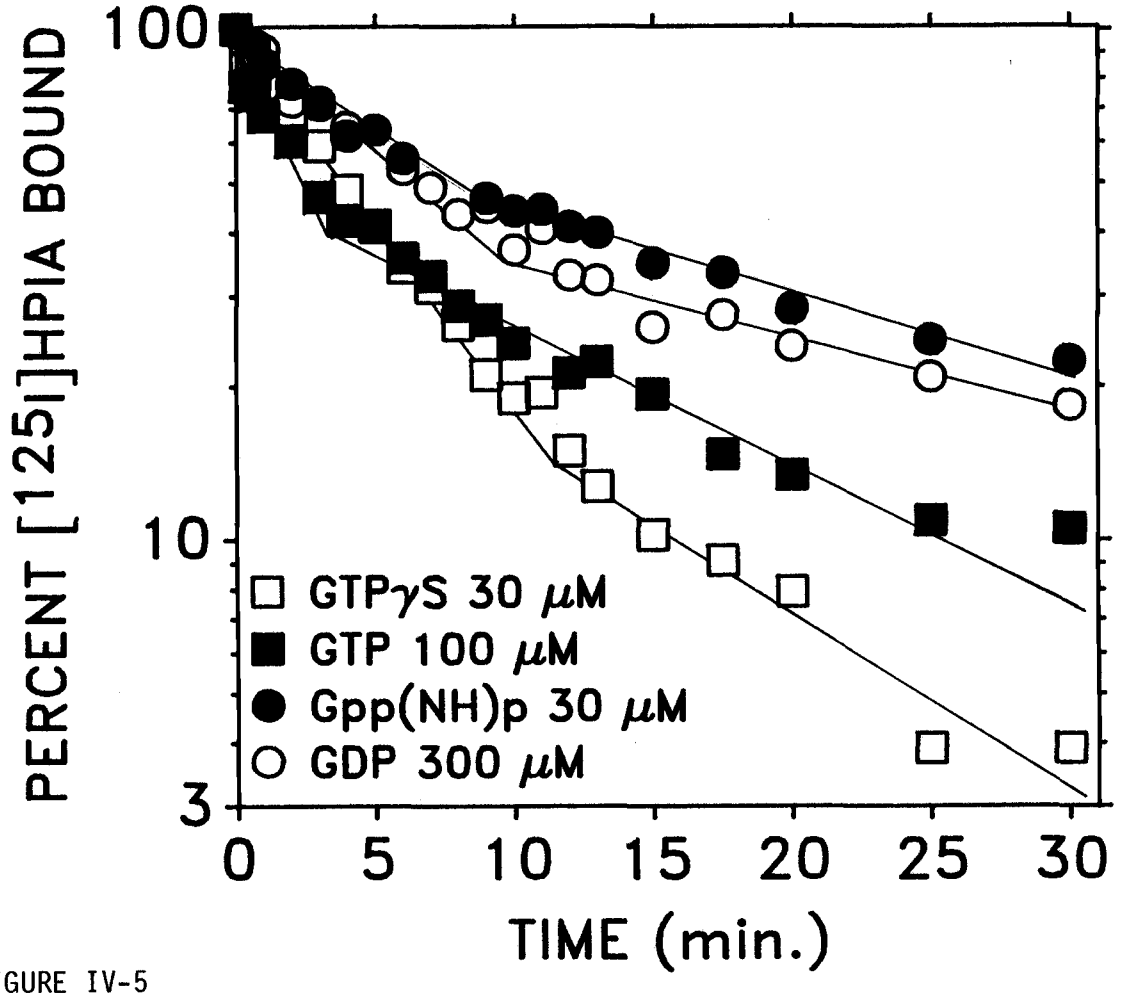
PERCENT [125I]HPIA BOUND
100
10
3
0
5
10
15
20
25
30
TIME (min.)
GTPγS 30 μM
GTP 100 μM
Gpp(NH)p 30 μM
GDP 300 μM

FIGURE IV-5

FIGURE IV-6

Dissociation of specifically bound [^{125}I]HPIA from the solubilized porcine atrial adenosine receptor initiated by GTPγS. 0.7-0.8 n*M* [^{125}I]HPIA was allowed to equilibrate with a solubilized porcine atrial adenosine receptor preparation (50 p*M* and 215 n*M* in adenosine receptor and [^{35}S]GTPγS sites, respectively) for 120 minutes, at which time dissociation was initiated by addition of the indicated concentrations of GTPγS (see below). *A*, 15 concentrations of GTPγS were used to initiate [^{125}I]HPIA dissociation, of which 6 are shown here. Theoretical curves drawn are based on parameter estimates obtained by fitting data to equations IV-3B. *Key*: ●, 10 n*M*; o, 30 n*M*; ■, 100 n*M*; □, 300 n*M*; ▲, 12 μ*M*; △, 30 μ*M*. *B*, Reciprocal relaxation times for the fast phase of GTPγS-initiated [^{125}I]HPIA dissociation vs. GTPγS concentration. Data were fitted with equation IV-4 which gave a k_{-1} for the fast phase of GTPγS-initiated [^{125}I]HPIA dissociation of (1.3 ± 0.1) x 10^{-1} min^{-1} and a K_D for GTPγS of 86 ± 20 n*M*. *Inset*, magnification of abscissa in the range of 0 - 1 μ*M* GTPγS concentration. Shown is the same theoretical fit described above. *C*, reciprocal relaxation times for the slow phase of GTPγS-initiated [^{125}I]HPIA dissociation vs. GTPγS concentration. Data were fitted as described in *B*, giving a k_{-1} for the slow phase of GTPγS-initiated [^{125}I]HPIA dissociation of (7.6 ± 0.3) x 10^{-2} min^{-1} and a K_D for GTPγS of 481 ± 76 n*M*. *Inset*, magnification of abscissa in the range of 0 - 1 μ*M* GTPγS concentration (same theoretical fit).

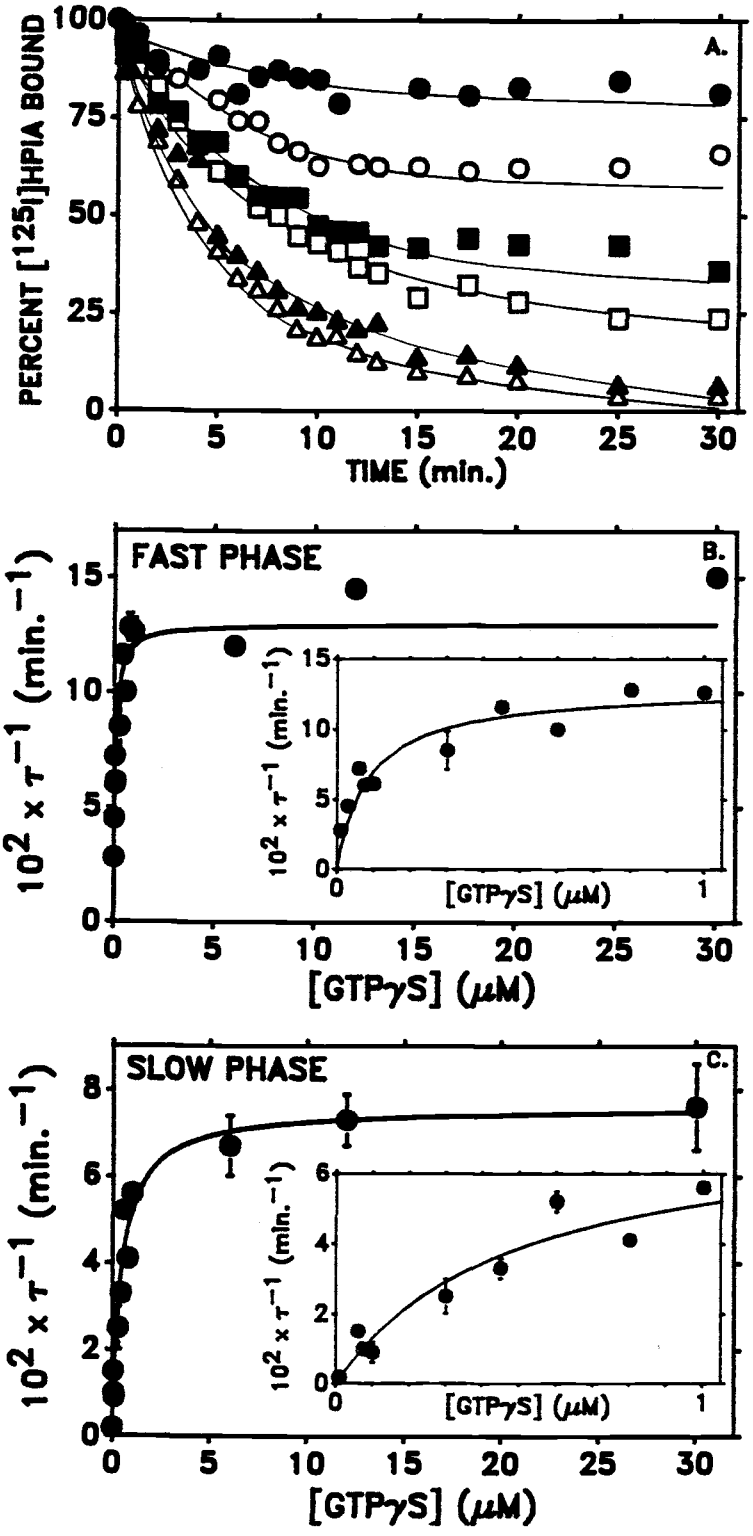
A.
PERCENT [125I]HPIA BOUND
TIME (min.)
B.
FAST PHASE
$10^2 \times \tau^{-1}$ (min.$^{-1}$)
[GTPγS] (μM)
C.
SLOW PHASE
$10^2 \times \tau^{-1}$ (min.$^{-1}$)
[GTPγS] (μM)

FIGURE IV-6

FIGURE IV-7

Adenosine receptor agonists and antagonists inhibiting the binding of [^{125}I]HPIA in solubilized porcine atrial adenosine receptor preparations. Receptor and [^{125}I]HPIA concentrations were fixed at approximately 40 and 750 p*M*, respectively. Each point represents the mean ± S.E.M. of 3-5 experiments. Lines drawn represent best fits as determined by EBDA software. Parameter estimates used in curve fitting are given in table 1 (*Theo.* = *Theophylline*).

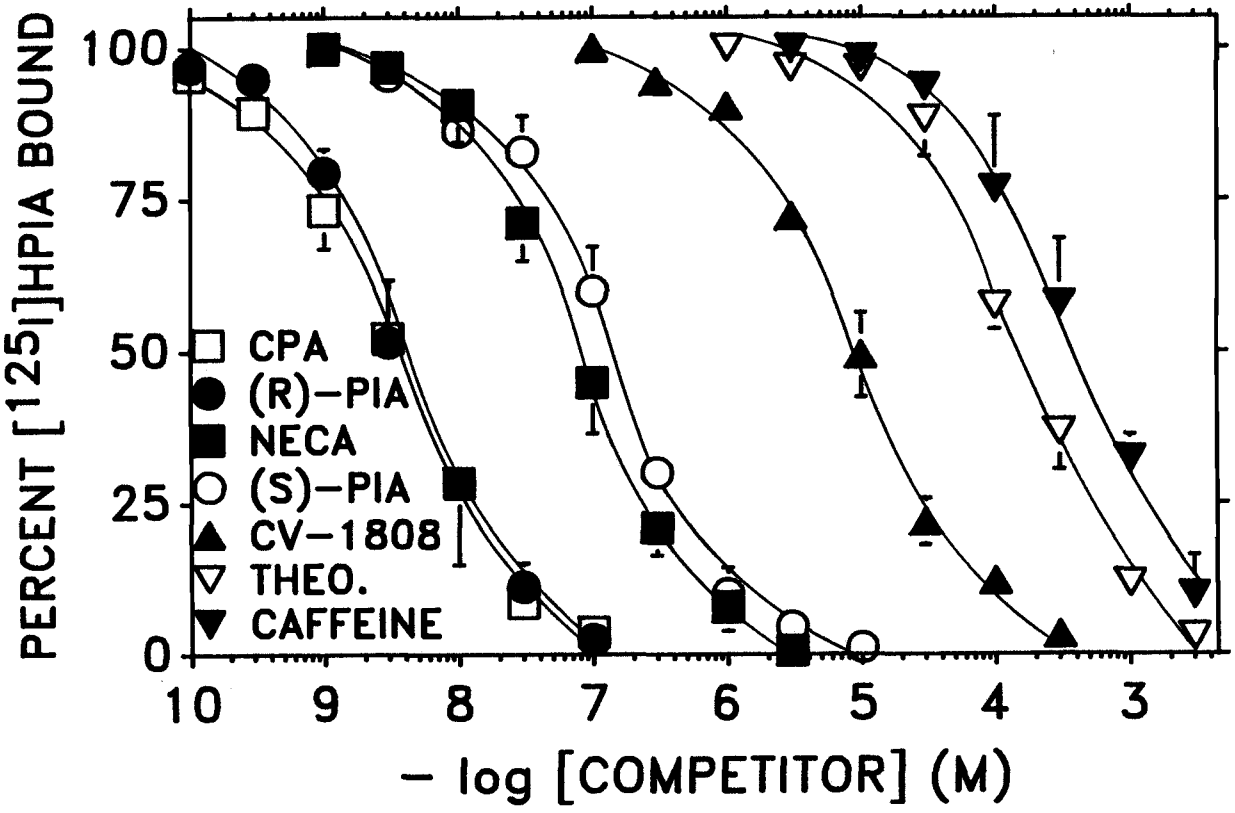
PERCENT [125I]HPIA BOUND
100
75
50
25
0
CPA
(R)–PIA
NECA
(S)–PIA
CV–1808
THEO.
CAFFEINE
10
9
8
7
6
5
4
3
– log [COMPETITOR] (M)

FIGURE IV-7

TABLE IV-1

Adenosine receptor agonists and antagonists inhibiting specific binding of [^{125}I]HPIA to the solubilized porcine atrial adenosine receptor. Receptor and [^{125}I]HPIA concentrations were approximately 40 and 750 p*M*, respectively. Parameter estimates were obtained using EBDA and represent the mean ± S.E.M. of 3-5 experiments.

COMPOUND	APPARENT K_D (n*M*)	SLOPE FACTOR
CPA	2.1 ± 0.8	0.98 ± 0.06
(*R*)-PIA	2.2 ± 0.5	1.01 ± 0.005
NECA	49 ± 11	1.05 ± 0.06
(*S*)-PIA	94 ± 20	0.95 ± 0.06
CV-1808	5640 ± 1940	1.00 ± 0.1
THEOPHYLLINE	106,000 ± 9000	1.08 ± 0.04
CAFFEINE	264,000 ± 95,000	1.00 ± 0.04

TABLE IV-2 Comparison of the binding properties of [^{125}I]HPIA to membrane-bound and solubilized porcine atrial A_1 adenosine receptors.

	MEMBRANE BOUND	SOLUBILIZED RECEPTOR
1. Mechanism of binding	Simple Bimolecular	Simple Bimolecular
2. k_{+1} (M^{-1} min^{-1})	$(1.9 \pm 0.2) \times 10^7$	$(3.36 \pm 0.10) \times 10^7$
3. k_{-1} (extrapolated, min^{-1})	$(4.5 \pm 0.1) \times 10^{-2}$	$(2.45 \pm 0.40) \times 10^{-2}$
4. k_{-1} (measured, min^{-1})	$(1.6 \pm 0.2) \times 10^{-2}$	$(1.6 \pm 0.1) \times 10^{-2}$
5. K_D (equilibrium)	2.5 ± 0.4 n*M*	1.4 ± 0.1 n*M*
6. K_D (kinetic)	2.4 n*M*	0.73 n*M*
7. B_{max} (fmol/mg of protein)	35 ± 3	88 ± 4
8. Specific binding at K_D	~ 35%	~ 90%
9. Agonist inhibition profile	CPA = (*R*)-PIA > NECA = (*S*)-PIA	CPA = (*R*)-PIA > NECA > (*S*)-PIA
10. Guanine nucleotide inhibition	70-80%	100%
11. Guanine nucleotide inhibition profile	Gpp(NH)p > GTPγS > GDP = GTP	GTPγS > Gpp(NH)p > GTP > GDP

ACKNOWLEDGMENTS

The authors gratefully acknowledge skillful membrane preparation done by Laurie Shoots, receptor solubilization done by Tony Lopez and the very helpful advice of Drs. Paul H. Franklin, Gary L. Peterson, Michael R. Tota and David J. Broderick.

CHAPTER V

DISCUSSION

Porcine atrial adenosine receptors which mediate cardioinhibitory effects of the nucleoside have been pharmacologically characterized. Due to the extremely low density of atrial adenosine receptors and the paucity of useful radioligands for this tissue, few attempts have been made to rigorously characterize this receptor. Such a low density of cardiac adenosine receptors is somewhat difficult to reconcile with the profound inhibitory effects of the nucleoside on nearly every parameter of myocardial function and suggests a functional localization of adenosine receptors within the myocardium. Such a localization has been recently described in guinea pig ventricle by Parkinson and Clanachan (72). Cardiac adenosine receptors (as labeled by [^{3}H]DPCPX using quantitative autoradiography) were found to be almost exclusively associated with ventricular conduction cells and in very low density on ventricular myocytes (72). However, adenosine uptake sites (responsible, in part, for termination of the action of the nucleoside) were uniformly distributed throughout ventricular tissue (72). This regional distribution of adenosine receptors in guinea pig ventricle may be involved in the exquisite sensitivity of this species to AV

nodal block induced by adenosine (1). The possibility of a regional distribution of adenosine receptors in atria has not yet been investigated, however, one may predict that these receptors would be localized to the SA node and surrounding tissue.

The present studies have used both agonist and antagonist radioligands to characterize atrial adenosine receptors. The antagonist radioligand, [^{3}H]DPCPX, proved to be particularly useful in studies employing membrane-bound atrial adenosine receptors. Agonist titration of [^{3}H]DPCPX binding allowed the first quantification of multiple agonist affinity states of a cardiac adenosine receptor. The observation that guanine nucleotides shifted agonist titration of [^{3}H]DPCPX binding from a two- to a one-site model of low affinity indicates that the high agonist affinity state of the receptor is derived exclusively from ternary complex formation in atrial membrane preparations. Kinetic characteristics of [^{3}H]DPCPX binding have not been previously investigated in any tissue. With regard to association rate experiments, a linear dependence of τ^{-1} on radioligand concentration suggests that [^{3}H]DPCPX interacts with the membrane-bound atrial adenosine receptor via a simple bimolecular reaction. However, it is possible that more complex association rate kinetics would be observed at higher [^{3}H]DPCPX concentrations. To investigate this possibility will require use of more sophisticated equipment, such as a stopped-flow apparatus (the half-time of association at 13 n*M* [^{3}H]DPCPX is approximately 45 seconds under these experimental conditions) but is certainly feasible with this radioligand.

[^{125}I]HPIA was only a marginally useful ligand for characterization of membrane-bound atrial adenosine receptors. Under ideal conditions, approximately 35% of total [^{125}I]HPIA binding was specific at a concentration equal to the K_D of the radioligand. This factor made exceeding concentrations of approximately 4 n*M* in equilibrium saturation or kinetic experiments extremely difficult due to diminished signal to noise ratios. Nonetheless, some novel observations were made over the course of these studies. It was found that τ^{-1} for association of this radioligand with membrane-bound atrial adenosine receptors was linearly dependent on [^{125}I]HPIA concentration. This finding would appear to be inconsistent with currently accepted models of receptor-G protein interactions (104):

$$H + R + \underset{\text{GDP}}{G_{\alpha\beta\gamma}} \overset{\text{FAST}}{\rightleftharpoons} HR + \underset{\text{GDP}}{G_{\alpha\beta\gamma}} \overset{\text{SLOW}}{\rightleftharpoons} \boxed{\underset{\text{GDP}}{HRG_{\alpha\beta\gamma}}} + GTP \overset{\text{FAST}}{\longrightarrow} H + R + \underset{\text{GTP}}{G_{\alpha}} + G_{\beta\gamma}$$

In this model, hormone or agonist radioligand (H) binds to free receptor (R) and HR interacts with a holo-G protein ($G_{\alpha\beta\gamma}$) via a reaction involving a conformational change to form a ternary complex (boxed). This ternary complex possesses high affinity for agonists and represents the source from which the signal measured in these experiments exclusively arises. Implicit in this model is that the step involving a conformational change is much slower than that of agonist binding to the free receptor, the latter of which approaches diffusion-limited kinetics (141). One may expect that

values of τ^{-1} for agonist association would be hyperbolically-dependent on [^{125}I]HPIA concentration and approach a limiting value corresponding to rate constant for the conformational change. However, since τ^{-1} for association of [^{125}I]HPIA with membrane-bound atrial adenosine receptors was linearly-dependent on ligand concentration, this model would not appear to properly describe the binding mechanism of this radioligand. A model that does describe the interaction of [^{125}I]HPIA with the membrane-bound atrial adenosine receptor is the following:

$$H + \underset{\text{GDP}}{RG_{\alpha\beta\gamma}} \overset{\text{FAST}}{\rightleftharpoons} \underset{\text{GDP}}{HRG_{\alpha\beta\gamma}} + GTP \overset{\text{FAST}}{\longrightarrow} H + R + \underset{\text{GTP}}{G_{\alpha}} + G_{\beta\gamma}$$

This model implies that the atrial adenosine receptor is precoupled (in the absence of agonist) to a G protein under these experimental conditions (5 m*M* $MgCl_2$, 37°C). α_2 adrenergic receptors have also been demonstrated to be precoupled to a G protein in human platelet membranes (141). Interestingly, α_2 receptors, like A_1 receptors, are coupled to adenylyl cyclase in an inhibitory manner via an interaction with G_i (141).

An alternative explanation for the observed [^{125}I]HPIA association rate kinetics is that [^{125}I]HPIA concentrations used in these experiments may simply have represented the initial linear phase of a rectangular hyperbola. In this case, [^{125}I]HPIA concentrations would be sufficiently low such that corresponding τ^{-1} values would not have exceeded the rate constant for

conformational change and the latter step would not appear rate-limiting. To resolve this issue would require use of [^{125}I]HPIA concentrations far greater that that which is technically feasible (see above). In any event, a kinetically-derived K_D was in excellent agreement with that parameter determined by equilibrium saturation analysis, assuming a simple bimolecular binding mechanism (2.4 and 2.5 n*M*, respectively).

Nearly all of the properties of membrane-bound atrial adenosine receptors, with respect to agonist radioligand binding, were found to be preserved after detergent solubilization. The mixed-detergent, double-extraction procedure employed in these studies afforded a 2.5-fold enrichment of adenosine receptor specific activity relative to porcine atrial membrane preparations. Technical aspects of radioligand binding experiments in solubilized receptor preparations were greatly facilitated by an enhanced signal to noise ratio of [^{125}I]HPIA binding (90% specific binding at K_D as compared to 35% specific binding in membrane preparations). This improved signal allowed a much more in-depth characterization of agonist radioligand interactions with atrial adenosine receptors. In addition, observations, questions and ambiguities which arose while conducting experiments with membrane-bound atrial adenosine receptors were more definitively answered using solubilized receptor preparations. In solubilized receptor preparations, it was conclusively shown that [^{125}I]HPIA interacted exclusively with a precoupled atrial adenosine receptor and this interaction was consistent with a simple bimolecular binding mechanism over a 100-fold range of radioligand

concentration. As indicated, atrial adenosine receptor maintain the ability to interact with G proteins in detergent solution. While such is not the case for some G protein-coupled receptors (muscarinic acetylcholine [126] and some catecholaminergic [127-129] receptors), it is not unprecedented. For example, α_2 adrenergic (142), D-2 dopamine (143), glucagon (144), fMet-Leu-Phe (145), neurotensin (146), serotonin 5-HT_{1A} (147), somatostatin (148), substance P (149), δ opioid (150), vasoactive intestinal peptide (151), vasopressin V_2 (152) and brain A_1 adenosine (42,45,122,123) receptors have all been shown to interact with G proteins in detergent solution.

The binding of the agonist radioligand [^{125}I]HPIA to solubilized atrial adenosine receptors was 100% sensitive to negative modulation by guanine nucleotides. All guanine nucleotides tested (GTP, GDP, Gpp(NH)p and GTPγS) elicited rapid and complete [^{125}I]HPIA dissociation which could be resolved into two kinetic phases. To address the mechanism by which guanine nucleotides induced biphasic agonist radioligand dissociation, kinetic characteristics of GTPγS-induced [^{125}I]HPIA dissociation were studied over a wide range of GTPγS concentration. Biphasic [^{125}I]HPIA dissociation was observed at every concentration of GTPγS examined and the magnitude of reciprocal relaxation times for each kinetic phase was observed to be hyperbolically-dependent on GTPγS concentration. The simplest model to explain this kinetic behavior was presented in chapter IV and involves the interaction of solubilized atrial adenosine receptors with two distinct populations

of G proteins possessing differing affinities for guanine nucleotide. While the nature of the proposed G protein heterogeneity remains unknown, several speculations can be made. As suggested in chapter IV, the atrial adenosine receptor may interact with two distinct G proteins, such as G_i and G_o. There is evidence for the existence of both G proteins in heart, albeit not in this species (132-138). Another possibility is that the atrial adenosine couples to isoforms of G_i. Linden's group has recently shown that bovine brain A_1 adenosine receptors copurify with $G_{i\alpha 1}$, $G_{i\alpha 3}$ and G_o (153). In addition, partially-purified brain adenosine receptors functionally interacted with these G proteins, but not $G_{i\alpha 2}$, in a reconstituted system (154). All three isoforms of G_i, as well as G_o, are expressed in atria (132-138,155). Thus, the possibility exists that biphasic guanine nucleotide-initiated [^{125}I]HPIA dissociation may arise from interaction of atrial adenosine receptors with distinct G proteins or isoforms of the same G protein.

The solubilized atrial adenosine receptor has recently been characterized with the antagonist radioligand [^{3}H]DPCPX (156). The enrichment of adenosine receptor specific activity upon solubilization was confirmed using this antagonist radioligand. However, while the solubilized receptor displayed an affinity for [^{125}I]HPIA comparable to the membrane-bound receptor (1.4 and 2.5 n*M*, respectively), the affinity of this receptor for [^{3}H]DPCPX was approximately 10-fold less than that of the membrane-bound receptor (4.7 and 0.4 n*M*, respectively). Moreover, preliminary kinetic experiments suggest that the association of [^{3}H]DPCPX with the

solubilized receptor is inconsistent with a simple bimolecular interaction (Leid, unpublished data). The influence of detergent solution on antagonist, but not agonist, binding properties suggests that the presence of digitonin/cholate may alter the accessibility of a hydrophobic binding domain on the receptor to the antagonist radioligand [^{3}H]DPCPX. Much more work will be required to rigorously address this issue.

An original goal of this thesis was to purify the atrial adenosine receptor to homogeneity in order to study interaction of purified receptor and G protein(s) in reconstituted systems, for physical studies, and as a first step in the molecular cloning of the gene encoding this protein. Purification of the receptor was not accomplished over the course of this thesis primarily due to the exceedingly low density of the receptor in atria and extreme lability of the resolved protein (Leid et al., unpublished data). Nonetheless, these studies represent a framework upon which further work, aimed at elucidating the mechanism(s) by which adenosine modulates myocardial function, may be built.

BIBLIOGRAPHY

1. Drury, A.N. and A. Szent-Györgyi. *J. Physiol. (Lond.)* 68:213-226 (1929).

2. Londos, C., D.M.F. Cooper, W. Schlegel, and M. Rodbell. *Proc. Natl. Acad. Sci U.S.A.* 75:5362-5366 (1978).

3. Londos, C., D.M.F. Cooper, and J. Wolff *Proc. Natl. Acad. Sci U.S.A.* 77:2551-2554 (1980).

4. Snyder, S.H., J.J. Katims, Z. Annau, R.F. Bruns, and J.W. Daly. *Proc. Natl. Acad. Sci U.S.A.* 78:3260-3264 (1981).

5. Hedqvist, P., B. Fredholm, and S. Olundh. *Circ. Res.* 43:592-598 (1978).

6. Murray, T.F., D. Sylvester, C.S. Schultz and P. Szot. *Neuropharmacol.* 24:761-766 (1985).

7. Daly, J.W. *J. Med. Chem.* 25:197-207 (1982).

8. Wolberg, G., T.P. Zimmerman, G.S. Duncan, K.H. Singer, and G.B. Elion. *Biochem. Pharmacol.* 27:1487-1495 (1978).

9. Fredholm, B.B. *Eur. J. Resp. Dis.* 61:29-36 (1980).

10. Petrack, B., A.J. Czernik, J. Ansell, and J. Cassidy. *Life Sci.* 28:2611-2615 (1981).

11. Born, G.V.R., R.J. Haslam, M. Gelman, and R.D. Lowe. *Nature (Lond.)* 205:678-680 (1975).

12. McKenzie, S.G., R. Frew, and H.-P. Baer. *Eur. J. Pharmacol.* 41:183-192 (1977).

13. Fredholm. B.B., K. Brodin, and K. Strandberg. *Acta Pharmacol. Toxicol.* 45:336 (1979).

14. Buckle, P.J. and I. Spence. *Naunyn-Schmiedeberg's Arch. Pharmacol.* 316:64-68 (1981).

15. Murphy. K.M.M. and S.H. Snyder. *Life Sci.* 28:917-920 (1981).

16. Sparks, H.V. and H. Bardenheuer. *Circ. Res.* 58:193-201 (1986).

17. Schrader, J., in *Regulatory Functions of Adenosine*, Berne, R.M., T.W. Rall, and R. Rubio, eds., Martinus Nijhoff, Boston, 1983, pp. 133-156.

18. Pearson, J.D. and J.L. Gordon. *Ann. Rev. Physiol.* **47**:617-627 (1985).

19. Su, C. *Ann. Rev. Physiol.* 47:665-676 (1985).

20. Lloyd, H.G.E., A. Deussen, H. Wupperman and J. Schrader. *Biochem. J.* **252**:489-494 (1988).

21. Deussen, A., M. Borst, and J. Schrader. *Circ. Res.* **63**:240-249 (1988).

22. Deussen, A., M. Borst, K. Kroll and J. Schrader. *Circ. Res.* **63**:250-261 (1988).

23. Newby, A.C. *Biochem. J.* **253**:123-130 (1988).

24. Headrick, J.P. and R.J. Willis. *Biochem. J.* **261**:541-550 (1989).

25. Richardt, G., W. Waas, R. Kranzhöfer, E. Mayer, and A. Schömig. *Circ. Res.* **61**:117-123 (1987).

26. Sattin, A. and T.W. Rall. *Mol. Pharmacol.* **6**:13-23 (1970)

27. Shimizu, H. and J.W. Daly. *Biochem. Biophys. Acta* **22**:465-473 (1970).

28. Burnstock, G. *Pharmacol. Rev.* 24:509-581 (1972).

29. Burnstock, G., in *Cell Membrane Receptors for Drugs and Hormones*, Bolis, L and R.W. Straub, eds., Raven, New York, 1978, pp. 107-118.

30. Van Calker, D., M. Muller, and B. Hamprecht. *J. Neurochem.* **33**:999-1005 (1979).

31. Belardinelli, L., J. Linden, and R.M. Berne. *Prog. Cardiovasc. Dis.* **32**:73-97 (1989).

32. Stiles, G.L., D.T. Daly, and R.A. Olsson. *J. Biol. Chem.* **260**:10806-10811 (1985).

33. Choca, J.I., M.W. Kwatra, M.M. Hosey, and R.D. Green. *Biochem. Biophys. Res. Comm.* **131**:115-121 (1985).

34. Klotz, K.-N., G. Cristalli, M. Grifantini, S. Vittori, and M.J. Lohse. *J. Biol. Chem.* 260:14659-14664 (1985).

35. Stiles, G.L. *J. Biol. Chem.* **261**:10839-10843 (1986).

36. Lohse, M.J., K.-N. Klotz, and U. Schwabe. *Mol. Pharmacol.* **30**:403-409 (1986).

37. Klotz, K.-N. and M.J. Lohse. *Biochem. Biophys. Res. Comm.* **140**:406-413.

38. Stiles, G.L. and K.A. Jacobson. *Mol. Pharmacol.* **32**:184-188 (1987).

39. Earl, C.Q., A. Patel. R.H. Craig, S.M. Daluge, and J. Linden. *J. Med. Chem.* **31**:752-756 (1988).

40. Green, A., C.A. Stuart, R.A. Pietrzyk, and M. Partin. *FEBS Letters* **206**:130-134 (1986).

41. Patel. A., R.H. Craig, S.M. Daluge, and J. Linden. *Mol. Pharmacol.* **33**:585-591 (1988).

42. Stiles, G.L. *J. Biol. Chem.* **260**:6728-6732 (1985).

43. Nakata, H. and H. Fujisawa. *FEBS Letters* **158**:93-97 (1983).

44. Cooper, D.M.F., S.-M.H. Yeung, E. Perez-Reyes, J.R. Owens, L.H. Fossom, and D.L. Gill. *Adv. Cyclic Nucleotide Res.* **19**:75-86 (1985).

45. Yeung, S.-M.H., E. Perez-Reyes and D.M.F. Cooper. *Biochem. J.* **248**:635-642 (1987).

46. Nakata, H. *Soc. Neurosci. Absts.* **15**:233 (1989).

47. Barrington, W.W., K.A. Jacobson, A.J. Hutchinson, M. Williams, and G.L. Stiles. *Proc. Natl. Acad. Sci. U.S.A. in press* (1989).

48. Berne, R.M. *Am. J. Physiol.* **204**:317-322 (1963).

49. Sollevi, A. *Prog. Neurobiol.* **27**:319-349 (1986).

50. Dole, W.P. *Prog. Cardiovasc. Dis.* **29**:293-323 (1987).

51. Kroll, K., E.O. Feigl. *Am. J. Physiol.* **249**:H1176-H1187 (1985).

52. Spielman, W.S., L.J. Arend, and J.N. Forrest, in *Topics and Perspectives in Adenosine Research*, Gerlach, E. and B.F. Becker, eds., Springer-Verlag, Heidelberg, 1987, pp. 249-260.

53. Berne, R.M., R.M. Knabb, S.W. Ely, and R. Rubio. *Fed. Proc.* **42**:3136-3142 (1983).

54. Berne, R.M. *Circ. Res.* **47**:807-813 (1980).

55. Sollevi, A. and B. Fredholm. *Acta Physiol. Scand.* **112**:293-298 (1981).

56. Ganger, H.J. and C.P. Norris. *Circ. Res.* **46**:764-770 (1980).

57. Schutz, W., O. Kraupp, S. Bacher, and G. Raberger. *Basic Res. Cardiol* **78**:679-684 (1983).

58. Kusachi, S., R.D. Thompson, and R.A. Olsson. *J. Pharmacol. Exp. Ther.* **227**:316-321 (1983).

59. Herlihy, J.T., E.L. Bockman, R.M. Berne and R. Rubio. *Am. J. Physiol.* **230**:1239-1243 (1976).

60. Ribeiro, J.A. and A.M. Sebastiao. *Prog. Neurobiol.* **26**:179-209 (1986).

61. Long, C.J. and T.W. Stone. *J. Pharm Pharmacol* **39**:1010-1014 (1987).

62. Kurtz, A. *J. Biol. Chem.* 262:6296-6300 (1987).

63. Fredholm, B. and A. Sollevi. *Clin. Physiol.* **6**:1-21 (1986).

64. West, G.A. and L. Belardinelli. *Pflugers Arch. Eur. J. Physiol.* **403**:66-74 (1985).

65. Szentmiklosi, A.J., M. Nemeth, J. Szegi, J.G. Papp, and L Szekeres. *Naunyn-Schmiedeberg's Arch. Pharmacol.* **311**:147-149 (1980).

66. Heller, L.J. and R.A. Olsson. *Am. J. Physiol.* **248**:H907-H913 (1985).

67. Coffin, V.L. and R.D. Spealman. *J. Pharmacol. Exp. Ther.* **241**:76-83 (1987).

68. Evans, D.B. and J.A. Schenden. *Life Sci.* **31**:2425-2432 (1982).

69. Belardinelli, L., F.L. Belloni, R. Rubio, and R.M. Berne. *Circ. Res.* **47**:684-691 (1980).

70. Belardinelli, L., G.A. West, and H.F. Clemo, in *Topics and Perspectives of Adenosine Research*, Gerlach, E. and B.F. Becker, eds., Springer-Verlag, Heidelberg, 1987, pp. 344-355.

71. Clemo, H.F. and L. Belardinelli. *Circ. Res.* **59**:427-436 (1986).

72. Parkinson, F.E. and A.S. Clanachan. *Am. J. Physiol. in press* (1989).

73. Dobson, J.G. *Circ. Res.* **52**:151-160 (1983).

74. Bruckner, R., A. Fenner, W. Meyer, T.M. Nobis, W. Schmitz and H. Scholz. *J. Pharmacol. Exp. Ther.* 234:766-773 (1985).

75. DeGubareff, T. and W. Sleator. *J. Pharmacol. Exp. Ther.* 148:202-214 (1965).

76. Dobson, J.G. *Am. J. Physiol.* 245:H468-H474 (1983).

77. Baumann, G., J. Schrader, and E. Gerlach. *Circ. Res.* 48:259-266 (1981).

78. Dobson, J.G. *Am. J. Physiol.* 245:H475-H480 (1983).

79. Bohm, M., R. Bruckner, W. Meyer, M. Nose, W. Schmitz, H. Scholz, and J. Starbatty. *Naunyn-Schmiedeberg's Arch. Pharmacol.* 331:131-139 (1985).

80. Dobson, J.G. *Circ. Res.* 43:785-792 (1978).

81. Schrader, J., G. Baumann and E. Gerlach. *Pflugers Arch. Eur. J. Physiol.* 372:29-35 (1977).

82. Jochem, G. and H. Nawrath. *Experentia* 39:1347-1349 (1983).

83. Pfaffinger, P.J., J.M. Martin, D.D. Hunter, N.M. Nathanson and B. Hille. *Nature (Lond.)* 317:536-538 (1985).

84. Kurachi, Y., T. Nakajima and T. Sugimoto. *Pflugers Arch. Eur. J. Physiol.* 407:264-274 (1986).

85. Hazeki, O. and M. Ui. *J. Biol. Chem.* 256:2856-2862 (1981).

86. Linden, J., C. E. Hollen, and A. Patel. *Circ. Res.* 56:728-735 (1985).

87. Martens, D., M. J. Lohse, B. Rauch, and U. Schwabe. *Naunyn-Schmiedeberg's Arch. Pharmacol.* 336:342-348 (1987).

88. Schutz, W., M. Freissmuth, V. Hausleithner, and E. Tuisl. *Naunyn-Schmiedeberg's Arch. Pharmacol.* 333:156-162 (1986).

89. Blair, T.A., M. Parenti, and T. F. Murray. *Mol. Pharmacol.* 35:661-670 (1989).

90. Isenberg, G. and L. Belardinelli. *Circ. Res.* 55:309-325 (1984).

91. Delahunty, T.M., M.J. Cronin, and J. Linden. *Biochem. J.* 255:69-77 (1988).

92. Petcoff, D.W. and D.M.F. Cooper. *Eur. J. Pharmacol.* 137:269-271 (1987).

93. Kendall, D.A. and S.J. Hill. *J. Neurochem.* **50**:497-502 (1988).

94. Clemo, H.F., A. Bourassa, J. Linden and L. Belardinelli. *J. Pharmacol. Exp. Ther.* **242**:478-484 (1987).

95. Lohse, M., D. Ukena and U. Schwabe. *Naunyn-Schmiedeberg's Arch. Pharmacol.* **328**:310-316 (1985).

96. Leid, M., P.H. Franklin, and T.F. Murray. *Soc. Neurosci. Absts.* **13**:1487 (1987).

97. Bruns, R.F., J.H. Fergus, E.D. Badger, J.A. Bristol, L.A. Santay, J.D. Hartman, S.J. Hays, and C.C. Huang. *Naunyn-Schmiedeberg's Arch. Pharmacol.* **335**:59-63 (1987).

98. Peterson, G.L. and M.I. Schimerlik. *Prep. Biochem.* **14**:33-74 (1984).

99. Cheng, Y. and W.H. Prusoff. *Biochem. Pharmacol.* **22**:3099-3108 (1973).

100. Lowry, O.H., N.J. Rosebrough, A.L. Farr and R.J. Randall. *J. Biol. Chem.* **193**:265-275 (1951).

101. Martinson, E.A., R.A. Johnson, and J.N. Wells. *Mol. Pharmacol.* **31**:247-252 (1987).

102. Daly, J.W., in *Physiology and Pharmacology of Adenosine Derivatives*, Daly, J.W., Y. Kuroda, J.W. Phyllis, H. Shimizu, and M. Ui, eds., Raven, New York, 1983, pp. 275-290.

103. Ukena, D., E. Poeschla, and U. Schwabe. *Naunyn-Schmidedberg's Arch. Pharmacol.* **326**:241-247 (1984).

104. Gilman, A.G. *Ann. Rev. Biochem.* **56**:615-649 (1987).

105. Snyder, S.H. *Ann. Rev. Neurosci.* 8:103-124 (1985).

106. Stiles, G.L. *Trends in Pharmacol. Sci.* **7**:486-490 (1986).

107. Schutz, W. and M. Freissmuth. *Trends in Pharmacol. Sci.* 6:310-311 (1985).

108. Haleen, S.J. and D.B. Evans. *Life Sci.* **36**:127-137 (1985).

109. Bohm, M., W. Meyer, A. Mugge, W. Schmitz and H. Scholz. *Eur. J. Pharmacol.* **116**:323-326 (1985).

110. Haleen, S.J., R.P. Steffen and H.W. Hamilton. *Life Sci.* **40**:555-561 (1987).

111. Linden, J., A. Patel and S. Sadek. *Circ. Res.* **56**:279-284 (1985).

112. Lohse, M.J., K.N. Klotz, J.L. Fotinos, M. Reddington, U. Schwabe and R.A. Olsson. *Naunyn-Schmiedeberg's Arch. Pharmacol.* **336**:204-210 (1987).

113. Leid, M., P.H. Franklin and T.F. Murray. *Eur. J. Pharmacol.* **147**:141-144 (1988).

114. Green, A. *J. Biol. Chem.* **262**:15702-15707 (1987).

115. Schimerlik. M.I. and R.P. Searles. *Biochemistry* **19**:3407-3413 (1980).

116. Jarv, J., B. Hedlund and T. Bartfai. *J. Biol. Chem.* **254**:5595-5598 (1979).

117. Luthin, G.R. and Wolfe, B.B. *Mol. Pharmacol.* **26**:164-169 (1984).

118. Chatterjee, T.K., C.E. Scott, D.M. Vazquez, and R.K. Bhatnagar. *Mol. Pharmacol.* **33**:402-413 (1988).

119. Stone, T.W., in *Purines: Pharmacology and Physiological Roles*, Stone, T.W., ed, VCH Publishers, Deerfield Beach, 1985, pp. 1-5.

120. Leung, E., M. M. Kwatra, M. M. Hosey, and R.D. Green. *J. Pharmacol. Exp. Ther.* **244**:1150-1156 (1988).

121. Leid, M., M. I. Schimerlik, and T. F. Murray. *Mol. Pharmacol.* **34**:334-339 (1988).

122. Gavish, M., R. R. Goodman, and S. H. Snyder. *Science (Wash. D.C.)* **215**:1633-1635 (1982).

123. Klotz, K. N., M. J. Lohse,and U. Schwabe. *J. Neurochem.* **46**:1528-1534 (1986).

124. Berrie, C. P., N. J. M. Birdsall, E. C. Hulme, M. Keen and J. M. Stockton. *Br. J. Pharmacol.* 82:853-861 (1984).

125. Sidhu, A. *Biochemistry* **27**:8768-8776 (1988).

126. Herron, G. S., S. Miller, W. L. Manley, and M. I. Schimerlik. *Biochemistry* **21**:515-520 (1982).

127. Limbird, L. E. and R. J. Lefkowitz. *Proc. Natl. Acad. Sci. (U.S.A.)* **75**:228-232 (1978).

128. Smith, S. K. and L. E. Limbird. *Proc. Natl. Acad. Sci. (U.S.A.)* **78**:4026-4030 (1981).

129. Leff, S. E. and I. Creese. *Biochem. Biophys. Res. Comm.* **108**:1150-1157 (1982).

130. Bruns, R. F., K. Lawson-Wendling, and T. A. Pugsley. *Anal. Biochem.* **132**:74-81 (1983).

131. Tota, M. R., K. R. Kahler and M. I. Schimerlik. *Biochemistry* **26**:8175-8182 (1987).

132. Halvorsen, S. W. and N. M. Nathanson. *Biochemistry* **23**:5813-5821 (1984).

133. Sternweis, P. C. and J. D. Robishaw. *J. Biol. Chem.* **259**:13806-13813 (1984).

134. Huff, R. M., J. M. Axton and E. J. Neer. *J. Biol. Chem.* **260**:10864-10871 (1985).

135. Mumby, S. M., R. A. Kahn, D. R. Manning and A. G. Gilman. *Proc. Natl. Acad. Sci. USA* **83**:265-269 (1986).

136. Luetje, C. W., P. Gierschik, G. Milligan, C. Unson, A. Spiegel and N. M. Nathanson. *Biochemistry* **26**:4876-4884 (1987).

137. Mumby, S., I. H. Pang, A. G. Gilman and P. C. Sternweis. *J. Biol. Chem.* **263**:2020-2026 (1988).

138. Luetje, C. W., K. M. Tietje, J. L. Christian and N. M. Nathanson. *J. Biol. Chem.* **263**:13357-13365 (1988).

139. Ashkenazi, A., J. W. Winslow, E. G. Peralta, G. L. Peterson, M. I. Schimerlik, D. J. Capon and J. Ramachandran. *Science (Wash. D.C.)* **238**:672-675 (1987).

140. VanDongen, A. M. J., J. Codina, J. Olate, R. Mattera, R. Joho, L. Birnbaumer and A. M. Brown. *Science (Wash. D.C.)* **242**:1433-1437 (1988).

141. Neubig, R.R., R.D. Gantzos, and W.J. Thomsen. *Biochemistry* **27**:2374-2384 (1988).

142. Cerione, R.A., J.W. Regan, H. Nakata, J. Codina, J.L. Benovic, P. Gierschik, R.L. Somers, A.M. Spiegel, L. Birnbaumer, R.J. Lefkowitz, and M.G. Caron. *J. Biol. Chem.* **261**:3901-3909 (1986).

143. Kazmi, S.M.I., J. Ramwani, L.K. Srivastava, G. Rajakumar, G.M. Ross, M. Cullen, and R.K. Mishra. *J. Neurochem.* **47**:1493-1502 (1986).

144. Welton, A.F., P.M. Lad, A.C. Newby, H. Yamamura, S. Nicosia, and M. Rodbell. *J. Biol. Chem.* **252**:5947-5950 (1977).

145. Williamson, K., B.F. Dickey, H.Y. Pyun, and J. Navarro. *Biochemistry* **27**:5371-5377 (1988).

146. Mills, A., C.D. Demoliou-Mason, and E.A. Barnard. *J. Neurochem.* **50**:904-911 (1988).

147. El Mestikawy, S., C. Cognard, H. Gozlan, and M. Hamon. *J. Neurochem.* **51**:1031-1040 (1988).

148. Knuhtsen, S., J.P. Esteve, B. Bernadet, N. Vaysse, and C. Susini. *Biochem. J.* **254**:641-647 (1988).

149. Too, H.-P. and M.R. Hanley. *Biochem. J.* **252**:545-551 (1988).

150. Wong, Y.H., C.D. Demoliou-Mason, and E.A. Barnard. *J. Neurochem.* **52**:999-1009 (1988).

151. Couvineau, A., B. Amiranoff, and M. Laburthe. *J. Biol. Chem.* **261**:14482-14489 (1986).

152. Aiyar, N., W. Valinski, P. Nambi, M. Minnich, F.L. Stassen, and S.T. Coock. *Arch. Biochem. Biophys.* **268**:698-706 (1989).

153. Munshi, R. and J. Linden. *J. Biol. Chem.* **264**:14853-14859 (1989).

154. Munshi, R., I.-H Pang, P.C. Sternweis, and J. Linden, in *Purine Nucleosides in Cell Signalling: Targets for New Drugs*, Jacobson, K.A., J.W. Daly, and V.C. Maganiello, eds., Springer, New York, 1989, in press.

155. Kim, S., S.-L. Ang, D.B. Bloch, K.D. Bloch, Y. Kawahara, C. Tolman, R. Lee, J.G. Seidman, and E.J. Neer. *Proc. Natl. Acad. Sci. U.S.A.* **85**:4153-4157 (1988).

156. Leid, M., P.H. Franklin, and T.F. Murray, in *Purine Nucleosides in Cell Signalling: Targets for New Drugs*, Jacobson, K.A., J.W. Daly, and V.C. Maganiello, eds., Springer, New York, 1989, in press.